DETERMINATION OF OPTIMUM HYDRAULIC DESIGN PARAMETERS OF A SETTLING BASIN FOR DISCRETE PARTICLES IN IRRIGATION SYSTEMS

PATRICK NAMU NJERU

MASTER OF SCIENCE

(Construction Engineering & Management)

JOMO KENYATTA UNIVERSITY OF AGRICULTURE AND TECHNOLOGY

2017

Determination 0f Optimum Hydraulic Design Parameters of a Settling Basin for Discrete Particles in Irrigation Systems

Patrick Namu Njeru

A Thesis Submitted in Partial Fulfillment of the Requirements for the Master of Science Degree in Construction Engineering & Management in the Jomo Kenyatta University of Agriculture and Technology

2017

DECLARATION

This thesis is my original work and has not been presented for a degree in any other University

Signature:……Date:……

Patrick Namu Njeru

This thesis has been submitted for examination with our approval as University supervisors.

Signature:……Date:……..

Prof. Dr.-Ing. Benedict M. Mutua, PhD
KIBABII, Kenya

Signature:……Date:……..

Dr. (Eng). James M. Raude, PhD
JKUAT, Kenya

DEDICATION

I owe much thanks to the Almighty God who guided me to achieve my dreams. To my dear wife Doreen Kawira Namu and beloved son Brandon Baraka, for their patience and encouragement during this research. Thirdly, to my beloved mother Mrs. Janet Marigu Elisha- my first mentor who shaped my destiny.

ACKNOWLEDEGEMENT

The completion of this thesis work was made possible through the Almighty God, to you my Father in heaven I say thank you. I owe the strengths of this work to many people who have contributed towards the success of this write up however small or big the contribution was. To confirm my heartfelt gratitude, I wish to mention just but a few contributors. Firstly, my supervisors; Dr. (Eng). James M. Raude and Prof. Dr.-Ing. Benedict M. Mutua for making me stay focused in this study. They guided me to synthesize my scattered and diverse research ideas.

My dear wife Doreen Kawira has been of great support and encouragement throughout this work. Your faith in me, gave me challenge to complete this research. My loving mother has always been there asking me whether I have completed the 'teacher's work', to you mom may you live to blow a thousand candles so that you may continue to enjoy the sweet fruits of making me what I am today and perhaps much better in the future. Thanks to my sister, Sophie Gitiri and her family for their prayers and encouragement throughout my higher education.

To Mr. James Njue, a friend in deed, who inspired me into completing my research, you a real brother to me. I also owe a lot of thanks to Mr. Steve Mungai and family of Superhighway training college-Thika. A kind hearted person who gave me his office with unlimited internet access to use during my studies. Through him, I have realized a friend in need is a friend in deed.

This acknowledgement will not be complete without the recognition of the vital assistance of Dr. Raphael Wambua who made constant calls to find out how far I was in my progress in thesis writing and was always there to guide

me on how to use ANN in Matlab. Lastly, to my friends Dennis Kiptoo, Denies Muriithi, Joseph Njiru, Michael Wafutu and colleagues in Mogadishu who kept encouraging me during my thesis writing may your love be greatly rewarded.

Let the Almighty God exceedingly bless all the above-mentioned persons beyond measure.

TABLE OF CONTENT

LIST OF TABLES

LIST OF FIGURES

LIST APPENDICES

ABBREVIATION AND ACRONYMS

ANN	Artificial Neural Networks
AV	Air Valve
CFD	Computational Fluid Dynamics
JKUAT	Jomo Kenyatta University of Agriculture and Technology
GI	Galvanized Iron
GOK	Government of Kenya
GUI	Graphical User Interface
MAE	Mean Absolute Error
MatLab	Matrix Laboratory
MBE	Mean Bias Error
MLP	Multi Linear Perceptron
MSE	Mean Square Error
MUSLE	Modified Universal Soil Loss Equation
MWI	Ministry of Water and Irrigation
NNN	Natural Neural Networks
PE	Processing Elements

PRbV	Pressure Reducing Valve
R	Coefficient of Regression
RBF	Radial Basis Function
RMSE	Root Mean Square Error
SB	Settling Basin
WO	Washout

DEFINITION OF TERMS

Data Training	Is the process of yielding the most accurate output by achieving the highest possible iteration/learning
Data Testing	Is evaluating/analyzing the performance of the developed model. At this stage un-seen data is exposed to the model.
Data Validation	Is the act of harmonizing the attributes of processed data in order to achieve more accurate outputs.
Discrete particles	Particles whose size, shape and specific gravity do not change with time.
Erosion	The initial dislodging of the sediment particles for eventual transport or movement.
Irrigation	The artificial application of water to the land or soil. It is used to assist in the growing of agricultural crops, maintenance of landscapes, and re-vegetation of disturbed soils in dry areas and during periods of inadequate rainfall.
Neural networks	System consisting of interlinked elements, which are able to process data and can be named as neurons.
Prediction	Is the aspect using available processed data to determine

	unknown incidences in a certain data sample.
Rangeland	The natural landscape in form of grasslands, shrub land, woodland, wetlands and deserts suitable for livestock to wander and graze.
Sediment	Material that is detached, transported and deposited in a new location by water.
Sedimentation	The condition whereby the solids are already at the bottom and in the process of settling.
Settling	A unit operation in which solids are drawn toward a source of attraction. That is particles are falling down the water column in response to gravity.
Settling basin	Are used as a separation mechanism to eliminate substances of different physical and chemical properties (i.e. waste solids management strategies) of a specified size and quantity in various fields, such as aquaculture, mining, dairy, food processing, alcohol production and wine making.
	System consisting of interlinked elements, which are able to process data and can be named as neurons.

ABSTRACT

Irrigated agriculture is faced with challenges that include sediment loading in the river basins and dams. The management of sediments in river basins and waterways has been an important issue for water managers throughout history. Water managers are faced with similar challenges caused by siltation of water reservoirs and irrigation water conveyance systems. As a copping strategy to counter the low irrigation application efficiency, designs of settling tanks are typically oversized. This is aimed at having enough detention time for the sediment particles to settle. This process is costly and tedious hence this study aimed at optimizing the hydraulic design parameters for settling basins with an intention of addressing such challenges. Artificial Neural Networks in MATLAB was used to build ANN models for predicting sediment settlement and eventually optimizing the hydraulic parameters of settling basins. The ANN was used to develop the relation between sediment settlement and different inflows by changing the different number of neurons in hidden layer from two to ten. The optimum hydraulic design parameters for a settling basin were calibrated using a physical model prepared in the Civil Engineering laboratory at Jomo Kenyatta University of Agriculture and Technology. Extensive data was collected to evaluate the physical and hydraulic parameters needed to calibrate and validate the ANN model. ANN model was trained and validated using a dataset obtained from the physical model. The developed simulated results were evaluated using recommended quantitative statistical analysis that compared the measured and the predicted data. The average accuracy between the artificial neural networks prediction and the real data in all the cases was over 90 %. The turbidity drop in a settling basin increased with the increase in flowrate and gave a biquadratic relationship, applicable in calculating turbidity drop. In addition, an ANN architecture of 1-9-1 was the best suited for predicting turbidity in Kiriku-Kiende settling basin where a quadratic relationship existed for flow rate against the optimum surface area for the settling tank. For flow rates of 5.7, 8.7, 9.9, 10.5 and 11.1 m^3/s, the critical settling velocity was found to be 0.0034, 0.0044, 0.0024, 0.0026 and 0.0034 m/s

respectively. The optimum surface areas for 5.7, 8.7, 9.9, 10.5 and 11.1 m^3/s flow rates was calculated as 2.42m^2, 3.04 m^2, 3.75 m^2, 4.20 m^2 and 4.71 m^2 respectively.

Further, on flushing, the settling tanks with continuous sediment removal gave a higher sediment efficiency flushing of 65.5% against 24.4% without flushing. Finally, ANN can be used as a decision making tool for turbidity prediction.

CHAPTER ONE

INTRODUCTION

1.1 Background information

Water quality control for irrigated agriculture requires that the sediments be controlled at their entrance point to the networks. This can be achieved by constructing a settling basin (SB) where better retardation of the sediments is realized by constructing large basins, cost notwithstanding (Shetab--Boushehri *et al*., 2010). However, one of the problems with surface irrigation water distribution is sedimentation control at the inlet to the irrigation networks. Walling and Fang (2003) approximated that 1% of the world's water storage capacity in reservoirs is lost every year through sediment deposition. This indicates that access to water for irrigation will become an issue of global concern and competition for the same in the future especially in the arid and semi-arid regions of the world. (Mengiste & Kidane, 2016).

Over the last half-century, significant productivity gains through water management in agriculture have protected the world from devastating food shortages and threats of mass starvation. According to Ngenoh *et al*. (2015), empirical evidences have shown that irrigation increases crop yield by between 100% to 400%. It is expected that, in the next 30 years 70% of grain production will be from irrigated land in the world (FAO, 2009). Therefore, water management, in both rain-fed and irrigated agriculture is instrumental in achieving these gains (FAO, 2003). Irrigation is important to global food production since about 15% of cropland and 5% of food production land, which includes rangeland and permanent crop land, is irrigated (Bjorneberg & Sojka, 2002). According to Mati (2011) and Valipour (2015), irrigation has a role to reduce poverty in the world through improvement of crop production. A research in the United States revealed that 15 million hectares of irrigated land corresponding to 21% is affected by soil erosion to some extent (Koluvek *et al*., 1993).

Irrigation induced soil erosion has been studied, primarily in the North western United States, since 1940, where a number of studies measured annual sediment yields from furrow-irrigated fields and it was found that the amount of sediment per year was 20 t/ha with some fields exceeding 100 t/ha per year (Shrestha, 2012). In addition, there is a substantial geographic variation in loss of reservoir storage from sedimentation. For example, in one study of 42 reservoirs in Iowa, Nebraska, and Missouri, 18 reservoirs lost 25 % of their storage capacity in 11 years (Clark *et al*., 1985; Reckendorf, 1995). The Yellow River that is the second largest River in China is known for its high sediment discharge with an average value of 1.6×10^9 tons/year. (Qingzhen *et al.,* 2015).

In Africa up to 80% of available water is used for agriculture (Josephine, 2009). The average rate of irrigation development in Sub-Saharan Africa countries between 1988 and 2000 was 43,600 ha/year (FAO, 2003). The Food and Agricultural Organization estimates that irrigated land in developing countries will increase by 27% in the next 20 years, but the corresponding quantity of water expected to be available for agricultural production will only increase by 12 % (FAO, 2009). Going by these projections, an additional one million hectares of land will be under irrigation in Africa by 2025 (Karina & Mwaniki, 2011). However, irrigated agriculture is faced with challenges such as sediment loading in the river basins and dams. For instance, the Orange River in South Africa is rated among the most turbid rivers in the world due to sedimentation (Compton & Maake, 2007).

The management of sediments in river basins and waterways has been an important issue for water managers throughout the history as from the ancient Egyptians managing sediment on floodplains (UNESCO, 2011). Currently, water managers are faced with similar challenges mainly resulting in siltation of water reservoirs (Yon & Lee, 2000). For instance, the large Borken dam in South Wello in Ethiopia despite having been constructed with multi-million dollars was silted within one rainy season. This was as a result of underestimation of the potential runoff and sedimentation during design (Habtamu, 2009). In another case, Compton & Maake (2007) identified that Caledon River in South Africa carries

the largest fine-mud suspended load, primarily from the erosion of Karoo sedimentary rock soils.

Unfortunately, Kenya is not exempted from the dangers posed by sedimentation and siltation in her water bodies. According to Onyando *et al*. (2005), a high proportion of sediments generated in the catchment areas is delivered through soil erosion to the rivers and lakes. A research by Herbert (2002) revealed that Gem-Rae irrigation scheme in Kisumu commissioned in 1985 had to be abandoned after 12 years of operation due to clogging of intake and main canals. In 1997 approximately 200 m^3 of sediment were removed weekly from this project intake. This is a clear indication that sediment management is important if irrigation potential in Kenya is to be exploited (Karina *et al*., 2011). Irrigation sector is among the long-term initiatives towards the achievement of a 10% annual economic growth envisioned in Vision 2030 (Ngenoh *et al.,* 2015).

According to a study conducted in Murang'a by Home and Ngugi (2012) on smallholder irrigation projects, sprinkler clogging caused by sediments resulted to low coefficients of uniformity in water application. The issue of sediments entering irrigation pipelines and power canals has been a major problem confronting hydraulic engineers (Sigh *et al*., 2013). As such, sediment settling basins have been designed and constructed at river water intakes. The sedimentation tanks are designed to remove most of suspended sediment which enters into the intakes by flowing water. The objective of Sedimentation basins which are hydraulic structures, designed and constructed where mostly there is water abstraction is to remove most of suspended sediments that enters the intake by flowing water (Heydari *et al*., 2013). The life of water reservoirs is usually reduced by the accumulation of sediment behind the upstream reservoir wall.

Effective management of sediments from rivers during irrigation water abstraction by use of settling basins has become increasingly important from an economic and environmental perspective. Many factors such as surface and solids loading rates, tank type, solids removal mechanism, inlet design, weir placement and loading rate affect the capacity and performance of a settling tank (Singh & Kumar, 2016). At times, these settling basins do not allow enough time for all the particles to

settle since the quantity of water abstracted also affect the settling time of the particles. Design guidelines do not adequately account for concentration or density gradients, flow variations, difference in tank shape and inlet-outlet structures. The design manuals provide design guidelines for particles greater than 0.2 mm (GOK, 2005). The smaller particles coagulate along the pipeline and finally block the sprinkler nozzles and emitters. As such, this study focused on optimizing the design parameters for settling basins to maximize the settling of discrete particles smaller than 0.2 mm in size.

1.2 Statement of the problem

The major problem in irrigation water management is sediment control in the inlet of water diversion to the settling basins and finally to the irrigation networks. Uncontrolled sediment has resulted to problems such as reduced capacity of water transport, annual irrigation acreage reduction and high maintenance cost for irrigation project. A research by Herbert revealed that Gem-Rae irrigation scheme in Kisumu had to be abandoned after 12 years of operation due to clogging of intake and main canals by sediment. In trying to cater for the low irrigation water application efficiencies, present-day designs typically oversize the settling tanks in view of having enough detention time for the particles to settle in the basin. As such, designers hope to cope with the poor design that is responsible for undesired and unpredictable system disturbances. This process is costly and tedious hence, this study aimed at optimizing the design parameters for settling basins for optimum sediment settlement.

1.3 Objectives of the study

1.3.1 Main objective

The main objective of this study was to optimize the hydraulic design parameters of irrigation settling basin using Artificial Neural Networks (ANN) model in MATLAB for efficient sediment and water management.

1.3.2 Specific objectives

The specific objectives of this study were to:

i) Determine the critical settling velocities of discrete particles for various flow rates in a sprinkler irrigation system.
ii) Develop a predictive model and determine the optimum dimensions for sprinkler irrigation settling basins in relation to different in-flow irrigation water turbidities.
iii) Evaluate the effect of continuous flushing on the sediment removal efficiency of surface irrigation system's settling basins.

1.4 Research questions

i) What is the critical settling velocity of discrete particles for various flow rates across a range of time in sprinkler irrigation system?

ii) What are the optimum design dimensions for a sedimentation basin based on different irrigation water inflow rates?

iii) What are the effects of continuous sediment flushing on the settling of particles in surface irrigation systems?

1.5 Justification

Without effective sediment control, settling basins and canals silt up reducing system discharge and conveyance capacities. This has been witnessed in a number of small scale irrigation project like Mitunguu irrigation scheme in Meru county which had to undergo a major rehabilitation to unblock the settling basin and water structures along conveyance line in 2011-2013. Sediments in irrigation network causes clogging and blocking of irrigation structures. This contributes to overall low irrigation water delivery to the farms. This study was to maximize the settling of particles, which will eventually increase the overall efficiency of irrigation systems. Consequently, there will be improvement in yields from crop production because of increased available irrigation water leading to improved food security in line with the country development agenda.

1.6 Scope and limitation

The study was carried out in Jomo Kenyatta University of Agriculture and Technology (JKUAT), at Civil Engineering laboratory where a physical model was designed and fabricated to resemble a physical settling basin. This was to

enable effective data collection which would reflect the behavior of sediment settling at different flow rates. The turbid water collected was tested for turbidity levels at soil laboratory in the Department of Soil, Water and Environmental Engineering. The research mainly focused on the performance of settling basin on how discrete particles settled against different flow rates. The major limitation to this study was that the baffles used in settling basins were not considered in the model even though they play a major role in dissipating kinetic energy of incoming flow. Lack of baffles may have affected the settling time of the particles.

CHAPTER TWO

LITERATURE REVIEW

2.1 Irrigated agriculture

The world's concern on access to adequate and nutritional food for a growing population has triggered the emergence of different strategies, programs and partnerships for provision of food. One of the strategies is to increase agricultural production through irrigated systems, especially under smallholder managed irrigation schemes that mainly produce food products for direct consumption or trading in the rural markets (FAO, 2006). To meet food requirements by 2020, the Food and Agriculture Organization for United Nations (FAO, 2000), estimated that food production from irrigated areas would need to increase from 35% in 1995 to 45% in 2020.

At present and more so in the near future, irrigated agriculture will take place under water scarcity. Insufficient water supply for irrigation will be the norm rather than the exception. Therefore, irrigation management will shift from emphasizing production per unit area towards maximizing the production per unit of water consumed, or the water productivity (Fereres *et al.,* 2007). It is estimated that 15-20 % of the worldwide total cultivated area is irrigated. Judging from irrigated and non-irrigated yields in some areas, this relatively small fraction of agriculture may be contributing to 30-40 % of gross agricultural output in the world (Jury & Vaux, 2005; FAO, 2006).

Irrigated agriculture is the primary user of diverted water globally, reaching a proportion that exceeds 70–80% of the total in the arid and semi-arid zones. It is therefore not surprising that irrigated agriculture is perceived to be a key driver behind agricultural productivity (Mengistie & Kidane, 2016). It is important that the scope of irrigation science is not limited to diversion and conveyance systems, nor solely to the irrigated field, or only to the drainage pathways. Irrigation is a system extending across many technical and non-technical disciplines. It only

works efficiently and continually when all the components are integrated effectively so that the overall efficiency improves with time (Chintokoma *et al.,* 2015).

In Kenya, smallholder irrigation development is one of the key strategies for land use intensification with expected positive effects on rural incomes and poverty alleviation. About 20% (106,600 ha) of the potential irrigable land is already under irrigation where 50% (53,300) of this area is under smallholder irrigation (FAO, 2003; Home & Ngugi, 2012; Kangau *et al*., 2012). Table 2.1 shows how the land under irrigation is utilized in Kenya per schemes while Table 2.2 presents the land under irrigation in each basin (Leonard & Timothy, 2016)

Table 2.1: Land under irrigation in Kenya

Type of Irrigation farming	**Area (Hectares)**	**Percentage (%)**
Large commercial farms	42,640	40
Government managed schemes	19,188	18
Smallholder schemes	44,772	42
Total	**106,600**	**100**

Source: Kangau *et al*., 2012

Table 2.2: Irrigation potential and development by basins

Basin	Total Potential for Irrigation (Hectares)	Developed Area (Hectares)	Balance
Tana	226,224	64,425	161,799
Athi	91,006	44,898	46,108
Lake Victoria basin	297,213	15,094	282,119
Kerio valley	101,753	9,587	92,166
Ewaso Ngiro	49,379	7,896	41,483
Total	**765,379**	**141,900**	**623,675**

Source: Leonard & Timothy, 2016

2.2 Sediment removal mechanisms

The plain sedimentation of discrete spherical particles described by Newton's Law, can be applied to sediment removal in sedimentation tanks. In discrete settling, the particle maintains its individuality and does not change in size, shape or destiny during settling (Lee & Shur, 2007). Various methods: Gravity separation, Settling tanks, Tube settlers, Hydro cyclones, Flotation, Foam fractionation and Ozonation are applied in settling discrete particles.

2.2.1 Gravity separation

Gravity separation is separation of two immiscible liquids or slurry containing fine solids by making use of the density difference. It is a set of unit processes in which gravity removes settleable solids, associated pollutants, floatables, and dispersed immiscible liquids (Mahajani & Umarji, 2009). In gravity settling separation, solid particles will settle out of a liquid phase if the gravitational force

acting on the droplet or particle is greater than the drag force of the fluid flowing around the particle (Brownell & Young, 2004). In gravity separation we have settling tanks, Tube settlers and hydro cyclones which are mostly applied to aid in particle settlement.

2.2.2 Tube settlers

Tube settlers are designed to improve the characteristics of the rectangular basin and to increase flow through the tank. They consist of a series of tubular channels sloped at an angle of 55°- 60° and adjacent to each other, which combine to form an increased effective settling area. This provides for a particle settling depth that is significantly less than the settling depth of a conventional clarifier, reducing settling times (Gregory *et al.,* 2010). Tube settlers capture the settleable fine floc that escapes the clarification zone beneath the tube settlers and allows the larger floc to travel to the tank bottom in a more settleable form. The tube settler's channel collects solids into a compact mass, which promotes the solids to slide down the tube channel (Brownell & Young, 2004; Gregory & Edzwald, 2010). Tube settles are mostly applied in water treatment works and rarely in irrigation purposes.

2.2.3 Hydrocyclones

Hydrocyclones are used to carry out sedimentation of particles in a liquid medium under enhanced separating force. The necessary force is generated by rotating the feed slurry rapidly in the cylindrical conical section (Hoffman & Stein, 2008). The cylindrical conical section is provided at the top and bottom of the cyclone so that fine particles and coarse particles can be withdrawn continuously. Hydrocyclones are simple, robust separating device which can separate both coarse and fine particles in a range of 4-500µm. When the slurry starts to rotate in the cylindrical body, the coarse or heavy particles are thrown outwards towards the wall that move downwards in a spiral path towards the underflow or an open orifice where they are ejected. During the process, fine particles remain near the center of the cyclone, close to the air core and eventually move in an upward spiral towards the overflow orifice. The size of cyclone and estimation of the number of stages required for a particular application depend upon the stream flow rate (Sinnot,

2005; Hoffman & Stein, 2008). A specific gravity difference must exist between solid and liquid phase in order for separation to take place, this is not the case in sedimentation tanks.

2.2.4 Filtration

Water filtration is a mechanical or physical process of separating suspended and colloidal particles from fluids (liquids and gases) by interposing a medium through which only the fluid can pass. Medium used is generally a granular material through which water is passed. Conventionally filtration follows coagulation, flocculation and sedimentation in water treatment process (Benham & Ross, 2009; Bar-Zeev *et al.,* 2012). Various methods are used for filtration that includes screens, Granular and Porous media filter. Screen filtration is applicable in sedimentation basins just before the water flows into the tank however granular and porous media filter are not common in surface irrigation due to the demand for manually cleaning and rinsing the membranes.

2.2.5 Screen filtration

Screening is the first unit operation used in wastewater treatment plants (WWTPs). Screening removes objects such as rags, paper, plastics, and metals to prevent damage and clogging of downstream equipment, piping, and appurtenances. Some modern wastewater treatment plants use both coarse screens and fine screens (Reynolds & Richards, 1996). Coarse and fine screens. Coarse screens remove rags, sticks, large solids and other debris ranging from 0.25 to 144 mm (EPA, 2003). They can be as simple as a trash rack or as complicated as a mechanically cleaned bar screen. Where coarse screens use bars or rods to remove solids, fine screens employ wire cloth, wedge wire elements or perforated plates. Fine screens are used to remove particles that may cause maintenance issues for process equipment and/or operational problems to the treatment process. Fine screen openings typically range from 1.5 to 6mm. The smaller size openings allow the fine screens to remove 20 to 35 percent of suspended solid and BOD (Crites & Tchobanoglous, 1998; EPA, 2003).

2.2.6 Granular media filter

Granular media filtration is the process for removal of suspended solids by passage of water through a porous medium. The filtration process results in a gradual accumulation of entrapped solids within the granular media; this requires intermittent removal by means of a filter backwash cycle. This cycle typically comprises both air scour and water wash phases, to effectively loosen and flush out the retained solids to waste (Viska, 2011). A sufficient flow of wash water is applied until the granular filtering medium is fluidized (expanded), causing the particles of the filtering medium to abrade against each other (Tabatabaei *et al.,* 2007). This method is mostly applied in water treatment processes and not for irrigation purposes.

2.2.7 Flotation

Flotation is a gravity separation process that exploits the differences in the surface properties of the particles. The separation process is based on the use of very fine gas bubbles that attach themselves to the solid particles in suspension to make them buoyant and drive them toward the free surface of the liquid. Flotation is especially useful to separate very small particles with low settling velocities (Spellman, 2009; Gregory *et al.,* 2010). A number of chemicals can be added to the flotation medium to meet the various requirements of the flotation process. One method of flotation is through foam fractionation and Ozonation which are discussed below.

2.2.8 Foam fractionation

Foam fractionation enhances sediment removal in a recirculating system. A typical foam fractionation unit is a bubble column where bubbles generated at the bottom rise upwards passing through a liquid in which solids are suspended. Solid mass transfer from the liquid to the bubble surface is mainly through diffusion and particle-bubble collision (Chen & Malone, 1991). Foam fractionation is primarily designed for dissolved, surface-active organics removal. The solids removed by foam fractionation are mostly fine particles with diameters smaller than 30µm (Lee & Shur, 2007). Solid removal in this process is affected by chemical properties of the solids in the system unlike in a sedimentation basin.

2.2.9 Ozonation

As an unstable reactive gas, ozone splits large organics into smaller biodegradable materials more easily removed by heterotrophic bacteria (Viska, 2011). Currently micro and nanoflotion with ozone (Dissolved ozone flotation, DOF) is in use. In this process, ozone is used instead of atmospheric air, whereby two processes are obtain in one unit that is; separation of solids and emulsion by gas bubbles (as in conventional flotation) and oxidation of soluble organic compounds which is done using strong oxidizing agent-ozone (Wilinski *et al.,* 2012; Jin *et al.,* 2015). Synergy of those two processes (separation and oxidation) can lead to better treatment effects. It can cause positive results by decreasing dosing coagulants and flocculants, pathogen removal, improvement of wastewater biodegradability, micro-pollutants removal, decreasing the amount of excess biological sludge (Jin *et al.,* 2006). However, ozonation is quite expensive for use in sediment management for surface irrigation systems.

2.2.10 Settling tanks

The simplest method of sedimentation is to use rectangular tanks with horizontal flow through them. The water with the particles in suspension is introduced at one end of the tank, then as the water flows to the other end of the tank settlement of particles in the water occurs. The aim is that a large proportion of the settling particles manage to reach the tank floor before the water is drawn out of the tank at the outlet end (Doroodchi *et al.,* 2006). Such horizontal flow tanks are usually built with a floor that slopes gently down to the inlet end to a hopper. The tank is fitted with a mechanism to scrape the sediment from the outlet end back to the inlet end and into the hopper from where it can be discharged hydraulically. In the design of such tanks detailed attention has to be given to the inlet and outlet ends so that the water flows from one end to the end as uniformly as possible (Sigh & Arun, 2013). Settling basins use the simplest technology with little energy input, relatively inexpensive to construct and operate with no specialized operational skills and therefore considered in this study.

2.3 Critical settling velocities of discrete particles

Settling basins are designed to retain water for a specified period with the aim of removing sediments. However, most settling basins built using these principles are oversized and inefficient because the critical design criteria are not considered or are inadequate (Shetab-Bousheri *et al*., 2010). For instance, while analyzing sediment settling and basin efficiency Jahseen (2009) was limited to only rectangular basins, with assumed uniform conditions across the full width of the basin. However, this condition is not always met as in practice flow expansion and contraction occurs in basin inlet and outlet zones.

The trapping efficiency of a settling basin is mainly governed by the geometry, generally size and shape as the main dominating parameters. Even flow distribution is the key to maintaining optimum trapping efficiency and reduced turbulence. It is very important to have a properly designed inlet and outlet geometry to ensure that even flow distribution over the depth and width of settling basin exists (Shrestha, 2012). The shape of the tank is very important for producing an even flow distribution in the basin (Yon & Lee, 2000; Heydari *et al.,* 2013).

A further consideration in the design of a sedimentation basin is the provision of adequate storage for settled sediment to prevent the need for frequent de-silting (Yon & Lee, 2000). The volume of accumulated sediment is estimated from regular monitoring of sediment levels, using a measuring post that is referenced against the top water level (Raju *et al.,* 1999). Generally, the recommended frequency of basin de-silting is once every five years, which is usually triggered when sediment accumulates to half the basin depth.

It is very important to trap sediment before feeding water into an irrigation scheme or power plant. However, it is not possible to trap all sediments. The main work of a settling basin is to reduce turbulence level in the water flow (Isam *et al*., 2013). This enables suspended sediment particles to settle out from the water body and deposit at the bottom of the basin. Deposited sediments are then

removed from the basin by use of the flushing system or through excavation if the amount of sediments is small at a pre-determine time (Shrestha, 2012).

Most of the particles bigger than 0.2 mm to 0.3 mm must be excluded to minimize costs related to sprinkler and emitter wear and generation losses during maintenance of the system (Reckendorf, 1995). It is therefore a general requirement to control sediment content in the water released for sprinkler and drip irrigation through continuous flushing of the settled sediment (Xueying *et al.,* 2016).

2.3.1 Sediment settling basins

Irrigation schemes are usually designed and implemented on the basis of assumed efficiencies in water conveyance, water distribution and water applications. However, over time, physical changes in the schemes such as poor maintenance of structures, soil property changes and deterioration of equipment may alter these efficiencies (Home & Ngugi, 2012).

One of the problems in irrigation water management is sediment control in the inlet to the irrigation networks (Heydari *et al.,* 2013). As a result, problems such as reduced capacity of water transport, annual irrigation acreage reduction and high maintenance cost emerge. To remove the sediment that has entered a canal or any conveyance line during diversion, the vortex tubes, tunnel type sediment extractors and settling basins are often used (Sigh & Arun, 2013). In the settling principle, particle settling is achieved by detaining water long enough for the suspended sediment to settle from the water under the influence of gravity before the water is discharged to uncontrolled environment (Raju *et al.,* 1999; Logan, 2012).

Settling of particles depends on two major factors namely: characteristics of the particle (Discrete particles and Flocculating particles) and concentration of the particles in suspension (Dilute or Concentrated) (Muhanned & Mohammed, 2013). These are summarized and shown in Figure 2.1

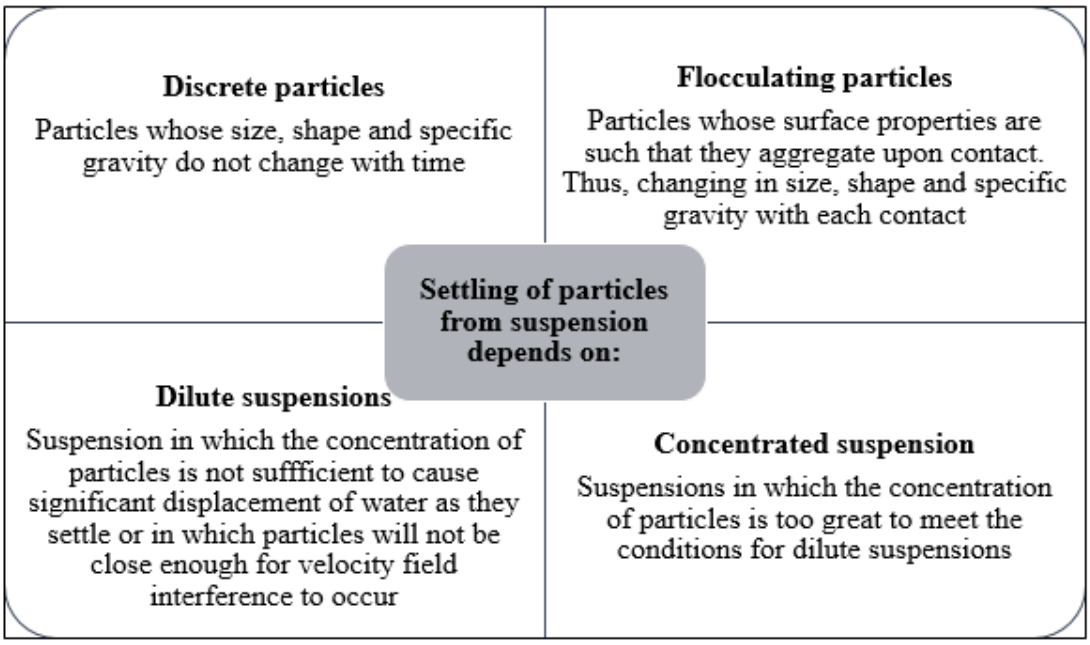

Figure 2:1: Factors affecting settling of particles

The current methods in which settling basins are designed and modified should be improved. Provision of a tool for optimizing the settling tank as well as, understanding, quantifying and visualizing the major process dominating the tank performance is important in smallholder irrigation systems management.

2.3.2 Principle of sediment particle settling

Suspended solids present in water having specific gravity greater than that of water tend to settle down by gravity as soon as the turbulence is retarded by offering storage. If a particle is suspended in water, it initially has two forces acting upon it. These forces are represented by Equations. Equation 2.1 represents the force of gravity acting on the particles while the Buoyant force is given by Equation 2.2. (Zhiyao *et al*, 2008).

$$F_G = \rho_p g \nu_p \quad (0.1)$$

$$F_B = \rho_w g \nu_p \quad (0.2)$$

Where:

F_G = Gravitation force (N)

F_B = Buoyant force (N)

ρ_p = Density of particle (kg/m^3)

V_p =Volume of particle (m^3)

g = Acceleration due to gravity (m/s^2)

e density of the particle differs from that of the water, a net force is exerted and the particle is accelerated in the direction of the force. This net force given in Equation 2.3 becomes the driving force.

$$F_{net} = (\rho_p - \rho_w) g V_p$$

(0.3)

Where:

F_{net} = Net force (N)

ρ_p = density of particle (kg/m^3)

ρ_w = density of water (kg/m^3)

V_p = volume of particle (m^3)

g = Acceleration due to gravity (m/s^2)

Once the motion is initiated, the drag force as given in Equation 2.4 is created due to viscous friction.

$$F_d = C_D A_p \rho_w \frac{V_s^{\,2}}{2}$$

(0.4)

Where:

C_D = drag coefficient

A_p = Cross-sectional area of particle perpendicular to the direction of movement (m^2)

V_s = Settling velocity of the particle (m/s)

Since the drag force acts in the opposite direction to the driving force and increases as the square of the velocity, acceleration occurs at a decreasing rate until a steady velocity is reached at a point where the drag force equals the driving force. The force balance for a settling discrete particle is given in Equation 2.5.

$$M_p \frac{dv_s}{dt} = F_G - F_B - F_D \quad (0.5)$$

After an initial transient period, the acceleration $\frac{dv_s}{dt}$ reduces to zero and the settling velocity becomes constant, as given in Equations 2.6 and 2.7.

$$M_p \frac{dv_s}{dt} = 0 = F_G - F_B - F_D \quad (0.6)$$

$$0 = (\rho_p g V_p) - (\rho_w g V_p) - \left(C_D A_p \rho_w \frac{V_s^2}{2} \right) \quad (0.7a)$$

This is re-arranged as given in Equation 2.7a

$$g V_p (\rho_p - \rho_w) = (C_D A_p \rho_w \frac{V_s^2}{2}) \quad (2.7b)$$

Substituting Equation 2.7 reduces to Equation 2.8 and given as:

$$V_s = \sqrt{\frac{2g(\rho_p - \rho_w)}{C_D \rho_w A_p}} \quad (0.8)$$

Equation 2.8 is the settling velocity equation of discrete particle in any shape while the settling velocity for spherical particle is presented in Equation 2.9 as:

$$V_s = \sqrt{\frac{4(\rho_p - \rho_w)gd}{3C_D\rho_w}}$$

(0.9)

The (C_D) used in Equation 2.9 is Newton's drag coefficient which is a function of, flow regime around the particle and particle shape.

For Spheres, C_D is given in Equation 2.10 as:

$$C_D = \frac{24}{\mathrm{Re}} + \frac{3}{\sqrt{\mathrm{Re}}} + 0.34$$

(0.10)

Where Re is Reynold's number, which is given by Equation 2.11 as:

$$\mathrm{Re} = \frac{V_s d}{V} = \frac{V_s d\rho}{\mu}$$

(0.11)

Hence in turbulent flow the values adopted are:

$\mathrm{Re} \triangleright 10^4$ and $C_D = 0.34\text{-}0.4$

Substituting Equation 2.11 in 2.9, it reduces to Equation 2.12, which is the equation for settling velocity of spherical discrete particles under turbulent flow conditions.

$$V_s = \sqrt{\frac{10g(\rho_p - \rho_w)d}{3\rho_w}}$$

(0.12)

2.4 Design parameters of a settling basin

When considering the process of sedimentation as applied to settling basins, discrete settling conditions could be assumed for relatively low inlet concentrations. Work by Hazen, in 1904, saw the first analysis of factors affecting the settling of solid particles from dilute suspensions and introduced the surface

loading concept (Concha & Burger, 2002; Margarita *et al.,* 2017). In the surface loading concept, the fall velocity of the sediment particle guides the design of settling basin. The fall velocity is dependent on density, size, shape and concentration of particles and to some extent on water temperature (Wisniewski *et al*., 2013). The design procedures of settling basin currently used are still based on the Sierp and Greely diagrams which considers surface overflow or surface hydraulic load and hydraulic retention time (Metcalf *et al.,* 2003; Chiang *et al.,* 2010).

The major design features and others considered in design of a settling basin are presented in Table 2.3.

Table 2.3: Major features considered in design of settling basin

Item	Description
1	Tank cross sectional area
2	Tank depth
3	Detention time
4	Type of flow (laminar or turbulent)
5	Density of the particle and fluid
6	Particle size and shape
7	Fluid temperature
8	Shear resistance of the particle

Sultana and Naik (2015), stated that the significant factors influencing the rate of sediment settling in a reservoir as; capacity to inflow rate, sediment content in the flowing water, texture and size of the sediment and the trapping efficiency. Capacity to inflow rate is defined by flow velocity and tank dimensions. According to Reckendorf (1995) the velocity of flow should not be greater than 30 cm/min in horizontal flow basin while tank dimensions should range between 2 to 5:1 for length to breadth ratio. The tank depth should range between 2.0 to 5.0 m while the surface overflow rate for plain sedimentation tank should be 12,000

to 18,000 L/d/m^2 tank area. In addition, thoroughly flocculated water to be between 24,000 to 30,000 L/d/m^2 tank area.

2.4.1 Design procedures for settling tanks

The design of current settling tank system is based on the principles of gravity settling. Gravity settling occurs in tanks of water with large cross-sectional areas where small influent and outward flows create a state of virtual quiescence in the system (Wisniewski, 2013). Particles with densities higher than that of the surrounding fluid will settle under the influence of gravity while lighter particles will float. The particles in the sedimentation tank are then retained in the sludge layer at the bottom of the tank as shown in Figure 2.2. (Doroodchi *et al.,* 2006).

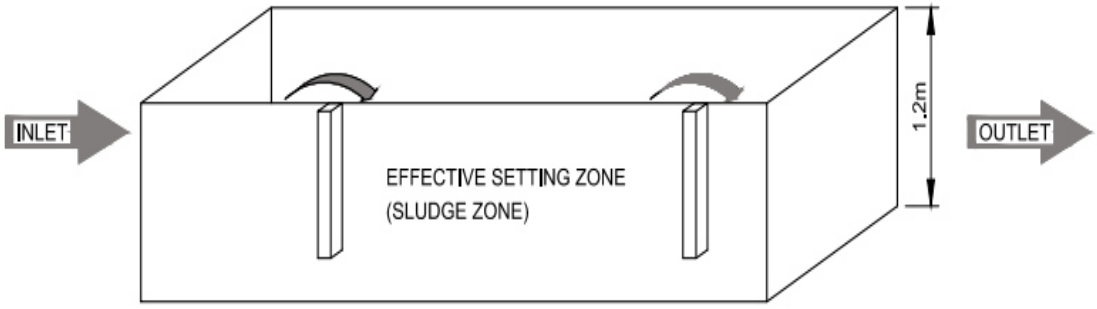

Figure 2:2: A typical settling basin model

Discrete settling occurs in the systems with small particle concentrations where particle aggregation is negligible and settling occurs by natural forces. In discrete settling, the terminal velocity or settling rate of the particles are calculated using Stoke's Law which assumes the rate depends only on the size, shape and density of the particle, viscosity and density of the fluid (Liyanage *et al.,* 2016). Equation 2.13 gives the Stoke's Law.

$$U_t = S_o = \frac{d^2 \times g \times (\rho - \rho_f)}{18 \times \mu} \quad (0.13)$$

Where:

d = Particle diameter (m)

g = Gravitational acceleration (m^2/s)

μ = Fluid viscosity (Ns/m^2)

ρ = Particle density (kg/m^3)

ρ_f = Fluid density (kg/m^3)

U_t = Terminal velocity (m/s)

S_o = Stoke's settling rate of particle (m/s)

The overflow parameter is a crucial parameter in the design of the sedimentation tank and is generally chosen to be half of the value of the stoke's settling rate (Ghawi *et al.,* 2012). For a fixed influent rate, adequate particle removal only depends on the surface area of the tank. Figure 2.3 is an illustration of an ideal settling tank.

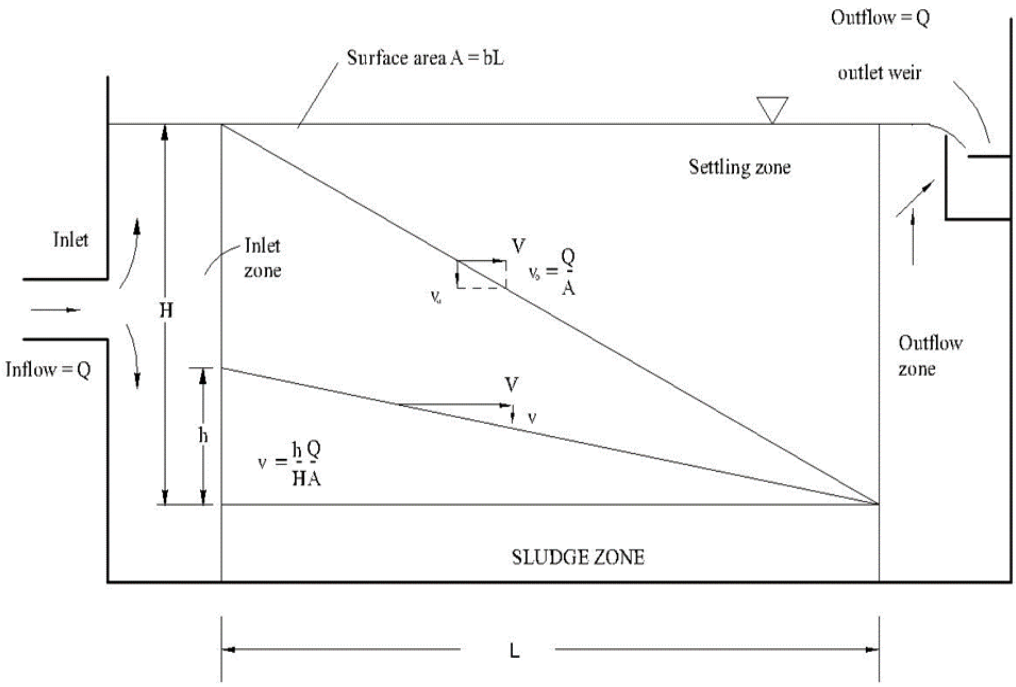

Figure 2:3: An ideal longitudinal section of settling tank illustrating the settling of discrete particles

It is apparent that aparticle will be settled at the sludge zone only if its settling velocity exceeds the water upflow velocity. In this case the the minimum upflow rate is given by the flow rate divided by the surface area of the tank given in Equation 2.14 (Islam *et al*., 2013).

$$v_0 = \frac{Q}{A} \tag{0.14}$$

Where:

Q = Flow rate (m^3/s)

A = Surface area of the tank (m^2), given as WL

v_0 = Settling velocity (m/s)

W = Tank width (m)

L = Tank length (m)

From the geometry of the tank the time required for the particle to settle, t_o is given by(Islam *et al*., 2013);

$$t_o = \frac{H}{V_p} = \frac{L}{V_h} \quad (0.15)$$

Where:

t_o = Settling time (s)

H = Depth of the tank (m)

L = Length of the tank (m)

V_h = Horizontal particle velocity (m/s)

V_p = Terminal settling velocity in the vertical direction (m/s)

Since Vh = Q/WH, then Vp = Q/WL , rearranging and noting that surface area A = WL, then the terminal settling velocity will be given by:

$$V_p = \frac{Q}{A} \quad (0.16)$$

The design of settling tanks for a given flow rate (Q), involves the selection of the surface loading rate (Q/A), from which the required tank surface area may be calculated, and either tank depth (H) or detention time (t). The task of proportioning the tank once major parameters are chosen is based on the simple design charts based on the above equations (GOK, 2005; Margarita *et al.,* 2017). The relationship in Equation 2.16 shows that settling efficiency is independent of tank depth. This condition is only true if the forward velocity is low enough to

ensure that the settled sediments is not scoured and re-suspended from the tank floor or the sludge zone.

2.4.2 Water Turbidity

Turbidity is caused by particles suspended or dissolved in water that scatters light making the water appear cloudy or murky. Particulate matter can include sediment especially clay and silt, fine organic and inorganic matter, soluble colored organic compounds, algae, and other microscopic organisms (Weixing *et al.,* 2015). The turbidity of water entering and leaving the settling basin should be tested regularly. This test is a direct measure of the efficiency of the settling process in removing suspended particles from water. Different methods are used in measuring turbidity levels. Such methods include the use of Nephelometric turbidity units (NTU), Turbidity tubes (T-tubes), Jackson turbidity units (JTU), Turbidity meter and use of Secchi disk.

Mathematical models can be used to increase the ability to predict flow rate and amount of sediment to be settled. In practice, the actual application of such models depends on the capability to perform the analysis and optimization for the relevant cases with reasonable effort (Lazarovitch *et al*., 2009).

2.5 Sediment flushing in a settling basin

A further consideration in the design of a sedimentation basin is the provision of adequate storage for settled sediment to prevent the need for frequent de-silting (Fornshell, 2000). The volume of accumulated sediment can be estimated from regular monitoring of sediment levels with a measuring post and reference against the top water level (Raju *et al*., 1999). As a rule, the recommended frequency of basin de-silting is once every five years, which is generally, triggered when sediment accumulates to half the basin depth. Flushing sediments through a reservoir has been practiced successfully to combat the storage loss for many reservoirs of the world. Worldwide average annual reservoir storage loss due to sedimentation is about 1.0 % (Yang, 2003; Rehman *et al.,* 2009; Shen, 2010).

Deposited sediments are removed from the basin by use of the flushing system or through excavation (de-silting) if the amount of sediments is small at a pre-

determine time (Isam *et al*., 2013). Flushing involves the opening of the settling basin bottom outlets and allowing the accumulated sediment to be re-suspended and flushed out. According to Pande (2015), flushing can be done without allowing the pool level in the basin to drop down significantly (partial drawdown flushing) or full drawdown flushing in which the basin level is allowed to be completely drawn down. Raju *et al*. (1999) examined the effect of flushing on the settling basin efficiency performance and proposed that the inflow channel up to the basin to be designed to carry more than the discharge requires as continuous flushing uses about 15 to 20% of the channel water.

2.5.1 Total solids

Total solids (TS) is the sum of total suspended solids (TSS) and total dissolved solids (TDS). Total solids is the material left in the evaporation dish after it has been dried for at least one hour or overnight in an oven at 103^0 C to 105^0C and is calculated according to Standard methods (APHA, 1975) as given in Equation 2.17.

$$\frac{MgTS}{L} = (A - B) \times 1000 \quad (0.17)$$

Where:

A = Weight of dried residue plus dish (mg)

B = Weight of dish (mg)

1000 = Conversion of 1000 mL/L

2.5.2 Total suspended solids

The Total suspended solids (TSS) refer to the non-filterable residue. The TSS standards for effluents are usually set between 12 mg/L and 30 mg/L (Lee, 2007). Total suspended solids (TSS) are particles that are larger than 2 microns found in the water column. Anything smaller than 2 microns (average filter size) is considered a dissolved solid. Most suspended solids are made up of inorganic materials, though bacteria and algae can also contribute to the total solids concentration (EPA, 2012).

These solids include anything drifting or floating in the water, from sediment, silt and sand to plankton and algae (Fondriest, 2014). As algae, plants and animals decay, the decomposition process allows small organic particles to break away and enter the water column as suspended solids (Murphy, 2007). Chemical precipitates are also considered as a form of suspended solids according to Langland *et al.* (2003).

TSS is calculated using Equation 2.18.

$$\frac{MgTSS}{L} = (C - D) \times 1000 \quad (0.18)$$

Where:

C = Weight of filter and crucible plus dried residue (mg)

D = Weight of filter and crucible (mg)

1000 = Conversion of 1000 mL/L

2.5.3 Settleable Solids

Settleable solids is the term applied to the material settling out of suspension within a defined time. It may include floating material (Lee, 2007). Settleable solids are an important pathway for pollutants found in river sediments. Special measurements are undertaken to determine the relationship between the settling distribution of settleable solids and their pollutant load - organic mass, chemical oxygen demand, heavy metals and organic micro-pollutants (Michelbach *et al.,* 1994).

2.6 Models commonly used in irrigation systems

Models are valuable tools that are used in the design and operation of fluid dynamics systems. Some models are used in optimizing and testing of control strategies especially in irrigation systems (Pedras *et al.,* 2009). Model results can be evaluated for different operating data before transferring the concepts to a full-scale plant. Moreover, choosing the most appropriate model helps to recognize

possible technical faults and to reduce operating costs of plants in the planning stage.

Agricultural system models play increasingly important role in the development of sustainable water and land management across diverse agro-ecological and socioeconomic conditions. This is because field and farm experiments require large amount of resources and may still not provide sufficient information in space and time to identify appropriate and effective management practices (Jones *et al.,* 2016). Models can help to identify management options for maximizing sustainability goals to water, land managers and policy makers across space and time as long as the needed information is available (Antle *et al.,* 2017).

To study improvements in the operation and management of irrigation and other water structures, various hydraulic models have been developed. Some of the commonly used models in irrigation are; SIC, CANALMAN, MIKE11, SOBEK, HECRAS, DUFLOW, SWAT, HSPF, SWRRB and ANN.

2.6.1 Simulation of irrigation canals (SIC)

The SIC software is one of the earliest hydraulic models developed by Cemagref in France in 1970s. SIC model has been used as a decision support tool by canal managers, especially in the daily operation and maintenance of the irrigation canal systems. The very first version of this model was developed for the International Irrigation Management Institute on a real canal located in the south coast of Sri Lanka (Kirindi Oya Right Bank Main Canal) (Dinshaw and Wytze, 1993). This model is only applicable with canals where the complete Saint Venant equations are solved using the classical implicit Preissmann scheme which was not the case in this study.

2.6.2 Canal management model (CANALMAN)

The Canal Management Software (CANALMAN) was developed for performing hydraulic simulations of un-steady flow in branching canal networks. The CANALMAN model was developed by Utah State University, Logan, Utah, USA (Merkley, 1995). This model is based on partial differential equations (the Saint-Venant equations for one-dimensional flow) that allow the flow rate and water

level to be computed as functions of space and time. The model has been used in Shingrai Minor of Upper Swat Canal irrigation system in NWFP Pakistan (Abdul *et al*., 2004). This model was not suitable in this study because it only computes the flow rate and water level simultaneously, and that the model more closely approximates the actual unsteady non-uniform nature of flow propagation in a canal within a network. While in this study the ideal model is one that can predict on the uncertainties of water turbidities. Secondly this study is considering water in a confined area of a settling basin and not in the distribution lines.

2.6.3 Hydrologic engineering center's river analysis system (HEC-RAS)

The Hydrologic Engineering Center's River Analysis System (HEC-RAS) was developed by U.S Army Corps of Engineers (2001) to study flow depths and total energy loss along a study reach of a river system. According to Imbenzi *et al.* (2014), HEC-RAS is a 1-D model that performs calculations for a steady or unsteady flow in gradually varied or rapidly varied flow analysis through computation of energy equation balance. This model is used to calculate water-surface profiles and energy grade lines in 1-D, steady state and gradually varied flow analysis. This study was not dealing with flow analysis but rather the analysis of falling rate of particles and therefore this model was not ideal for this study.

2.6.4 MIKE 11

The Danish Hydraulic Institute (DHI) developed the MIKE 11 model in 1995. It is a one-dimensional unsteady flow hydraulic model used for the simulation of flow in rivers. The MIKE 11 is a modeling package for the simulation of surface runoff, flow, sediment transport, and water quality in rivers, channels, estuaries and floodplains. The model uses a

1-D implicit, dynamic wave routing based on the St.Venant equations for unsteady flow (Malaterre and Baume, 1997). This model has been applied in many study sites, for instance, it was applied in the Euphrates River in Iraq; the stream length used for this model was 1.6 km (Ammar, 2008). The only limitation to this model is that it was designed to perform detailed modeling of rivers,

including special treatment of floodplains, road overtopping, culverts, gate openings and weirs and this is beyond the scope of this research.

2.6.5 Hydrological simulation program-FORTRAN (HSPF)

Johanson *et al.* (1984) developed the Hydrological Simulation Program-FORTRAN (HSPF) model to simulate both basin hydrology and water quality. A continuous time model, HSPF allows simulation of contaminant runoff with instream water quality and sediment interactions. The instream component includes not only nutrient process such as nitrogen and phosphorous movement, but also benthic algae, phytoplankton and zooplankton (Saenyi, 2002). Extensive revisions and modifications on HSPF codes have been performed. HSPF simulates three sediment types (Sand, silt and clay) in addition to a single organic chemical and transformation products of that chemical. Re-suspension of silts and clay (cohesive solids) are defined in terms of shear stress at the sediment-water interface (Bicknell *et al.,* 1996). For, sands the capacity of the system to transport sand at a particular flow is calculated and settling is defined by the difference between sand in suspension and the capacity. Calibration of the HSPF model requires data for each of the three solid types. According to Patil *et al.* (2016), the drawback to HSPF is the data intensive nature of the input parameters making the calibration/verification of such a model to be complicated and tedious.

2.6.6 The simulator for water resources in rural basins (SWRRB)

The Simulator for Water Resources in Rural Basins (SWRRB) was developed for simulating hydrologic and related processes in rural basins. The objective in model development was to predict the effect of management decisions on water and sediment yields with reasonable accuracy for un-gaged rural basins (Williams *et al*., 1985; Arnold *et al.,* 1990). The SWRRB model was developed by modifying the Chemicals, Runoff, and Erosion from Agricultural Management Systems (CREAMS) which is a daily rainfall hydrology model for application to large, complex, rural basins. According to Williams *et al.* (1985), besides water, SWRRB also simulates sediment yield using the Modified Universal Soil Loss Equation (MUSLE) and a sediment routing model. The use of MUSLE equation is

a limitation to this present study since the study was not focusing on the quantity of sediment being loaded into the settling basin.

2.6.7 Artificial neural networks model (ANN)

Artificial Neural Networks (ANNs) are a form of computing that attempt to simulate the operation of human brain and nervous system (Chia-Ling & Chung-Sheng., 2012). Although the concept of artificial neurons was first introduced in 1943 (McCulloh & Pitts, 1943), research into applications of ANNs has blossomed since the introduction of the back-propagation training algorithm for feed-forward ANNs (Rumelhart *et al.*, 1986; McCelland & Rumelhart, 1988).

The intention of this study is to apply an alternative approach to sediment settling prediction in sedimentation basin. This is by predicting the turbidity of water in a given lead time based on given historical data. Since ANN has been successfully applied in water resources hence considered for this research. ANN has been used cause of its ability to model the non-linear relationship between a set of input variables and the corresponding outputs without need for predefined mathematical equations.

2.7 The neural networks

2.7.1 Natural neural networks

One efficient way of solving complex problems is following the lemma “divide and conquer”. A complex system may be decomposed into simpler elements, in order to understand it. Also simple elements may be gathered to produce a complex system (Raghuwanshi *et al*., 2006; Maier *et al.,* 2010) and to achieve this, networks approach is used. There are a large number of different types of networks, but they are all characterized by a set of nodes and connections between nodes. The nodes can be seen as computational units. They receive inputs, and process them to obtain an output. This processing might be very simple such as summing the inputs, or quite complex where by a node might contain another network.

Many authors for instance Hertz *et al.,* (1991) and (Zurada, 1992; Masters, 1993) have described the structure and operation of Natural Neural Networks (NNNs).

The NNNs of which the brain is an example, consist of billions of densely interconnected nerve cells called Neurons. Each neuron receives the combined output signals (information) of many other neurons through synaptic gaps by input transmission paths called dendrites (Patil *et al.,* 2016). The transmitted signals are electrochemical, which means that they are electronic impulses that are transmitted across the synaptic gaps to the dendrites by means of chemical process (Rahim and Amina, 2015). Consequently, the connection between neurons is chemical and the strength of this connection is modified by the action of the chemical transmitters and as the brain learns.

The dendrites collect the incoming signals and send them to the cell body, or the soma, of the neuron. The soma sums the incoming signals and, if the charge of these signals is strong enough, the neuron is activated and produces an output signal (Ansari and Athar, 2013). Otherwise, the neuron remains inactive. The output signal is then transmitted to the neighboring neurons through an output structure called axon. The axon of a neuron divides and connects to dendrites of the neighboring neurons through junctions called synapses. The way neural networks receive, process and transmit the electrochemical signals, as well as the action of the chemical transmitters, comprise the basic memory mechanism and communication system of the human brain. (Rietjes *et al.,* 2008). This is summarized in Figure 2.4 which was modified from Fausett (1994).

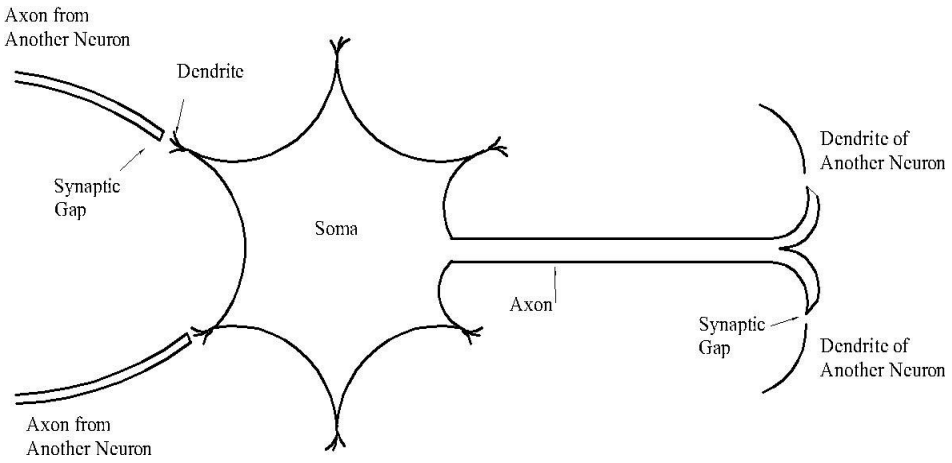

Source: Fausett, 1994

Figure 2:4: Typical structure of biological neuron

2.7.2 Artificial neural networks

Artificial neural networks (ANNs) are a computational tool, based on the properties of biological neural systems (Maitha *et al.,* 2011; Wambua *et al*., 2016). Neural networks excel in a number of problem areas where conventional computer systems have traditionally been slow and inefficient (Nourani *et al.,* 2009). The matrix laboratory (MATLAB) is an ideal tool for working with Artificial Neural Networks for a number of reasons. First, MATLAB is highly efficient in performing vector and matrix calculations. Secondly, MATLAB comes with a specialized Neural Network Tool box, which contains a number of useful tools for working with artificial neural networks. Thirdly, MATLAB allows easy matrix manipulation, plotting of functions and data, implementation of algorithms, creation of user interfaces and interfacing with programs in other languages according to Akif and Amina (2015). It also allows quick and easy coding in a very high-level language and it further allows the users to develop their own functions and specialized programs as compared to other models (William, 1998). As such, ANN model in MATLAB was used in this study.

Over the past two decades Artificial neural network (ANN) models have been widely used for prediction and forecast in various areas including finance, medicine, power generation, water resources and environmental sciences (Anzy *et al.,* 2016). Some examples include; drought forecasting using ANN for upper Tana River Basin in Kenya. Prediction of missing hydro-meteorological data series using ANN. Use of ANN to predict suspended sediment concentration with hydrology and hydrodynamics, use of ANN as a prediction model for water quality index in Juru River-Malaysia and many other applications (Chutachindakate *et al.,* 2007; Mohd *et al.,* 2011; Wambua *et al.,* 2016). This is due to their ability to give input-output relationship without any understanding of the physical process (Kumar *et al*., 2010 ; Ramapulana, 2011). It is a highly nonlinear tool that can capture complex interactions among the input and output variables without any prior knowledge about nature of these interactions (Kisi & Murat, 2011; Khalil *et al.,* 2012). In recent years, the Artificial Neural Network technique has shown excellent performance in regression, especially when used for pattern recognition and function estimation (ASCE, 2000).

The structure of ANN consists of an input layer, one or more hidden layers and an output layer. The input from each processing element (PE) in the previous layer is multiplied by connection weight. These connection weights are adjustable and may be likened to the coefficients in statistical models. At each PE, the weighted input signals are summed and a bias or threshold value is added or subtracted (Maier & Dandy, 2000). This combined input is then passed through a non-linear transfer function (logistic sigmoid or hyperbolic tangent transfer functions) to produce the output of the PE (Wambua *et al*., 2014a). The output of one PE provides the input to the PEs in the next layer as summarized and presented under Equations 2.19 and 2.20 and illustrated in Figure 2.5 developed by (Maier & Dandy, 2000).

If node *j*, is in the output layer, δ_j can be calculated by applying the *delta rule*, as follows:

$$\delta_j = (y_j - d_j) f'(I_j) \quad \text{.....(0.19)}$$

Where:

$f'(I_j)$ = the derivative of the activation function f with respect to the weighted sum of inputs of node *j*.

If node j is in the hidden layer, the generalized delta rule, can be used as illustrated in Equation 2.20 and Figure 2.5.

$$\delta_j = [\sum_{1}^{m} \delta_m w_{mj}] f'(I_j) \quad \text{.....(0.20)}$$

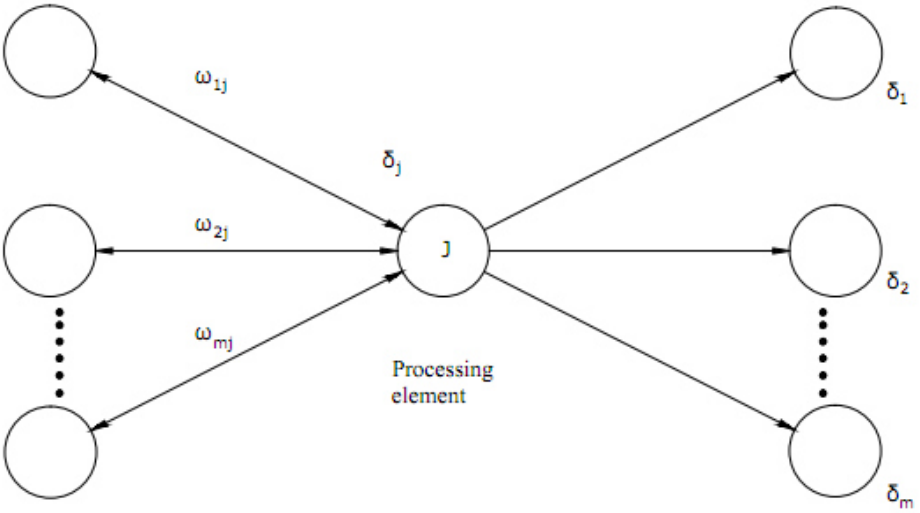

Figure 2:5: Node *j* in a hidden layer Source: Maier & Dandy, 2000

The back propagation training algorithm uses a gradient descent technique to adjust the weights. This process involves changing the weights from their initial random state by an amount proportional to the partial derivative of the error function, *E*, with respect to the given weight. According to Rumelhart *et al*.

(1986), the error function, for node *j*, can be calculated using the following Equation 2.21.

$$E = \frac{1}{2}\sum (y_j - d_j)^2 \quad \text{.....(0.21)}$$

Where:

E = the global error function,

y_j = the predicted output by the network and

d_j = the desired (historical or measured) actual output.

The global error function, *E*, is minimized by modifying the weights using the gradient descent rule and presented in Equation 2.22 as follows:

$$\Delta w_{ji} = -\eta \frac{\partial E}{\partial w_{ji}} \quad \text{.....(0.22)}$$

Where:

Δw_{ji} = weight increment from *i* to node *j*,

η = learning rate, by which the size of the step taken along the error surface is determined.

Equation 2.22 can be further defined by the *delta rule* as follows:

$$\Delta w_{ji} = \eta \delta_j x_i \quad \text{.....(0.23)}$$

Where:

x_i = input from node I, i = 0, 1,……., n

δ_j = error value between the predicted and desired output for node *j*.

The weights were then updated by adding the delta weight, Δw_{ji} to the corresponding previous weights as follows:

$$w_{ji}(n+1) = w_{ji}(n) + \Delta w_{ji} \quad \text{.....(0.24)}$$

Where:

w_{ji} (n) = the value of a weight from node *i* to node *j* at step n (before adjustment),

w_{ji} (n+1) = the value of the weight at step (n+1) (After adjustment).

The global error between the output predicted by the network and the actual desired output are calculated using an error function. According to Masters (1993), the mean squared error (MSE) function is usually preferable for the following reasons:

a) The subsequent derivatives of this function are simple.

b) It gives more attention to large errors and,

c) It lies close to the heart of the normal distribution in which, if the errors can be assumed to be normally distributed, minimizing the MSE is optimal. Hence it will be used to draw the conclusion on the use of ANN model.

2.7.3 Application of ANN in modeling irrigation and water related systems

ANN is capable to model any arbitrary complex non-linear process that relates sediment load to continuous water discharge (Lohani and Krishan, 2015). It is a very practical and promising modeling tool in the context of sediment load prediction. The output of ANN can potentially be used in solving environmental problems including water resources modeling and management problems (Yun-Mei zhu, 2007; Nikolos *et al.,* 2008; Najah et al., 2011).

The basic strategy for developing an Artificial Neural Network based model of system behavior is to train the network on examples of the system (Garcia and Shigidi, 2006). If the example contains the relevant information about the system behavior, then the trained neural network would contain sufficient information about the system behavior to qualify as a system model (Ghumman *et al.,* 2011). Such a trained neural network is not only able to reproduce the results of examples it was trained on, but also through its generalization capability, it is able to approximate the results of other examples.

ANNs may thus be considered a relatively new tool in the field of prediction and forecasting. Recently, ANNs have been applied successfully to a wide range of areas including classification, estimation, prediction and functions synthesis (Yaseen *et al.,* 2015). Moreover, ANNs have also been used successfully in predicting business failure, speech production and recognition, pattern recognition, medical diagnosis and treatment, control problems (Lin, 2005) and many fields of engineering, including geotechnical engineering (Daliakopoulos *et al.,* 2005; Garcia *et al.,* 2006; Lee *et al.,* 2017). In water and environmental science, numerous works have applied ANN for modeling the rainfall-runoff processes, sediment loading and for predicting environmental responses such as typhoon storm, stream flow, tide, flood and water quality (Palani *et al*., 2008;Archana, 2008; Lee, 2009; Juan *et al.,* 2017).

To establish an integrated stage discharge sediment concentration relation, Ghorbani *et al*. (2016) used the ANN approach. The authors have shown that the ANN results were much closer to the observed values than the conventional technique. Further, Archana *et al.* (2015) applied ANN to model the sediment discharge relationship of alluvial river. Khan *et al*. (2016) presented an ANN model to predict the discharge and water level for Ramganga River catchment of Ganga basin in India. Gagliardi *et al*. (2017) applied ANN models to forecast short-term water demands up to 24 hours ahead based on the representation of the periodical patterns that typically characterized water demands, such as seasonal and weekly patterns of daily water demands. ANN models were developed to predict both runoff and sediment yield on a daily and weekly basis for Upper Siwane River watershed in India (Raghuwanshi *et al.,* 2006). ANN were applied to predict the monthly, weekly and daily suspended sediment in a catchment by relating it to average rainfall, temperature, rainfall intensity and water discharge (Yun-Mei *et al.,* 2007). Rai and Mathur (2008) developed a feed forward back propagation ANN for computation of event based temporal variation of sediment yield from the watersheds.

ANNs learning/training is ‘by example’ in which an actual measured set of output variables and the corresponding outputs is presented to determine the rules that

govern the relationship between the variables (Mohd *et al.,* 2011). Consequently, ANNs are well suited to model complex problems where the relationship between the variables is unknown and where non-linearity is suspected (Ghamari *et al.,* 2010; Maier *et al*., 2010).

Since ANN has an ability to learn from examples without the need of explicit physics, it can be applied in different science and management fields (Chia-Ling and Chung-sheng, 2012). In this research, a neural network's methodology is applied in sediment settlement to produce a quantitative estimation of particle settlement in different water flow rates. Multi-layer feed-forward networks were chosen to estimate the turbidity levels of different flow rates. The feasibility of using feed-forward networks for this application was studied based on the following observations (Ghamari *et al.,* 2010)

1. ANNs are very effective in relating quantities for which a physical or empirical model is not fully described.
2. The given data set requires a supervised learning model.
3. Multilayer feed-forward neural networks are the most suitable networks for generating non-linear relationships for a given problem.

The connections determine the information flow between nodes. They can be unidirectional, when the information flows only in one sense, and bidirectional, when the information flows in either sense. The interactions of nodes through the connections lead to a global behavior of the network, which cannot be observed in the elements of the network. This global behavior is said to be emergent (Mubiru *et al*., 2008). This means that the abilities of the network through nodes connections supersede the ones of its elements, making networks a very powerful tool. Networks are used to model a wide range of phenomena in physics, computer science, biochemistry, ethology, mathematics, sociology, economics, telecommunications, and many other areas (Toth *et al.,* 2000; Mohamed, 2003; Daliakopoulos *et al.,* 2005; Garcia *et al.,* 2006; Kumar *et al.,* 2011).

2.7.4 Structure and operation of artificial neural networks

Artificial neural networks (ANNs) attempt to mimic some of the behavior of the basic biological and chemical processes of NNNs. Many authors have described the structure and operation of ANNs (Hecht-Nielsen 1990; Maren *et al*., 1990; Zurada 1992; Ripley, 1996). ANNs consist of a number of artificial neurons variously known as 'processing elements' (PEs) nodes. These nodes or units represent the neurons in NNNs. Processing elements in ANNs are usually arranged in layers namely input layer, an output layer and one or more intermediate layers also referred to as hidden layers (Sengorur *et al.,* 2015), A modified schematic diagram after Maier and Dandy (2000) is presented in Figure 2.6.

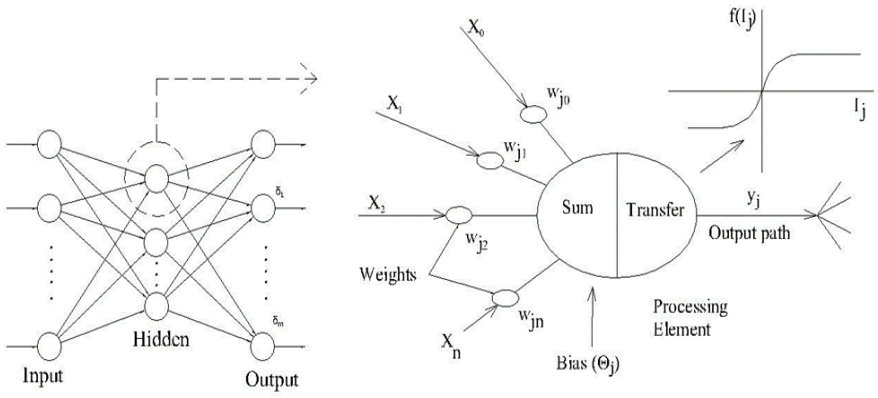

Figure 2:6: Typical structure and operation of ANNS Source: Maier and Dandy, 2000

Each processing element in a specific layer is fully or partially, connected to many other processing elements via weighted connections. The weight in each connection represents the synaptic strength in NNNs (Holger & Graeme, 1996). The scalar weights determine the strength of the connections between interconnected neurons. A zero weight refers to no connection between two neurons and a negative weight refers to a prohibitive relationship. From many other processing elements, an individual processing element receives its weighted inputs, which are summed and bias unit or threshold is added or subtracted (Rumelhart *et al.,* 1986; Ranjithan *et al.,* 1993). The bias unit is used to scale the

input to a useful range to improve the convergence properties of the neural network (Maren *et al.,* 1990). The result of this combined summation is passed through a transfer function to produce the output of the processing element (Engelbrecht, 2007). For node *j*, this process is summarized in Equations 2.25 and 2.26.

$$I_j = \sum_{i=1}^{n} w_{ji} x_i + \theta_j$$

(0.25)

Summation

$$y_j = f(I_j) \quad \text{...(0.26)}$$

Where:

I_j = the activation level of node *j;*

w_{ji} = the connection weight between nodes I and j;

Xi = the input from node i, i=0, 1... n;

$Ø_j$ = the threshold for node *j*;

y_j = the output of node j;

$f(I_j)$ = the transfer function

The propagation of information in ANNs starts at the input layer where the input data are presented (Vahid *et al.*, 2009). The inputs are weighted and received by each node in the next layer. The weighted inputs are then summed and passed through a transfer function to produce the nodal output, which is weighted and passed to processing elements in the next layer (Rumelhart *et al.*, 1986). The network adjusts its weights on presentation of set of training data and uses a learning rule until it can find a set of weights that will produce the input-output mapping that has the smallest possible error. This process is known as ‘learning’ or ‘training’ (Maanen *et al.*, 2010).

2.7.5 Classification of artificial neural networks

ANNs can be categorized on the basis of two major processes:

i) The learning rule used and

ii) The connections between processing elements.

Based on learning rules, ANNs as mentioned earlier, can be divided into supervised and unsupervised networks. (Wambua *et al*., 2014b) Two examples of supervised networks are multi-layer perceptron and neuro-fuzzy networks (Masters, 1993). Based on connections between processing elements, ANNs can be divided into feed-forward and feedback networks. In feed-forward networks, the connections between processing elements are in the forward direction only (Figure 2.7a). In feedback networks, connections between processing elements are in both the forward and backward directions (Figure 2.7b).

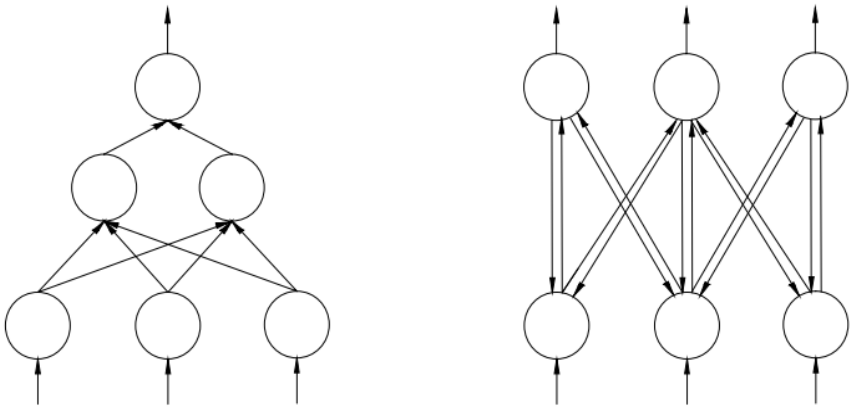

(a) Feed-Forward network (b) Feed-back network

Source: Masters, 1993

Figure 2:7: **Connections between PEs for different neural network types**

2.7.6 Transfer functions

Transfer functions can take a variety of forms. The logistic sigmoid and hyperbolic tangent transfer functions are the most common functions in neural networks (Csabragi *et al.,* 2015). The logistic sigmoid function is usually used

when the desired range of output values is between 0 and 1, whereas the hyperbolic tangent function is often used when the desired range of output values is between -1 and 1 (Ramapulana, 2011; Xueying *et al.,* 2016). The logistic sigmoid and hyperbolic functions are shown in Figures 2.8, 2.9 and Equations 2.26, and 2.27 respectively (Maanen *et al.,* 2010; Wambua *et al.,* 2014a). Usually, the same transfer function is used for all processing elements in a particular layer.

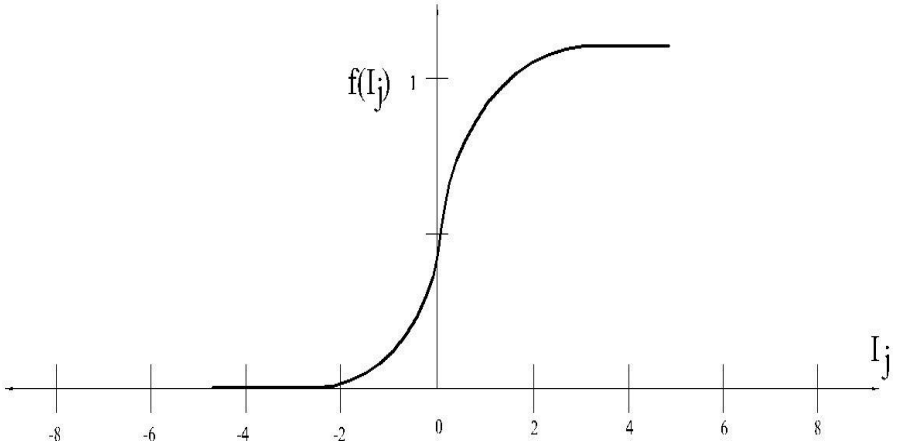

Figure 2:8: The logistic sigmoid function

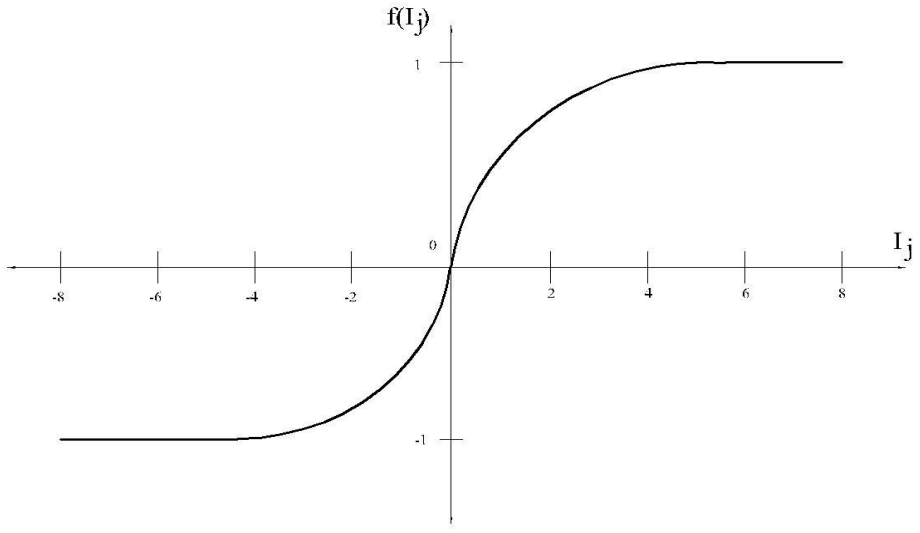

Source: Ramapulana, 2011

Figure 2:9: The hyperbolic sigmoid function

$$f(I_j) = \frac{1}{1 + e^{-(I_j)}} \quad \text{..... (0.27)}$$

$$f(I_j) = \frac{e^{(I_j)} - e^{-(I_j)}}{e^{(I_j)} + e^{-(I_j)}} \quad \text{.....}$$

(0.28)

2.7.7 Neural network topology

The number of layers, number of nodes (or neuron units) determine neural network architecture in each layer and the weighted connections between nodes. The nodes and their connections define the topology of a neural network (Ramapulana, 2011). The number of layers includes the input layer, hidden layers and the output layer. Thus, a three layer network will have one hidden layer (in addition to the input and output layers).

The determination of the network architecture is one of the most important steps in developing a model for a given problem. Although neural network construction has been extensively, researched (German *et al.,* 1992) there is no known procedure or algorithm for this process for the general case. Two approaches have been proposed, namely constructive and destructive methods. In both constructive and destructive methods, the numbers of hidden nodes are considered (Kwok & Young, 1995).

Constructive methods start with a small number of network units, which is usually under-parameterized, and then proceed to increase the number of units during training until the performance of the network reaches a satisfactory level. Some of the most popular methods are the Cascade Correlation Algorithm (Fahlman & Lebiere, 1990) and the Upstart Algorithm (Frean, 1991). Destructive neural network methods, also called pruning methods, determine a suitable neural network structure by starting with a large number of units and then progressively removing some of these units during training until some or other performance criterion are met.

A constructive approach was adopted in this research, since this approach is more suitable to the problem of time series prediction and was shown to be more successful in general (Saharia & Bhattacharjya, 2012). The most used neural network for prediction and forecasting applications is the feed-forward networks, whereby nodes in one layer are connected to nodes in the next layer. Feed-forward networks are the most commonly used network architecture, but both feed-forward and recurrent networks are used for time series prediction. Unlike feed-forward networks, recurrent networks have the ability to "remember" past events and they are generally regarded to be more effective for time series prediction problems. However, feed-forward architectures (Figure 2.10) also perform well under certain circumstances (Lallahem & Hani, 2017).

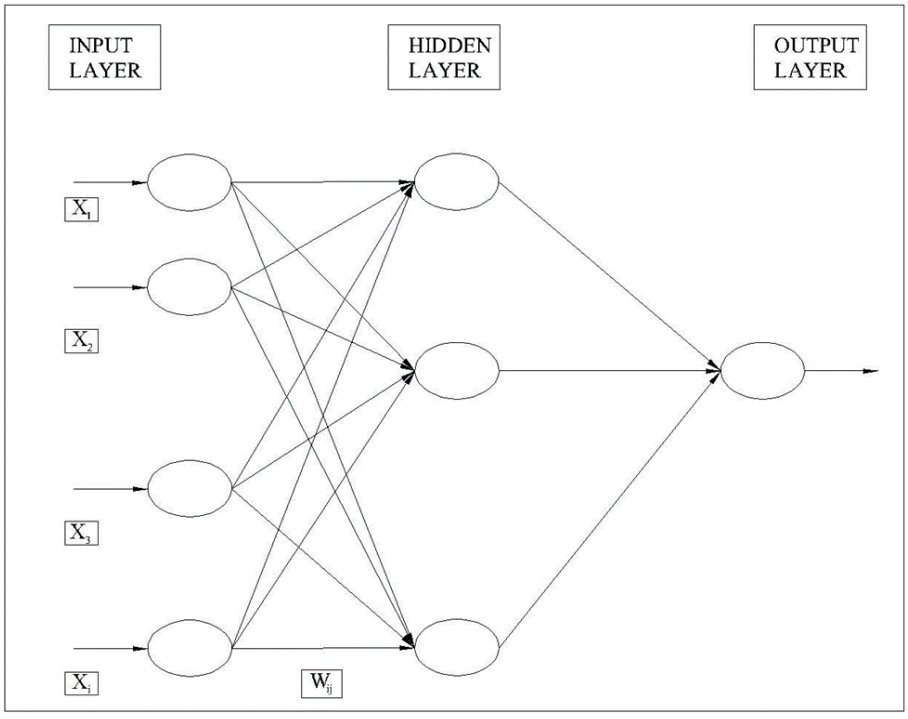

Figure 2:10: Feed Forward neural network Source: Lallahem & Hani, 2017

Recurrent networks have the ability to cater for moving average components whereas feed-forward networks cannot. However, feed-forward networks have been used almost exclusively for the prediction and forecasting of water resources

variables, as such they process data faster than the other models that are currently in use in this field (Rientjes & De Vos, 2008). While recurrent networks have potential advantages for time series applications they do not provide specific benefits over feed-forward networks for data limited by a number of time steps. For such time windows, feed-forward networks have been found to perform well in comparison with recurrent networks in many practical applications (Bouzeria *et al.,* 2017). Both feed-forward and recurrent network architectures are used with different numbers of hidden nodes for prediction experiments as shown in Figure 2.11.

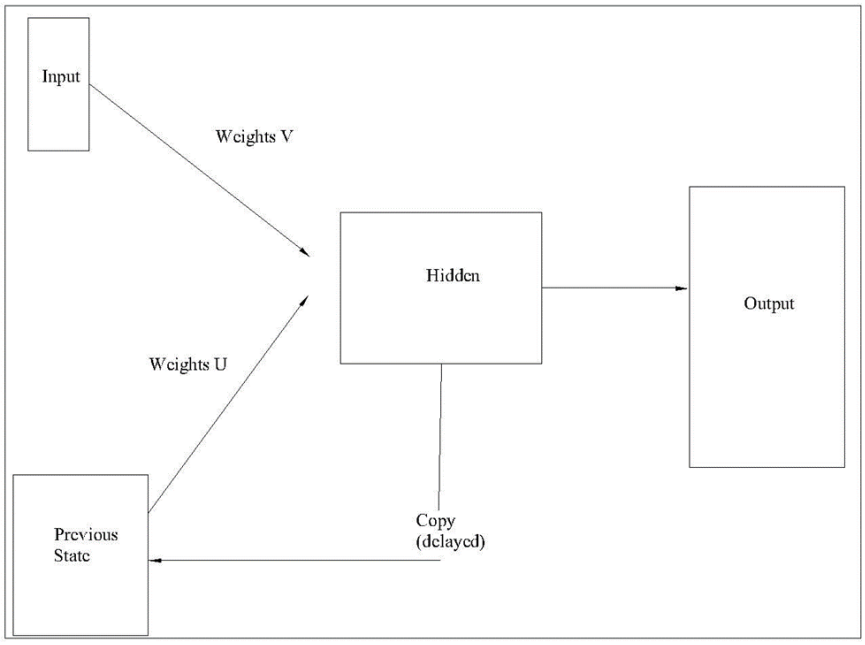

Source: Lallahem & Hani, 2017

Figure 2:11: A Simple recurrent network

The neural network topology can be determined in two ways, namely by fixing the number of hidden nodes and by selecting the number of connection weights to each node. The relative properties of smaller and larger networks must also be considered when selecting the network. Smaller networks requires less storage and have higher processing speed during training and testing; however the error graph can be more complicated and such networks sometimes contains more local minima (Hutchins, 1995). Larger networks tend to learn quickly in terms of the

number of training cycles required and have an increased ability to avoid local minima in the error surface. However, they require a large number of training samples in order to achieve better generalization ability (Zurada, 1992).

2.7.8 Neural network time series modeling

Time series modeling has been extensively researched, and the use of neural networks is an established technique (Nagy *et al*., 1997). Typical examples of neural network applications are market predictions, meteorological and network traffic forecasting (Chan *et al*., 1993; Collobert *et al*., 1995, Dorffner, 1996; Davey *et al*., 1997).

A time series T is a sequence of vectors, tuples or patterns, x (t), t = 0, 1. . .

Where:

t = the elapsed time instant.

That is;

T = {x(t0), x(t1), . . . , x(ti), . . .} (Davey *et al*., 1997)
……(0.29)

The sequence *x(t)* may be scalar values or structured objects such as vectors or images. Since turbidity is a scalar value, we consider here only sequences of scalars, although these concepts can easily be transferred to series of structures. The value *x* can vary continuously with *t*, such as turbidity, but in practice it is sampled as a series of discrete data values usually at equal time intervals (Chandra & Zhang, 2012; Faruk, 2010). In our case, turbidity values are sampled per experiment at the same time with different flow rates. The sampling rate determines the temporal resolution of the time series. However, it is not always the case that the highest resolution will produce the best predictive performance; it may be the case that every *n*-th point in the series produces an improved prediction model.

The forecasting problem can be stated as developing a model *f* that can be used to estimate a future value from a set of values up to the present time. Formally, this can be stated as finding the function *f* such that *f*: R*N* → R that is used to obtain

an estimate of x at time $t + d$ by using the historical values of x for N time steps preceding the time step t.

2.8 Programming the neural network model

MATLAB is a numerical computing environment and a programming language. It allows easy matrix manipulation, plotting of functions and data, implementation of algorithms, creating user interfaces and interfacing with programs in other languages. The Neural Network Toolbox contains the MATLAB tools for designing, implementing, visualizing and simulating neural networks. It also provides comprehensive support for many proven network paradigms, as well as graphical user interfaces (GUIs) that enable the user to design and manage neural networks in a very simple way.

In this study MATLAB (R2015a) was used for developing MLP and RBF ANN models and performance functions for calculating the model performance error statistics such as R, RMSE and MBE.

2.8.1 Calibration and validation of ANN model

Model calibration is an iterative procedure of parameter evaluation and refinement, because of comparing simulated and observed values of interest. The ultimate goal of calibrating the ANN model was to incorporate spatial processes into the calibration techniques (Wambua *et al.,* 2016). However, the models are only tools to aid in the decision process and are never a substitute for user understanding of the processes occurring in the settling basin, to guide calibration (Moriasi *et al.,* 2007). First is to study the settling basin thoroughly, understand the processes involved, identify the specific project needs and scenarios to be analyzed, parameterize ANN for the SB, then compare the model prediction with observed data, and then develop and implement a calibration plan.

Model validation is in reality an extension of the calibration process, the purpose of which is to ensure that, the calibrated model properly assesses all the variables and conditions. This can affect model results, and demonstrate the ability to predict field observations for periods separate from the calibration effort (Mustafa *et al*., 2011). The available data for ANN was divided into three sub phases;

training phase, validation phase and testing phase (Mohd *et al.*, 2011; Cigizoglu, 2004). The rule of thumb is to optimize the geometry or input parameters by trial and error (Maier *et al.,* 2000). The size of input and hidden neurons of network are varied depending on the prediction horizon whereas the output has single node (Daliakopoulos *et al.,* 2005).

2.8.2 Data set generation

Split-sample training is a common ANN training method. The basic idea behind this approach is to withhold a small subset of the data for validation, and to train the network on the remaining data (Moselhi *et al.,* 1992; Chung & Lee, 2009). However, it might be difficult to construct a representative validation set when a limited amount of data is available. The authors indicated that the holdout method is the only method, which maximizes utilization of available data. A small percentage of the training data set, is set aside in order to determine whether there is improvement in generalization thus avoiding over-training.

This subset of the data is used as a testing set in a trial phase to determine how long training should continue in order to achieve acceptable generalization ability. The testing subset can then be added to the initial training data set and the whole data set can ultimately be used to train the network for a fixed number of epochs, based on the results from the trial phase (Yitian & Gu, 2003; Cigizoglu *et al.,* 2006).

The generalization ability of a neural net refers to the ability of this net to correctly provide responses, for instances that the network has not been trained on previously unseen, extrapolated or interpolated data inputs (German *et al,* 1992). Generalization ability is affected by the number of times a given data pair, is used to train the network and the number of parameters in the neural network (the latter, indicated by the number of trainable weights in the neural network).

If the same instance or set of instances are not representative of the entire function space and they are repeatedly presented to a neural network, then the network might fit that particular sample set too closely, and could be unable to extrapolate beyond the range of the data used for training (Rietjes *et al.,* 2008). Such a

network is said to be over-trained. Conversely, if a neural network is not sufficiently trained on a representative sample set, the trained network might fit the training data too loosely. Such a neural network is said to be under-trained.

The cross validation technique is also frequently used in ANN training. However, this method substantially compromises the amount of data available for training. In this method, the complete data set is split into two sub-sets, namely a training set and an independent validation set (Maanen *et al*, 2010).

2.8.3 Learning (Training) of ANN

Learning or training is the process of adjusting the weights in accordance with a learning rule and on the presentation of the training data. Learning in ANNs is usually divided into supervised and unsupervised learning (Gaya *et al.,* 2017). In supervised learning, the network is presented with a historical set of model inputs and the corresponding (desired) outputs. The actual output of the network is compared with the desired output and an error is calculated. This error is used to adjust the connection weights between the model inputs and outputs to reduce the error between the historical outputs and those predicted by the ANN. The number of training samples presented between weight updates is called an epoch (Sietsma & Dow, 1991; Yun-Mei Zhu *et al.,* 2007). The network may choose to be updated after each training record is presented; the entire set of training data is presented or a certain number of training samples is presented.

In unsupervised learning, the network is only presented with the input stimuli and there are no desired outputs. The network itself adjusts the connection weights according to the input values (Lee & Jeng, 2002). The idea of training in unsupervised networks is to cluster the input records into classes of similar features. Unsupervised learning is similar to the way learning takes place in the NNNs of the human brain (Rajurkar *et al.,* 2010).

Learning in the context of neural networks is defined as a process by which the free parameters of a neural network are adapted through a process of presenting signals from the environment in which the network is embedded. The type of learning is determined by the manner in which the parameter changes take place

(Palani *et al.,* 2008). The notion of learning in a neural network is the process of guiding the network to provide a particular output or response for a specific given input.

The objective of the learning process is to minimize the errors between the predicted and actual outputs (Hammerstrom, 1993; Faraway & Chatfield, 1998). This minimization process can be achieved by the error function with respect to all variables in the neural network (connection weights, network architecture, learning rate and threshold). For simplicity and since the connection weights are the most influential variable, Emamgholizadeh *et al*. (2014) proposed the back-propagation algorithm in which the error function is used in a backward manner to adjust the weights.

A neural network learns about its environment or a dynamic system through an iterative process of adjustments applied to its weights and biases (Jain *et al.,* 2001; Khairi *et al.,* 2015). The environment is characterized by a set of exemplars, which is typically a group of patterns of "environmental" variables. The network becomes more "knowledgeable" about its environment after each iteration of the learning process. Like learning in human beings and animals, neural network learning is an inferred process, which cannot be perceived directly, but can be assumed to have happened by observing changes in performance (Lin & Namin, 2005).

2.8.4 The Learning rate

The learning rate is a constant used in error back-propagation learning that affects the speed of learning. The smaller the learning rate, the more steps it takes to get to the stopping criterion. (Weiss & Kulikowski 1991). The learning rate is usually determined prior to training and while it can remain fixed during training, more sophisticated training algorithms can vary this value as training proceeds. The learning rate should ideally be decreased as training progresses, since the network weights tend to approximate the desired function more closely as training continues.

The weights between the hidden layer and the output layer are adjusted first, followed by the weights between the hidden layer and the input layer (Hutchins, 1995). This process is repeated which propagates the error term needed for weight adjustment until the network can obtain a set of weights, which have the input/output mapping that has the minimum error (Najah *et al.,* 2011). Once the desired learning is achieved, the weights are fixed and the neural network can be deployed and used in practice.

The back-propagation algorithm is sensitive to the initial conditions in that, the initial values of the weights, as a result of its gradient descent nature. For example, training may start with a set of initial weights that are positioned in a flat region of the error surface from which convergence becomes very slow (Sharma *et al.,* 2015). Moreover, training may start from an unfavorable position in weight space from which the network may get stuck in a local minimum and cannot escape (Maier *et al.,* 2010).

The choice of learning rate is critical and the optimum learning rate is usually determined by trial and error. If the learning rate is selected to be small, convergence will be achieved, however, it will be very slow. In addition, convergence will be subject to the local minimum in the error surface that is closest to the random starting position. On the other hand, if the learning rate is selected to be large, convergence will never occur. Wang et *al*. (2015; Sharma *et al.,* 2015) described a process to solve the above problem without leading to oscillation. This process is simply to add a momentum term (μ) to the weight adjustment that is proportional to the amount of the previous weight change. Once an adjustment is carried out, it is saved and used to modify all subsequent weight adjustments. According to Vicente *et al.* (2012) the weight change of the current step should carry some momentum of the weight change from the previous step. Therefore, the modified adjustment equations are given as (Vicente *et al.* 2012):

$$\Delta w_{ji}(n+1) = -\eta \frac{\partial \mathrm{E}}{\partial w_{ji}} + \mu \Delta w_{ji}(n) \quad \text{.....(0.30)}$$

and

$$w_{ji}(n+1) = w_{ji}(n) + \Delta w_{ji}(n+1) \quad \text{(0.31)}$$

A momentum value of 0.9 is customarily set, for both on-line and batch training modes, (Sarle, 1994). Ripley (1996) argued that it is often better to use momentum values of 0.99 or 0.999 for on-line training mode and a smaller value of 0.5 for batch training mode. However, Sarle (1994) argued that the best momentum can be determined by trial-and –error.

There are several other algorithms for training MLPs that are described by Hertz *et al.* (1991). Most of these algorithms are based on the assumption that the learning rate is constant from epoch to the next and from one weight to another. However, some researchers' for example (Chan and Fallside, 1987; Jacobs, 1988) challenged the above assumption by proposing learning rules that use varying learning rates and provided guidelines for learning rate update. This can decrease the number of cycles required for training, however, it has been argued that the automatic methods of updating learning rates have the risk of being trapped in local minima (Mukherjee & Deshpande, 1997).

Despite the effectiveness of MLPs that are trained with the back-propagation algorithm for solving many engineering problems, they suffer from a number of shortcomings. MLPs trained with the back-propagation algorithm may be slow to converge (Wasserman1989; Vitela & Reifman, 1997). This is attributed to fact that these networks rely on non-linear transfer functions for learning. If node activation is large, nodal outputs may tend to get stuck in the flat spots at the extreme values of the transfer functions. The changes used to update the weights are a function of the derivative of the transfer functions. At the extreme values of the transfer functions the derivative is near zero.

Another limitation of MLPs trained with the back- propagation algorithm is that when the network tries to find the global minimum of error surface, it can get trapped in a local minimum. However, for many applications, the local minima

are not a significant problem, as they occur relatively infrequently (Kolen & Pollack, 1990).

Finally, feed-forward neural networks that are trained with the back-propagation algorithm are often criticized for being black boxes. The knowledge acquired by these networks during training is stored in their connection weights and bias values in a complex manner that is often difficult to interpret (Touretzky & Pomerleau, 1989; Hegazy *et al.,* 1994; Shaopei & Boru, 1998). Consequently, the rules governing the relationships between input/output variables are difficult to quantify, especially for large networks that have a large number of PEs. One way to overcome this problem is to use neuro-fuzzy networks. In this study, several numbers of hidden nodes have been explored during the training of both feed forward and recurrent networks, with each architecture providing a different performance when increasing and decreasing hidden nodes.

One of the most common problems in the training process is the over fitting phenomenon. This happens when the error on the training set is driven to a very small value, but when new data is presented to the network, the error is large. This problem occurs mostly in case of large networks with only few available data. Demuth and Beale (2002) have shown that there are a number of ways to avoid over fitting problem. Early stopping and automated Bayesian regularization methods are most common. However, with immediate fixing the error and the number of epochs to an adequate level (not too low/ not too high) and dividing the data into two sets; training and testing; one can avoid such problem by making several realizations and selecting the best of them (Wasserman, 1989; Vitela & Reifman, 1997).

In this study, the ANN Toolbox in MATLAB R2015a multi-purpose commercial software was used in order to implement training of the data. In this technique, the available data was divided into two subsets. The first subset is the training set, which is used for computing the gradient and updating the network weights and biases. The second subset is the test set. This method works by modifying the performance function, which is normally chosen to be the sum of squares of the network errors on the training set (Weiss & Kulikowski, 1991). The typical

performance function that is used for training feed forward neural networks is the mean sum of squares of the network errors (Wang *et al.,* 2015).

2.8.5 Sensitivity analysis

Sensitivity analysis (SA) is an important step before starting a simulation process (Schladow & Hamilton, 1997; Al-Abed *et al.,* 2002; Chung *et al.,* 2009). The analysis of model sensitivity represent the simulation results that are more sensitive to some parameters than others (Montano *et al.,* 2003; Jack, 2007). This involves identification of inputs that contribute most to output variability, identification of parameters that are most highly correlated with the output and once the model is in use, the consequence results from changing a given input parameter. It is important to comprehend the parameters of ANN to avert needless waste of time in the process of parameter training and validation (Chia-Ling *et al.*, 2012).

Both the graphical method and the sensitivity- index approach can be used to display the sensitivity of the output parameters over the entire range of the tested input parameters (Walker, 1996; Jacomino and Fields*,* 1997; Ehasan *et al.,* 2010). When parameters are relative to one another, it would be difficult to get definite sensitivity analysis results. Therefore, it is significant to ensure that each parameter is independent in the process of sensitivity analysis (Chang *et al.,* 2007). This study uses a single-value sensitivity index to evaluate the effect of parameters of ANN on simulation results. The index is defined as (Chang *et al.,* 2007):

$$S = (O_2 - O_1 / I_2 - I_1)(I_{ave} / O_{ave}) \quad \text{.....(0.32)}$$

Where:

S = the sensitivity index,

I_1 and I_2 = the smallest and the largest input-values respectively;

O_1 and O_2 = the model output values corresponding to I_1 and I_2 respectively;

I_{ave} and O_{ave} are respectively the average I_1 and I_2 and the average O_1 and O_2. The greater the value of S, the greater the effect an input parameter has on a particular output (Walker, 1996).

2.9 Performance evaluation criteria

The performance of the models is evaluated using different statistical measures. The evaluations measures included are correlation coefficient (R), mean absolute error (MAE), mean square error (MSE), Root mean square error (RMSE) and Nash–Sutcliffe Efficiency (NSE).

2.9.1 The correlation coefficient

The correlation coefficient (R) was used to determine the statistical relationship between the measured and the predicted turbidities (Moriasi *et al,* 2007; Bouzeria *et al.,* 2017). The fundamental function was customized to the respective δ values using the relation:

$$R = \frac{\sum_{i=1}^{n} \left[\partial_{ms} - \overline{\partial}_{ms}\right]\left[\partial_{pd} - \overline{\partial}_{pd}\right]}{\sum_{i=1}^{n} \left[\partial_{ms} - \overline{\partial}_{ms}\right]\left[\partial_{pd} - \overline{\partial}_{pd}\right]^2} \quad \text{.....(0.33)}$$

Where:

R = correlation coefficient

∂_{ms} = measured value of the turbidity

$\overline{\partial}_{ms}$ = mean of the measured values of the turbidity

∂_{pd} = predicted value of the turbidity

$\overline{\partial}_{pd}$ = mean of the predicted values of the turbidity

n = number of data points considered

The R is a measure of the strength of the linear relationship between the measured and predicted δ values. It varies from 0 to 1. The values of 0 and 1 indicate a poor and perfect prediction capability of the model respectively.

2.9.2 Mean absolute error

The mean absolute error (MAE) was determined from the relation:

$$MAE = \frac{1}{n}\sum_{i=1}^{n}\left|\partial_{ms} - \partial_{pd}\right| \qquad \text{(0.34)}$$

Where:

MAE = the mean absolute error

∂_{ms} = measured value of the turbidity

∂_{pd} = predicted value of turbidity

n = number of data points

The MAE was used to measure the average magnitude of errors of the set of predicted values. The values of MAE increase from zero to large positive values. The higher the value of MAE, the higher the discrepancy between predicted and measured values (Kim & Valdes, 2003; Moriasi *et al.*, 2007).

2.9.3 Mean square error

The Mean square error (MSE) is a measure of the difference between the measured and predicted values from different indices. It measures the average of the squares of the errors between two values being compared. MSE is an indication of the average deviation of the predicted values from the corresponding measured data and can provide information on long term performance of the models; the lower MSE the better is the long term model prediction. A positive MSE value indicates the amount of overestimation in the predicted turbidity value and vice versa (Wambua *et al.*, 2014b). In this study, Equation (2.35) was adapted for calculating MSE associated with turbidity prediction.

$$MSE = \frac{1}{n}\sum_{i=1}^{n}\left(\partial_{pd} - \partial_{ms}\right)^2$$

(0.35)

Where:

MSE = mean square error

∂_{ms} = measured value of the turbidity

∂_{pd} = predicted value of the turbidity

n = number of data points

The *MSE* ranges from 0 to 1. The smaller the MSE value the better the prediction capability of the model.

2.9.4 Nash-sutcliffe efficiency

The Nash–Sutcliffe Efficiency (*NSE*) is a normalized statistic that determines the relative magnitude of the residual variance compared to the measured data variance (Nash & Sutcliffe, 1970). NSE indicates how well the plot of observed versus simulated data fits the (1 to 1) line. Mathematically *NSE* is given as shown in Equation 2.36.

$$NSE = 1.0 - \left[\frac{\sum_{i=1}^{n}\left(\delta_i^{ms} - \delta_i^{pd}\right)^2}{\sum_{i=1}^{n}\left(\delta_i^{ms} - \overline{\delta_i^{ms}}\right)^2}\right] \quad \text{.....(0.36)}$$

Where:

NSE = Nash–Sutcliffe Efficiency

δ_i^{ms} = measured value of turbidity

δ_i^{pd} = predicted value of turbidity

$\overline{\delta_i^{ms}}$ = mean of measured value of turbidity

n = total number of observations

The resulting values of NSE are compared with those given as acceptable levels of the efficiency as per Nash-Sutcliffe (1970) criterion. Where NSE ranges between $-\infty$ to 1.0

(1 inclusive), with NSE=1 being optimal value. Values between 0.0 and 1.0 are generally viewed as acceptable levels of performance.

2.9.5 Modified index of agreement

The modified index of agreement (d_1) is applied in performance testing to supplement the other methods used because it is more sensitive to the differences on predicted and observed data values than correlation coefficient R, (Anzy *et al.,* 2016). This index gives the ratio of mean square error and the potential error and is mathematically expressed as:

$$d_1 = 1.0 - \frac{\sum_{i=1}^{n}\left|\delta_{ms} - \delta_{pd}\right|}{\sum_{i=1}^{n}\left(\left|\delta_{pd} - \overline{\delta_{ms}}\right| + \left|\delta_{ms} - \overline{\delta_{ms}}\right|\right)} \quad \text{.....} \quad (0.37)$$

Where:

d_1 = modified index of agreement

δ_{ms} = measured value of turbidity

δ_{pd} = forecasted value of turbidity

$\overline{\delta_{ms}}$ = mean of the measured values

n = number of observations.

2.9.6 Root mean square error

The Root Mean Square Error (RMSE) (also called the root mean square deviation, RMSD) is a frequently used measure of the difference between values predicted

by a model and the values actually observed from the environment that is being modelled (Kanda *et al*., 2016). These individual differences are also called residuals, and the RMSE serves to aggregate them into a single measure of predictive power. RMSE provides information on the short term performance which is a measure of the variation of predicted values around the measured data. The lowest the RMSE, the more accurate the prediction is (Mohd *et al.*, 2011).

The RMSE of a model prediction with respect to the estimated variable X_{pd} is defined as the square root of the mean squared error as shown in Equation 2.38:

$$RMSE = \sqrt{\frac{\sum_{i=1}^{n} (X_{ms,i} - X_{pd,i})^2}{n}} \quad \text{.....(0.38)}$$

Where:

X_{ms} =is measured values and

X_{pd} =is predicted /modelled values at time i.

n =number of observations.

The RMSE values is used to distinguish model performance in a calibration period with that of a validation period and to compare the individual model performance.

CHAPTER THREE

METHODOLOGY

3.1 Study area and location

The Kiruku-Kiende Irrigation project is located in Gaturi South in Nembure division of Embu West Sub-County in Embu County at coordinates 9949924N, 336052 E and at an average elevation of 1508m above sea level as shown in Figure 3.1.

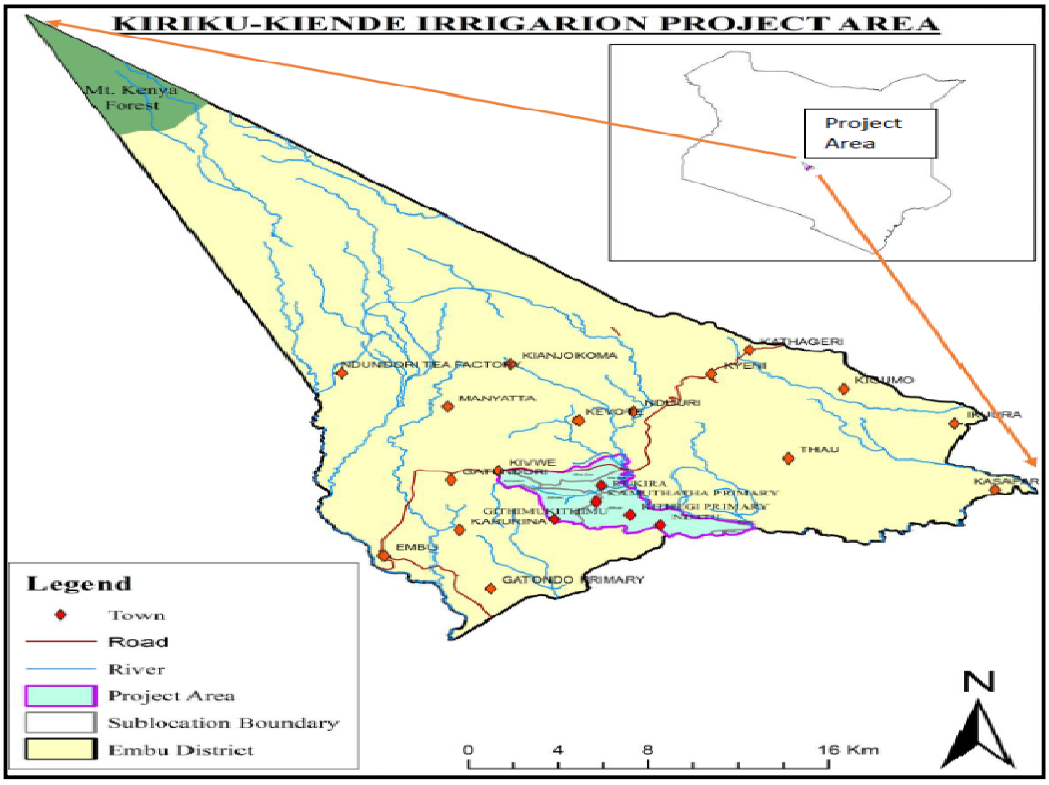

Figure 3:1: Map of study area

Legend

Town

Road

River

Project Area

Embu Sub-County

The scheme covers a gross area of 2,261.5 hectares with about 52 hectares being irrigable area. The water source for Kiriku Kiende Irrigation Project is Kirurumwe River in the Tana Sub-basin. The River originates from the foot of Mt. Kenya near Manyatta with many tributaries along its reach. High flows occur in the months of April and low flows in the month of September. An estimated flow available in the river during critical dry months is about 0.048 m^3/s per second (District Water Office, Embu, 2005).

The water samples were drawn from Kirurumwe River where Kiriku-Kiende irrigation project abstracts its water. Kirurumwe River basin is characterized with loose red soil and a steep slope and as such during rainy season there is a lot of soil erosion. This soil is carried into Kirurumwe River which makes the river highly turbid. Sediment yield and turbidity are serious problems being experienced by the project management in the area. The turbidity of the water at the inlet and outlet of the settling basin in Kiriku-Kiende irrigation project in Embu Sub-County was determined. Water from this project was to serve as a guideline on the reality of river water turbidity so as to have a model representative of a real situation.

3.1.1 The experimental set-up

A physical model of settling basin with a header tank was fabricated (Annex 5) and used to run the various experiments. The study was carried out in the Civil Engineering Laboratory at Jomo Kenyatta University of Agriculture and Technology (JKUAT). The schematic diagram is shown in Figure 3:2.

Using settling velocity for sand particle formula in Equation 2.16 (Zhiyao *et al.*, 2008) and a tank sizing ratio of ratio 4:1 for linear measurements, the dimensions of physical model for settling basin were taken as Length of 2 m, breadth of 0.5 m and a height of 0.4 m. The inflow pipe used was of diameter 20 mm connected to a header tank at a height of 1.6 m with a measuring flow meter next to the control valve. In this height there was considerable minimum head for water to flow in the settling tank by gravity and also considering this is the minimum head required to rotate a sprinkler.

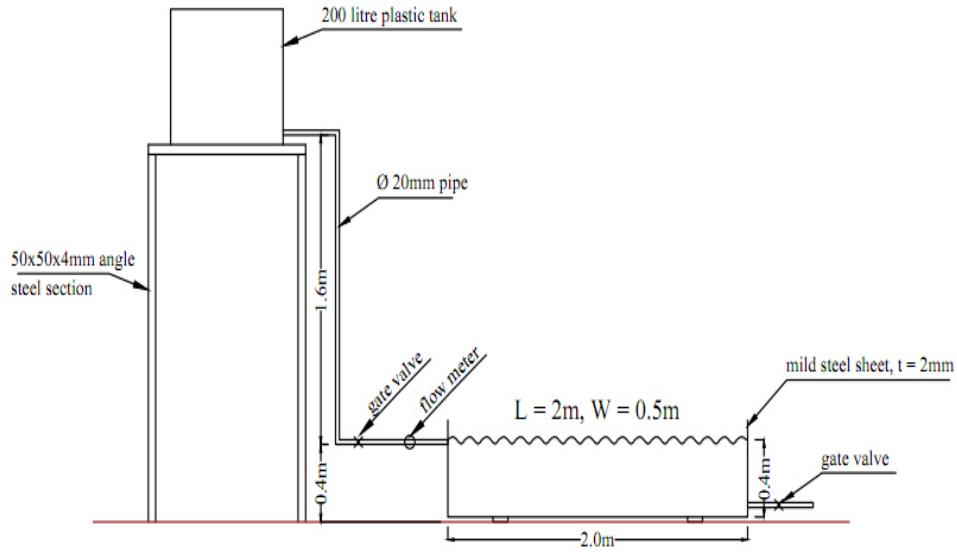

Figure 3:2 Schematic diagram for the experimental set up

To prepare turbid water, Sand particles were prepared by sieving through a 0.20 mm diameter of sieving mesh. Turbid water was then filled in the 200 litres tank; the turbidity for this water was measured and recorded and was maintained between 390 to 470 Nephelometric turbidity units (NTU). The reason was to maintain the water turbidity in a state similar to that of Kirurumwe River. The turbidity at the intake of Kiriku-Kiende project during rainy season was 426 NTU and 192 NTU during dry spell. Considering these extreme Kirurumwe river turbidities then the range of high and low turbidities was chosen. The water flowed by gravity to the settling basin at an increasing flow velocity. The flow was regulated by a gate valve fixed next to a flow meter and was used in recording the flow rate. Water was drawn from the super surface of the settling basin and put in the measuring bottles after every 20 minutes. At time interval of 20 minutes was chosen as notable change in turbidity value could be recorded. This was repeated over a period of 300 minutes since at this time the water in the settling tank was almost clear to a level acceptable for irrigation purposes. The collected samples from turbid water was then tested for turbidity level in the soil laboratory at the Soil, Water and Environmental Engineering Department, JKUAT

(SWEED, JKUAT) using turbidity meter shown in Figure 3.3a. This was repeated for ten (10) different flow rates, corresponding to the range of water flow rates, details in Appendix 2. The experiment was conducted between 4th May 2016 and 20th May 2016 for a set of data at different times.

Figure 3:3 (a) The turbidity meter **(b) Turbid water samples for testing**

The data collected was split into three where parts and used for: training the model, part two for model validation and part three for analyzing and testing the model using the Artificial Neural Networks in MatLab model. Measured turbidity values and settling time were set as input parameters whereas predicted turbidity was considered as system output. A data base consisting of 160 data sets obtained from the experimental set-up was used to develop the predictive model. The raw data is presented in Appendix 2.

3.2 Critical settling velocities of discrete particles

The sand particles for preparing turbid water were passed through sieve no.100 with sieving mesh of 0.20 mm in diameter in order to achieve the discrete sand particles for the experiment. In practice the smallest particle expected to be settled in a settling basin is of diameter 0.2 mm for irrigation purposes (GOK, 2005). However, particles less than 0.2 mm in size coagulate and settle as mass and others fall independently within the tank.

The turbidity of natural raw water varies from 10 to 500 NTU (Sunita & Sonal, 2014). Hence, the experiment was carried out by making synthetic turbid water. About 350 grams of graded sand was added to 200 liters of clean water in the header tank. The suspension was stirred for one hour to achieve uniform homogeneous sample (Sasikila & Muthurama, 2016). The turbidity of this homogenous solution was recorded as 465 NTU and then let in to the model settling basin at a pre-determined flow rate. The preparation of turbid water was repeated for 463, 424, 395 and 196 NTU water samples.

Different flow rates of 4.8 l/min, 5.7l/min, 8.7l/min, 9.9 l/min, 10.5 l/min, and 11.1 l/min were set using a gate valve and water released from the header tank into the model-settling basin. Turbidity levels were then monitored in the model tank and recorded for every 20 minutes over a period of 300 minutes for each flow rate. A time range of 20 minutes corresponded to a notable turbidity drop on the settled sediments. The flow rates were determined and regulated by the gate valve in order to realize the expected openings corresponding to a given flow. The gate valve was opened half-way per test progressively to achieve the flow rates.

The turbid water in the header tank was stirred after every 5 minutes to maintain uniformity and to ensure that the particles do not settle in the tank. This process was repeated for lower turbidities ranging from 180 to 250 NTU for flow rates of 8.7 l/min, 9.9 l/min, 10.5 l/min and 11.1 l/min respectively. The settling velocity of the particles was then computed using Equation 2.12.

3.3 Optimum Hydraulic Parameters

3.3.1 Model calibration and optimization

The learning process or training forms the interconnection between neurons. The input-target training data was preprocessed using Equation 3.1 in order to improve the numerical condition for optimization problem and for better behavior of the training process. The normalized data (Appendix 3) was fed into the ANN for each flow rate whereby using a trial and error method training was performed. The model was set such that 70% of the input data was allocated for training, 15% for validation and 15% for testing. The training automatically stopped when the

generalization stopped improving as indicated by an increase in the MSE of the validation sample. The optimization was typically carried out in such a way that the sequence of model output signals generated by training was close as possible to the corresponding set of observations. To achieve this the value of regression and mean sequence error was monitored as training was being done.

3.3.2 Model validation

A validation data set was used as input into the performance measures; correlation coefficient, mean absolute error and mean square error to validate the models. A performance criterion after Moriasi *et al* (2007) and Wambua *et al* (2016) for each performance measure was adapted as presented in the following sections. The validation data set was used for cross validation to evaluate the neural network performance during training. The testing data set was used to evaluate the neural network performance after training had been completed (Dandy and Maier, 2000). Poor turbidity prediction can be expected when the validation data contain values outside of the range of those used for training.

Different scenarios of sediment concentration (ranging from 390 NTU to 470 NTU) against discharges were used with Artificial Neural Networks toolbox within Matlab. These were used to give the prediction of the desired irrigation water turbidity at different lag times of 20, 40, 60 and 80 minutes and thereafter the optimum tank dimensions required to settle the particles was calculated.

3.3.3 Sensitivity analysis

Prior to calibration of the ANN, a sensitivity analysis was performed to identify key calibration input variables. The parameter considered here are, training times, settling time and the number of neurons in the hidden layer. Each parameter was varied while the rest two were kept constant. This was repeated for each parameter while holding others constant. For every training the R^2 for both training and validation parameters were recorded. Equation 2.32 was then applied to calculate the sensitivity index S. The results of sensitivity analysis are shown in Table 4.1.

3.3.4 Designing the ANN models

Designing ANN models followed a number of systemic procedures. The five basics steps are: (1) collecting data, (2) pre-processing data, (3) building the network, (4) training and (5) testing performance of model. The process is schematically presented in Figure 3.4.

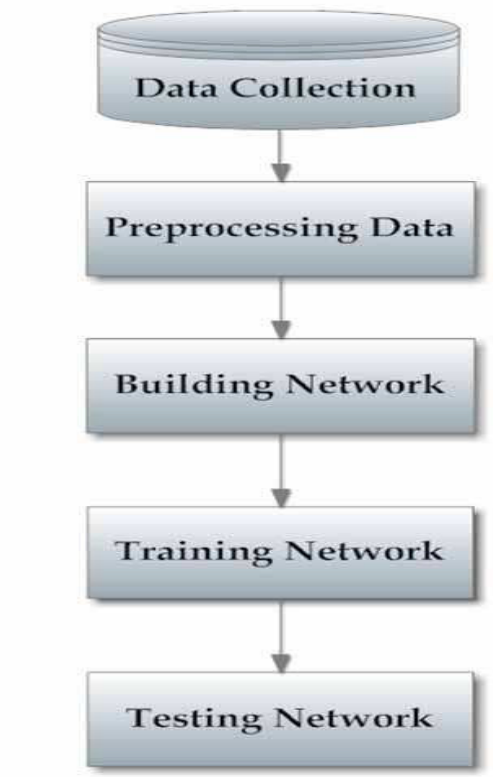

Figure 3:4: Basic flow for designing ANN model

3.3.4.1 Data collection

Collecting and preparing sample data is the first step in designing ANN models as out-lined in Section 3.1.1, different turbidity levels were recorded for each flow rate over a duration of 300 minutes at an interval of 20 minutes. A total of six (6) different flow rates with turbidities ranging from 390 to 470 NTU (referred to as highly turbid water) were set, these are 4.8 l/min, 5.7 l/min, 8.7 l/min, 9.9 l/min, 10.5 l/min and 11.1 l/min. This process was repeated for lower turbidities ranging

from 180 to 250 NTU for flow rates of 4.8 l/min, 8.7 l/min, 9.9 l/min, 10.5 l/min and 11.1 l/min respectively (referred as low turbid water) as shown in Appendix 2.

The process in section 3.2 was repeated but discharge rates used were 4.8 l/min and 11.1 l/min per each sediment concentration, this was measured using a calibrated bend meter located in the supply line. The major assumption in the development of the model was that the flow field was the same for all positions within the basin.

3.3.4.2 Data pre-processing

After data collection, three data pre-processing procedures were conducted to train the ANNs more efficiently. These procedures were: (1) data normalization (2) data randomization and. (3) data segregation (Martin, 2006). Normalization procedure before presenting the input data to the network is generally a good practice, since mixing variables with large magnitudes and small magnitudes will confuse the learning algorithm on the importance of each variable and may force it to finally reject the variable with the smaller magnitude (Tymvios *et al.,* 2008). The output of network was turbidity value. In view of the requirements of the neural computation algorithm, the data of both the inputs and output were normalized to an interval by transformation process. In this study normalization of data (inputs and outputs) was done for the range of [−1, 1] using, Equation 3.1 (Mustafa *et al.,* 2011).

$$p_n = p_{\min} + \left(\frac{p - p_{\min}}{p_{\max} - p_{\min}} \right) (p_{\max} - p_{\min}) \quad \text{.....(0.1)}$$

Where;

p_n = the normalized parameter,

p = actual parameter,

p_{min} = minimum of the actual parameters and

p_{max} = maximum of the actual parameters.

About 70% or 112 out of 160 of the data sets were selected randomly as train data and 15% (equivalent to 24 data sets) for validation and another 24 for test purposes. Annex 3 shows the normalized data set for feeding in the input of ANN training.

3.3.4.3 Training the network

During the training process, the weights were adjusted in order to make the actual outputs (Predicted) close to the target (measured) outputs of the network. In this study, 112 data entries for turbidity levels against flow rate were used for training as it is outlined in Section 3.2. Fourteen different types of training algorithms were investigated for developing the network for every flow rate. MATLAB has Hyperbolic Tangent Sigmoid (logsig) as in-built transfer function that was used in this study. The use of this transfer function caused the network to have smaller weights and biases, and this forced the network response to be smoother and less likely to over fit (Demuth and Beale, 2002).

3.3.4.4 Testing the network

The next step was to test the performance of the developed model. At this stage the data was exposed to the model. In order to evaluate the performance of the developed ANN models quantitatively and verify whether there is any underlying trend in performance of ANN models, statistical analysis involving the coefficient of determination (R), the Root Mean Square Error (RMSE), and the Mean Square Error (MSE) were conducted. The expressions for the aforementioned statistical parameters are:

$$MSE = \frac{1}{n}\sum_{i=1}^{n} (\partial_{pd} - \partial_{ms}) \quad \text{.....(0.2)}$$

$$RMSE = \sqrt{\frac{1}{n}\sum_{i=n}^{n} (\partial_{pd} - \partial_{ms})^2} \quad \text{.....(0.3)}$$

Where δ_{pd} denotes the predicted turbidity in the settling basin in NTU, δ_{ms} denotes the

Measured turbidity in the settling basin in NTU, and n denotes the number of observations.

3.3.4.5 Developing the ANN model architecture

A total of twenty eight neural network models (see Figure 4.1) were developed in order to study the turbidity as predictive variable for sediment settlement in a settling basin. Neural networks were trained, verified and tested on data for one hundred and twenty data set. The aim of these training simulations was to determine the neural network architecture that would yield the best sediment settlement predictive performance.

When the performance of the training parameters (weights and biases) on the validation dataset showed no improvement during training, the optimization process was stopped and no new weights or biases were generated and as such overfitting of the training dataset was avoided by an early typical stopping technique. This study considered ANNs with the simplest structure, a number of hidden nodes ranging from 2 to 10 and only one hidden layer. Faraway and Chatfield (1998) shown that increasing the number of nodes can sometimes cause ANN performance to decay (overtraining).

In trying to determine the weights and biases resulting in the global minimum of the differences between observations and ANN predictions, some local minima were encountered (whose presence depended on the initial values assigned to biases and weights) and this may have halted the optimization process. There was no clear solution to this problem, hence the reason why most authors preferred to train ANNs using different random seeds to generate initial weights and then analyze the best ANN (Faraway and Chatfield, 1998). Therefore, this study adapted this approach and generated 240 ANN models with different initial random seeds.

In naming the models (e.g. PN 204) the first two letters (PN) refer to Predicted Network, then the first two numbers refer to lead-time that is 20, 40, 60 and 80 minutes lead time respectively. The last third number represented the flow rate

where by 1, 2, 3, 4, 5,6 and 7 represents 4.8 l/min, 5.7 l/min, 8.7 l/min, 9 l/min, 9.9 l/min, 10.5 and 11.1 l/min respectively.

3.4 Effects of sediment removal by continuous flushing

Two types of experiments were conducted: The first set of runs pertain to the removal efficiency of the settling basin when there was no flushing, and the next set of runs pertain to the removal efficiency of the settling basin when flushing was introduced.

The discharge was measured using a calibrated bend meter positioned in the supply line. Uniform flow of 11.1 l/min in the approach channel was established by operating the gate valve. The desired sand concentration of 500g was added to the water in the header tank, stirred and then let into the settling basin. The sediment was allowed to settle for 300 minutes after which water was slowly drained using a wash out by opening the control valve mounted at the sub surface of the tank. The settled wet sediments were collected dried in the oven and the weights recorded. The oven temperature was set at 110^0c and the sand was dried for 30 minutes, this was to ensure a steady state condition of the sand was reached with about 10-20% of moisture according to procedures outlined in BS 1377: part 2: 1990 (Chudley *et al.*, 2008). This procedure was repeated for four different experiments with the same flow rate and weight recorded.

On the second experiment, the same flow of 11.1 l/min was set and the same quantity of 500 grams of graded sand added into the header tanks. The flushing outlet pipe was set at 4.8 l/min. The turbid water was let into the basin and after 60 minutes, the outlet (flushing) pipe was opened for 15 minutes and then closed. The amount of sediment remaining in the basin was then collected and dried in the oven and the weight recorded in accordance with the procedure of drying earlier described. This was repeated for four other experiments where the flow rate was set at 11.1 l/min and water in the header tank mixed with 500g of graded sand. After settling for 60 minutes the wash out was opened at 4.8 l/min for 15 minutes. The settled sand was then removed and oven dried. Results are presented in Table 4.10 while the complete system for the experiment is shown in Appendix 5.

According to Revel *et al*. (2013) sediment flushing efficiency of the tank was then calculated using Equation 3.4.

$$\lambda = \frac{S_{out}}{S_{in}} \quad \ldots\ldots\ldots\ldots\ldots\ldots\ldots\ldots\ldots\ldots\ldots\ldots \quad (0.4)$$

Where:

λ = the tank sediment flushing efficiency

S_{out} = is the flushed sediment amount out of the tank (gram)

S_{in} = is the sediment inflow into the tank (gram)

CHAPTER FOUR

RESULTS AND DISCUSSION

4.1 Determination of critical settling velocity

Figure 4.1 presents a summary of turbidity values at different flow rates (Q_1, Q_2, Q_3, Q_4 and Q_5) measured at 4.6 l/min, 9.9 l/min, 10.5 l/min, 11.1 l/min and again 9.9 l/min with low turbidity value respectively. Retention time as particles were settling is represented by T_1, T_2 up to T_{16} where T_1 represents turbidity at zero (0) minutes and time increases at constant interval of 20 minutes.

During the experiment, it was noted that after five (5) hours the turbidity dropped significantly to levels acceptable for irrigation purposes, hence further collection of data was terminated. There are no uniform guidelines that exist for acceptable turbidity values for irrgation water purposes, therefore, monitoring of turbidity is impo

In Figure 4.1 the behavior of sediment settling for different flow rates is presented against turbidity values. The graph for flow rate Q_1 (4.8 l/min) corresponds to the lowest flow rate in this experiment and the corresponding turbidity levels recorded shows that there was very little turbidity change after every 20 minutes which means that at low flow rates sediments take time to settle at the bottom of the basin. The flow rates of Q_3, Q_4 and Q_5 shows a similar trend in sediment settlement where by the sediment settle gradually, but after 60 minutes the turbidity levels begin to rise again (T6 to T10), this is attributed to the eddy currents which tend to distribute the sediment particles in an uneven manner. However, after 120 minutes the sediment settling tend to stabilizes and particles are settling in an even manner. Flow rate Q_2 and Q_5 are the same but with different sediment concentration. Q_2 and Q_5 have a turbidity value of 465.33 NTU and 196.00 NTU respectively. These two turbidities are represented cumulatively in the linear graph as $Q_2 = Q_1+Q_2$ (424.33+465.33) = 889.66 NTU and $Q_5 = Q_1+Q_2+Q_3+Q_4+Q_5$ (424.33+465.33+463+395+196) = 1943.66 NTU. The linear graphs for both Q_2 and Q_5 flow rates on sediment settling show almost similar

slope, which shows that irrespective of the sediment concentration settling of sediment is affected, by flow rate in the same way.

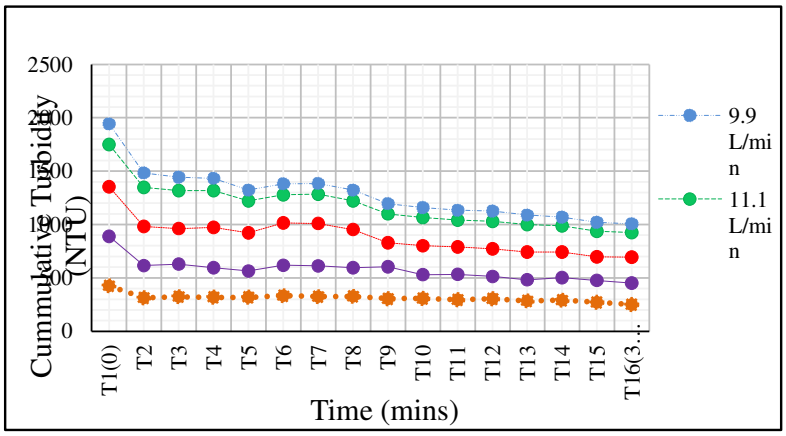

Figure 4:1: Turbidity versus time

Table 4.1 shows the turbidity values for five different flow rates at time intervals of forty minutes. The turbidity drop indicates that as the discharge into the settling basin increases, the sediment settling increases leading to less sediment concentration in the water. At flow rate of 11.1 l/min there is reduced turbidity drop irrespective of a higher flow rate than preceding flow rate of 10.5 l/min. This was attributed to the low concentration of sediments in the water compared to others and as such fewer particles settled.

Table 4.1: Turbidity drop at different flow rates

	Time in minutes								
FLOW RATE (l/min)	**0**	**40**	**80**	**120**	**160**	**200**	**240**	**280**	**Turbidity drop**
5.7	424.33	324.00	317.33	325.33	305.33	295.67	284.00	271.48	152.85
8.7	425.00	332.00	382.67	372.00	311.00	275.33	269.33	240.00	185.00
9.9	465.33	304.00	245.33	287.33	297.33	236.67	198.67	206.00	259.33
10.5	463.00	334.67	358.33	396.00	227.67	257.00	260.00	219.67	243.33
11.1	395.00	354.67	299.33	274.67	269.33	251.00	256.33	240.00	155.00

From design principles, settling velocity (Vs) is computed from the flowrate (Q) and the effective settling area of the tank (A).

$$V_s = \sqrt{\frac{4(\rho_p - \rho_w)gd}{3C_D\rho_w}} \quad (0.1)$$

Where:

V_s = Settling velocity (m/s)m

ρ_p =Density of sand particle (kg/m^3)

ρ_w =Density of water (kg/m^3)

g =Acceleration due to gravity (taken as 9.81m/s^2)

d =Particle size (m)

C_D =Drag coefficient (taken as 0.37 for turbulent flow)

Equation 4.1 is applied to calculate the optimum dimensions for a settling tank

$$V_s = \frac{Q}{A} \quad (0.2)$$

Where:

V_s = Settling velocity (m/s)m

Q = Flow rate (m^3/s)

A = Effective surface area of the tank (m^2)

From equation 4.2, the basin retention time for different turbidities can be calculated.

The critical settling velocity is the settling velocity of the particles which are almost 100% removed from the basin. As seen from Table 4.3 the critical settling velocities (0.0024 to 0.0044 m/s) are higher than the particle settling velocity (0.000038 to 0.00011 m/s) which is an indication that some particles settled faster at the sludge zone of the basin. In each flowrate the collection efficiency which is the settling efficiency was calculated and ranged from 40% (Q=5.7 l/s) to 58% (Q=11.1 l/s). The behavior of Vp at Q10.5 was abnormal which could have been contributed by human error for not stirring the water after 5 minutes during data collection.

Table 4.2: Critical settling velocity for different flow rates

Flow Rate (l/min)	Particle settling velocity (m/s) **Vp**	Critical settling velocity (m/s) **Vc**	Removal Efficiency (%)
5.7	3.8 x 10-5	3.4 x 10-3	40
8.7	7.0 x 10-5	4.4 x 10-3	48
9.9	8.6 x 10-5	2.4 x 10-3	52
10.5	8.4 x 10-5	2.6 x 10-3	48
11.1	1.07 x 10-4	3.4 x 10-3	58

The particle settling velocity is increasing with increase in flow rate from 0.000038 to 0.00011 m/s. The collection efficiency increased with increase in flowrate from 40% to 58%, which is an indication that as inflow rate is increased more sediment tend to settle at the bottom of the basin. A plot of turbidity drop against flow rate is presented in Figure 4.2.

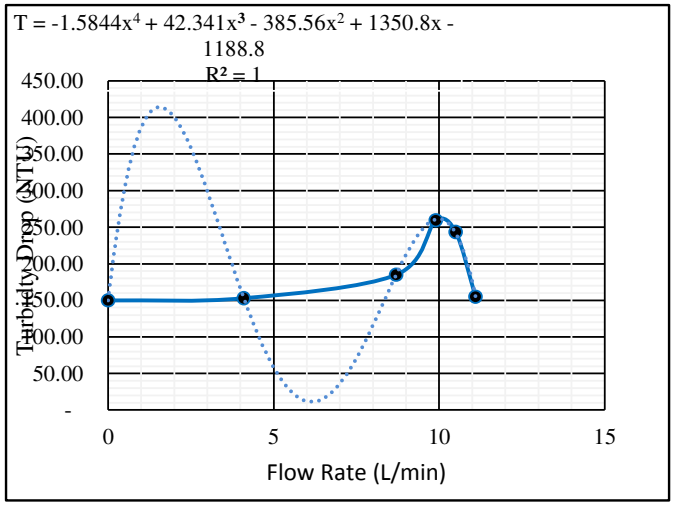

Figure 4:2: Turbidity drop against Flow rate

Figure 4:2 shows that as the flow rate is increased, the turbidity drop also increases up to a critical flow rate of 9.9 l/min then it starts to drop forming a curve with a polynomial curve shape, which is reduced to quartic equation or biquadratic equation with an R^2 value of one. This indicates that the equation can be used to accurately calculate the expected turbidity drop in any turbid water with a given flow rates.

$$T = -1.5844x^4 + 42.341x^3 - 385.56x^2 + 1350.8x - 1188.8 \quad (0.3)$$

Where;

T = Expected turbidity drop value (NTU)

x = Flow rate (L/min).

The quartic equation for calculating turbidity in a given settling basin is given by Equation 4.3 with flow rate limits of x=4.8 and 11.1 l/min

It was observed that the sediment concentration at the sludge zone increased with increase in flow rate as shown in Table 4.2. These findings are similar to results by Martin (2006) who while researching on sediment load and sediment concentration prediction, observed that the highest sediment concentration was with high flows. Haiyan *et al*. (2013) observed similar trend in that with increase of flowrate from 0.7 m/s to 1.1 m/s the concentration of phosphorous (sediment) in the overlying water increased and then tended to be stable thereafter. While investigating flow simulation and analysis in a vertical flow sedimentation tank, Guihua *et al*. (2012) noted that with increased inlet velocity the raw sewage rapidly settled in a uniform distribution of the entire radial extent of sedimentation tank.

4.2 Optimum hydraulic parameters

4.2.1 Sensitivity analysis

Table 4.3 shows results of different simulations when the parameters of ANN were changed. These are, training times, settling time and number of neurons in the hidden layer.

Table 0.3(a-c): Changes of prediction accuracy under different parameters of ANN

a) Scenarios with various training times

Scenario	A-1	A-2	A-3	Base
Number of neurons in hidden layer	9	9	9	9
Training times	7	7	6	9
Settling time (minutes)	20	20	20	20
R^2 (parameter training)	0.5898	0.5537	0.9675	0.9999
R^2 (parameter validation)	1.0000	0.9999	1.0000	1.0000

b) Scenarios with settling time

Scenario	B-1	B-2	B-3	Base
Number of neurons in hidden layer	9	9	9	9
Training times	9	9	9	9
Settling time (minutes)	80	60	40	20
R^2 (parameter training)	0.9848	0.7957	0.9255	0.9999
R^2 (parameter validation)	1.0000	0.9999	1.0000	1.0000

c) Scenarios with different number of neurons in hidden layers

Scenario	C-1	C-2	C-3	Base
Number of neurons in hidden layer	2	4	6	9
Training times	9	9	9	9
Settling time (minutes)	80	60	40	20
R^2 (parameter training)	0.9848	0.7957	0.9255	0.9999
R^2 (parameter validation)	1.0000	0.9999	1.0000	1.0000

The values of the three parameters above were regarded as input into the model and R2 between measured and predicted water turbidity as model output. The R2 value is high since one input is considers and other variables are being held constant and are given a maximum value unlike when all the three variables are being fed at the same time in to the model. Sensitivity index (S) was calculated for each scenario using Equation 2.32. The results are presented in Table 4.4

Table 0.4: **Sensitivity analysis using sensitivity index**

Item	Parameter	Sensitivity (S)
1	Training times	0.0005
2	Settling time	0.0044
3	Number of neurons in hidden layer	0.0570

The results presented in Table 4.4 shows that the R^2 between measured and predicted water turbidity for training and validation are different for various scenarios with different parameters. Table 4.5, which shows the sensitivity analysis index indicates that ANN is more sensitive to the transfer function of hidden layer. This is in agreement with the sensitivity analysis carried out by Chia-Ling and Chung-Sheng (2012) in assessing the effect of the parameters of ANN on the prediction of turbidity of raw water in the water treatment plant. The simulation result of water turbidity prediction are more sensitive to the transfer function of the number of neurons in hidden layer than training and settling times.

4.2.2 ANN for turbidity prediction

To avoid the negative effect of oversize and undersize, the input data were normalized to a specific range by transformation processes. Equation 3.1 was used to transform the input data into the interval of [−1, 1] before feeding it into the

Artificial Neural Network model for training and predictions on settlement of particle against the flow rates. The normalized data is shown in Annex 3.

ANN modeling analyzed the 112 sample values for training (training sets) and statistically predicted the possible output of the trained data. The model validated the output by iteration and testing the data against regression (correlation) and mean square error for training, validation and testing data set. As the inputs are applied to the network, the network outputs are then compared with the targets. Table 4.5 shows the results for the trained data, validation and the predicted turbidity values for both high and low turbidities.

Table 0.5: Results for training, validation and predicted turbidity

Flow rate (l/s)	Measured Turbidity	Trained Turbidity	Validated Turbidity	Predicted Turbidity	Error
5.7	250.62	249.16	249.17	249.19	1.43
8.7	228.00	226.86	226.84	226.85	1.15
9.9	200.00	199.24	199.24	199.25	0.75
10.5	219.67	218.78	218.77	218.77	0.90
11.1	233.67	232.21	232.22	232.23	1.44
5.7	108.67	107.88	107.90	107.91	0.76
8.7	128.33	127.21	127.23	127.24	1.09
9.9	81.67	80.93	80.95	80.97	0.70
10.5	57.00	56.70	56.71	56.72	0.28
11.1	164.00	162.23	162.25	162.26	1.74

4.2.3 Model performance

The accuracy of the models was evaluated by plotting line graphs that show actual data versus the values predicted by the models for the five flowrates. However, the five more formal quantitative measures of accuracy of time series modeling techniques were employed that is the MAE, MSE, R, NSE and RMSE. The results for different lead-time with their best ANN models are shown in Table 4:6 where PN-201 represents the model name.

Table 0.6: ANN models for different lead times

Table 4:6a: 20-Minutes lead-time

Model Name	ANN Arch	MSE	R	RMSE	MAE	d1	NSE
PN-201	1-4-1	3.726E-07	1.0000	0.5345	0.1333	0.2431	0.6043
PN-202	1-5-1	5.837E-03	0.9722	0.5345	0.1333	0.2285	0.6624
PN-203	1-3-1	3.009E-03	0.9945	0.4432	0.1105	0.3742	-0.3226
PN-204	1-9-1	1.150E-09	1.0000	0.5102	0.1273	0.1469	0.8839
PN-205	1-6-1	2.771E-03	0.9805	0.5319	0.1327	0.1295	0.9133
PN-206	1-2-1	1.795E-02	0.9989	0.4855	0.1211	0.2676	0.4913
PN-207	1-5-1	9.960E-04	0.9965	0.5345	0.1333	0.1921	0.7810

Table 4:6b: 40-Minutes lead time

Model Name	ANN Arch	MSE	R	RMSE	MAE	d1	NSE
PN-401	1-7-1	3.898E-04	0.9981	0.9009	0.2408	0.4380	-1.1804
PN-402	1-10-1	4.711E-08	1.0000	0.6654	0.1778	0.3212	0.1617
PN-403	1-7-1	1.468E-04	0.9996	0.6042	0.1615	0.6774	-12.3350
PN-404	1-8-1	5.283E-06	1.0000	0.6777	0.181	0.2108	0.7251

					2		
PN-405	1-2-1	7.686E-04	0.9943	0.7209	0.1927	0.1900	0.7870
PN-406	1-5-1	2.991E-15	1.0000	0.8106	0.2166	0.5032	-2.5695
PN-407	1-7-1	1.044E-03	0.9968	0.9509	0.2541	0.3524	-0.0977

Table 4:6c: 60-Minutes lead time

Model Name	ANN Arch	MSE	R	RMSE	MAE	d1	NSE
PN-601	1-4-1	1.763E-04	0.9994	1.0661	0.2957	0.5903	-5.7302
PN-602	1-3-1	7.725E-04	0.9959	0.7937	0.2201	0.4045	-0.6675
PN-603	1-5-1	1.533E-03	0.9993	0.9198	0.2551	1.3558	-15.7500
PN-604	1-6-1	1.814E-03	0.9961	0.8866	0.2459	0.2982	0.3228
PN-605	1-10-1	3.395E-03	0.9939	0.9444	0.2619	0.2605	0.5295
PN-606	1-2-1	3.744E-05	0.9999	1.0547	0.2925	0.7342	-19.7623
PN-607	1-5-1	2.235E-06	1.0000	1.3649	0.3786	0.5074	-2.6429

Table 4:6d: 80-Minutes lead time

Model Name	ANN Arch	MSE	R	RMSE	MAE	d1	NSE
PN-801	1-10-1	3.2543E-13	1.0000	1.3908	0.4015	0.79233	-32.5215
PN-802	1-6-1	5.8053E-16	1.0000	0.9380	0.2708	0.51979	-2.9431
PN-803	1-4-1	8.360E-04	0.9985	1.1078	0.3198	2.08264	-19.9931
PN-804	1-10-1	3.270E-03	0.9995	1.0593	0.3058	0.37853	-0.3440
PN-805	1-7-1	1.3212E-20	0.9998	1.1540	0.3331	0.34196	0.0076
PN-806	1-6-1	5.7138E-05	0.9999	1.3769	0.3975	0.99282	-46.7281
PN-807	1-4-1	2.55E-23	1.0000	1.7332	0.5003	0.645132	-8.9701

The results presented in Table 4.6 (a-d) refer to the ANN that displayed the lowest error herein defined as the mean square error and the Nash–Sutcliffe Efficiency (Maanen *et al*., 2010) for every lead-time. These were further analyzed to give the best ANN predictor for sediment settlement in a settling basin using NSE error evaluation for elimination method for each category resulting to the four best ANNs. Table 4.7 shows the four best ANN models.

Table 4.7: The best four ANN models

Model Name	ANN Arch	MSE	R	RMSE	MAE	d1	NSE
PN-204	1-9-1	1.150E-09	0.99990	0.5102	0.1273	0.1469	0.8839
PN-402	1-10-1	4.711E-08	1.00000	0.6654	0.1778	0.3212	0.1617
PN-605	1-10-1	3.395E-03	0.99399	0.9444	0.2619	0.2605	0.5295
PN-805	1-7-1	1.3212E-20	0.99980	1.1540	0.3331	0.34196	0.0076

Figure 4.3 below is a plot of RMSE, MAE, modified index agreement and NSE versus the errors for the test set of 112. The bar graphs shows a linear relationship where the RMSE is increasing with increase in water flow rates. The minimum RMSE was used as a criterion for selecting the best neural network. Based on this criterion the network trained to 0.51 (PN-204) would be chosen as the better network. Figure 4.3 also shows results of MAE, where the error is increasing with increase in flow rate, which shows increase in discrepancy of the observed and predicted data. Using MAE as a criterion for selecting the best neural network the training error of 0.13 corresponding to PN-204 model was selected.

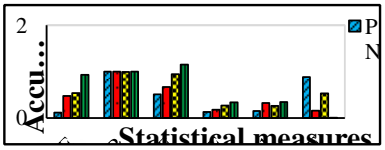

Figure 4:3: Comparison of quantitative measures of accuracy for the four ANN models

Figure 4.3 further shows results for modified index agreement (d_1) which shows PN-204 has least error while PN-805 has highest error. A computed value of 1 indicates a perfect agreement between measured and predicted while a d_1 of 0 indicates poor agreement (Willmott, 1981). Using this criterion ANN model PN-805 of 0.34 error forms the best neural network.

Finally, the NSE error values for the four models show that PN-204 with an error of 0.88 has exceptionally large error than others. Using NSE as a criterion, NSE ranges from $-\infty$ to 1 with NSE = 1 being optimal. Values of 0.0 to 1.0 are generally viewed as acceptable levels of performance (Nash and Sutcliffe, 1970). Based on that the PN-204 with an error of 0.88 is the best ANN model as summarized in Table 4.8.

Figure 4.4 shows the correlation (R) for the four best flows under consideration as analyzed by the model, Analysis of the four shows the strength of the linear relationship between the observed and the predicted turbidity values for best neural network. The values of 0 and 1 indicate poor and perfect prediction capability respectively. Based on this criteria PN-402 with 1.0 is slightly higher than PN-204 at 0.9999 which means that PN 402 has higher possibility of prediction than PN-204.

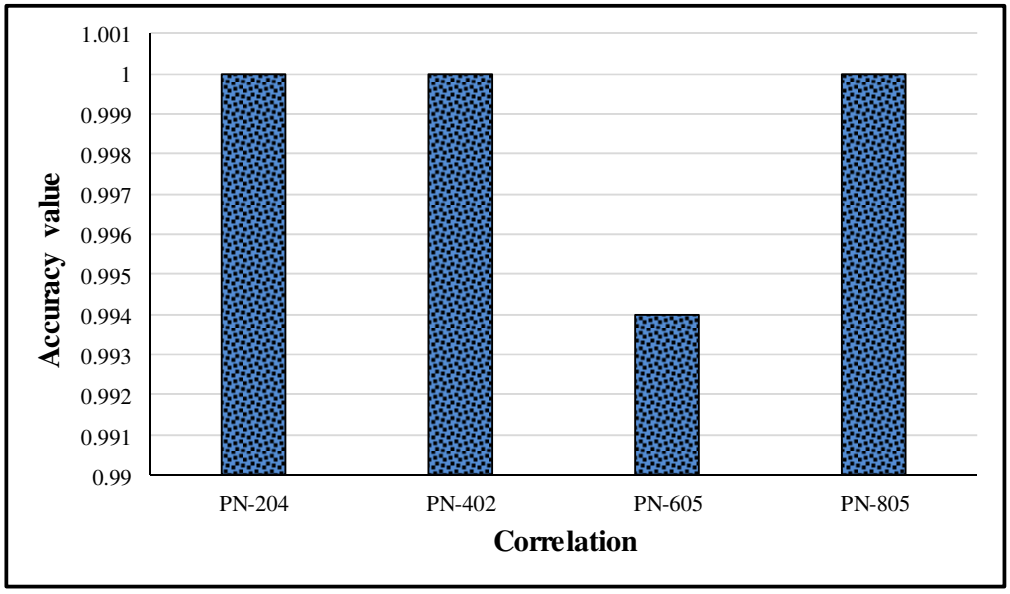

Figure 4.4: Correlation for the four best ANN models

The four ANN models in Table 4.7 were used to develop the relation of sediment settlement and the flowrate for discrete particle setting in a settling basin. The number of hidden neurons in each activation layer was selected by trial and error method. From the statistical analysis of each model presented earlier, the ANN model PN-204 is the best for predicting water turbidity for irrigation purposes, this is because it has the least RMSE, MAE and NSE values. On the correlation, PN-204 is almost the same with PN-402 hence going for PN-204, which has met all the criteria for selection. A strong correlation was also found between the observed and estimated sediment load values for the same model as the value of Nash-Sutcliffe model efficiency coefficient was found to be quite high at 0.9999. Table 4.8 shows the summary of the best ANN and their associated statistical measure values. From this summary, it is clearly deduced that ANN model PN-204 has best values for the statistical measures used in this experiment hence forming the best ANN predictive model.

Table 4.8: Summary of the best ANN with their respective statistical values

S/No	Statistical Measure	Best ANN	Value
1	Mean Square Error	PN 204	0.12
2	Correlation (R)	PN 204	0.99
3	Root mean square error (RMSE)	PN 204	0.51
4	Mean absolute error	PN 204	0.13
5	Modified Index (d1)	PN 804	0.34
6	Nash-Sutcliffe error (NSE)	PN 204	0.88

Figure 4:5 shows the training, testing and validation mean square error values for Levenberg Marquardt algorithm with 1-9-1 model architecture. In this architecture, the minimum R values for the best model training and validation is 0.99978 and 1.00000 repectively at Epoch 5 as shown in Figure 4.6.

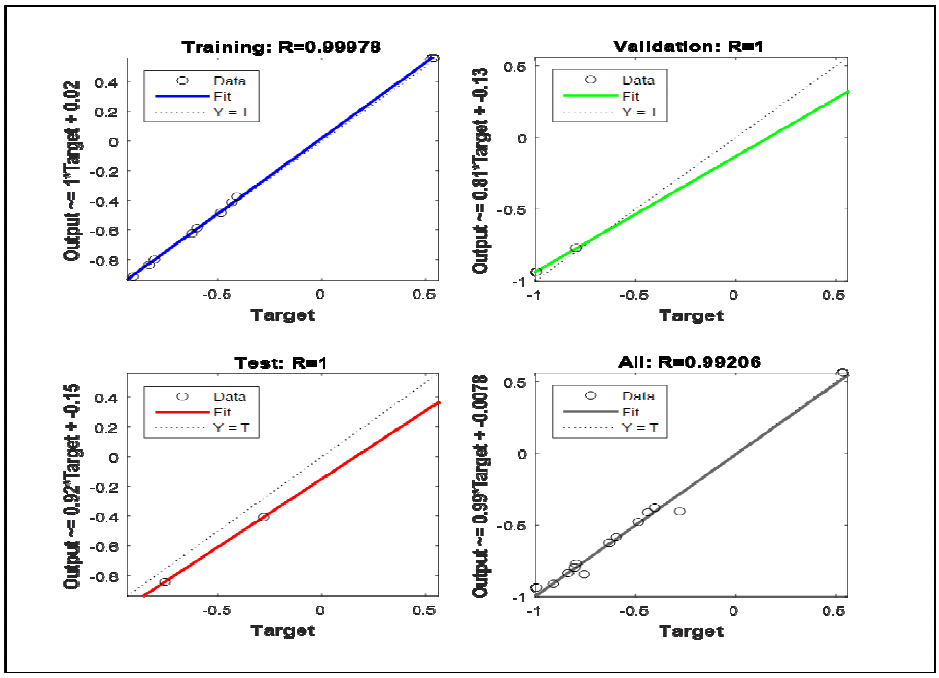

Figure 4.5 Regression of the best ANN of turbidity prediction at 8.7l/min

Figure 4.6 shows that the fifth epoch out of the six epoches iterated gave the best epoch when all the data trained achieved the least error possible. The performance of that epoch was noted as 0.0021691.

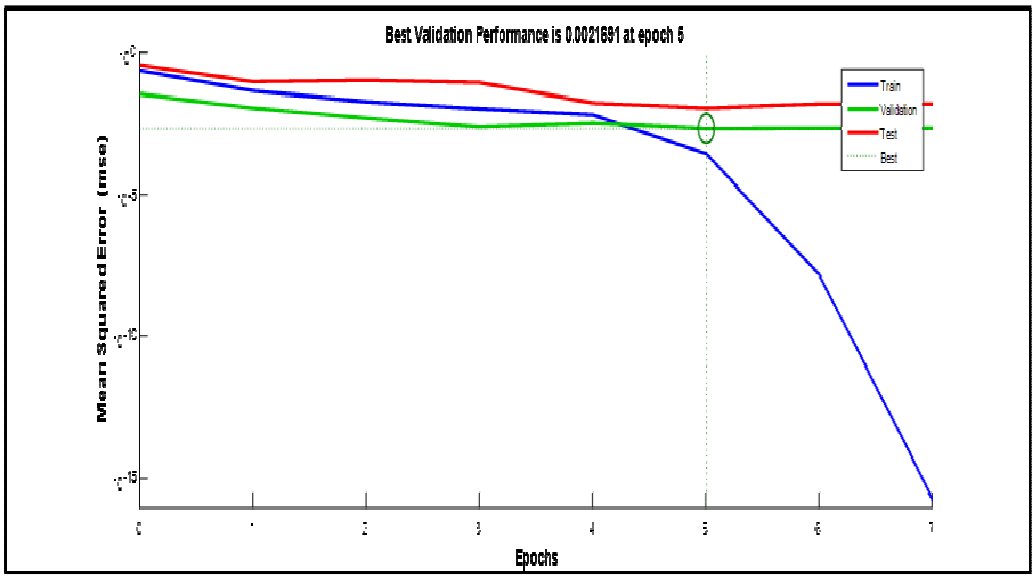

Figure 4.5: MSE results for L-M algorithm at 8.7 l/min

The gradient value in Figure 4.7 was noted to be above zero and revealed a relative data consistency.

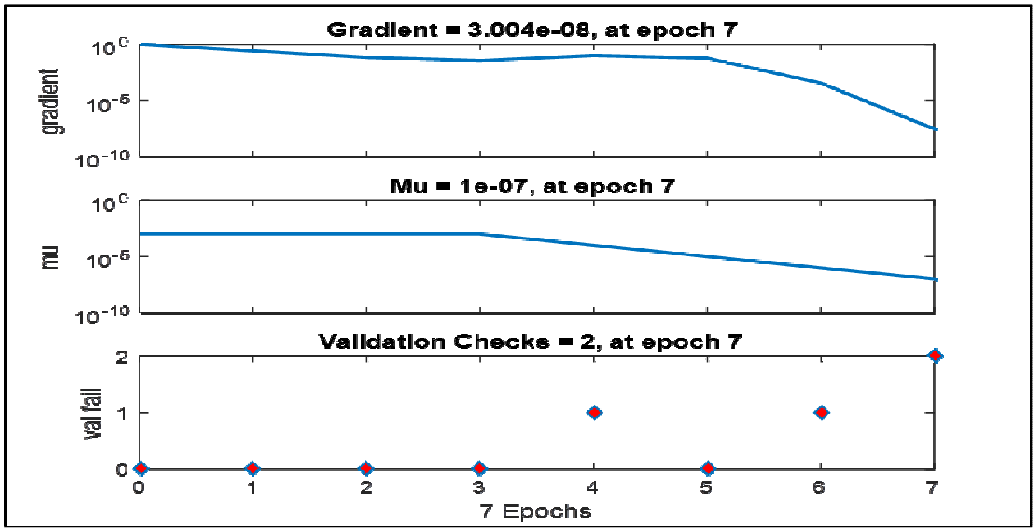

Figure 4.6: The validation check

Time series response in Figure 4:8 clearly indicates a downward trend of turbidity over time. This indicates the turbidity was predicted well within the model. The turbidity of water is expected to decrease with increased time for settlement as shown in the output-time series targent response graph.

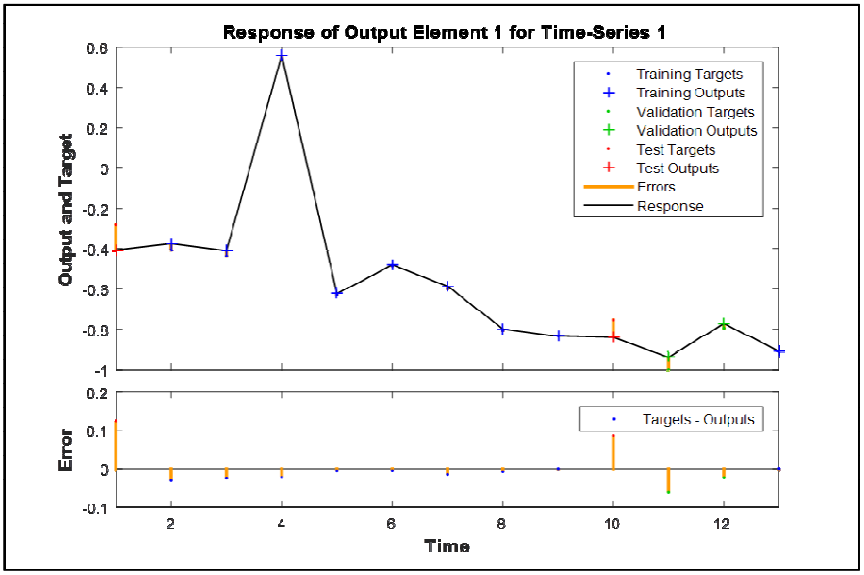

Figure 4.7: Output and time series target response

Figure 4.9 shows that all spikes are within the confidence limit. This indicates that the data is random and organised. This is true since turbidity was recorded at regular intervals of 20 minutes.

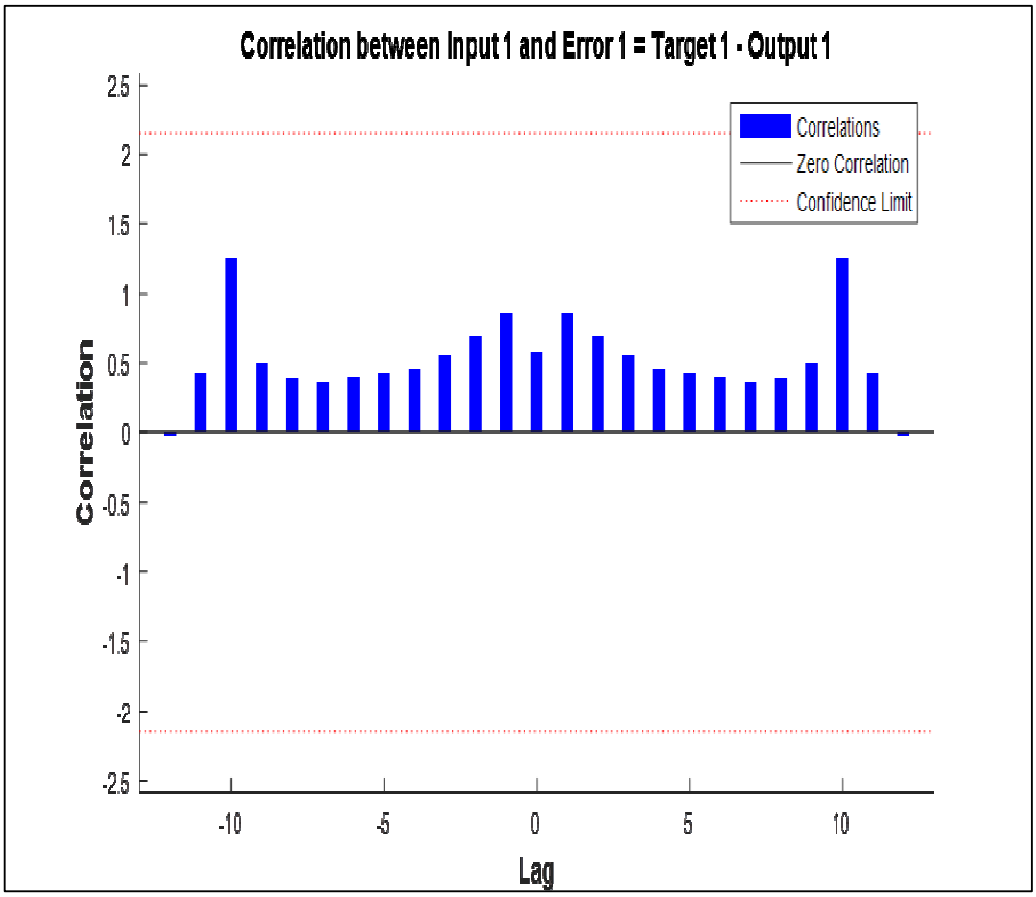

Figure 4.8: Correlation error plot graph

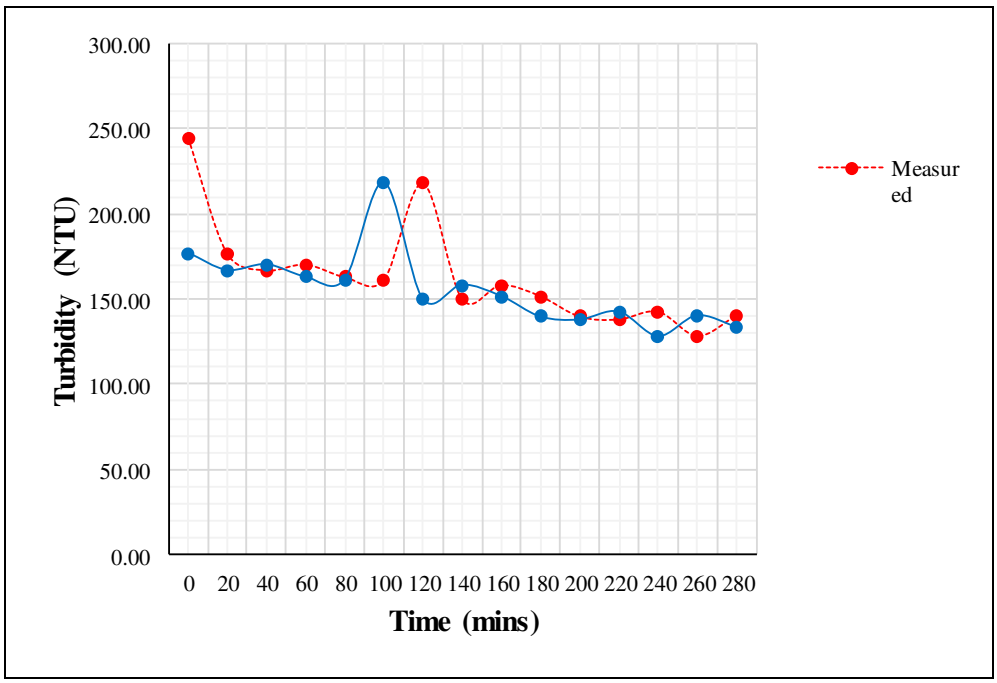

Figure 4.9: The measured and predicted turbidity

From Figure 4.11, the best line of fit shows that there is a good relationship between the observed turbidity values and the predicted turbidity values with a gradient of 0.5 hence making the model a more predictive tool for sediments settlement.

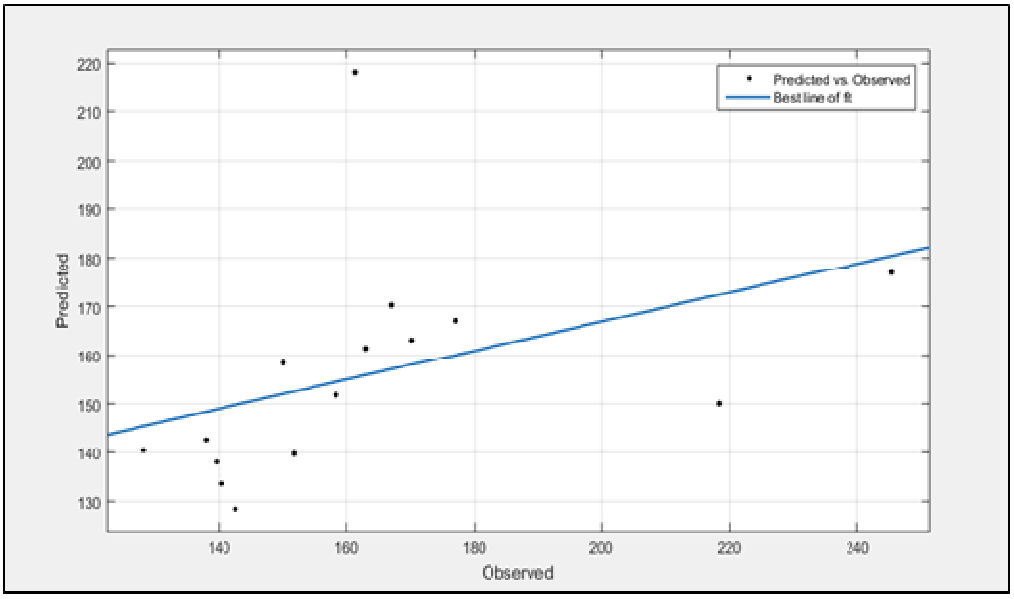

Figure 4.10: The Relationship of the observed and predicted turbidity

The coefficient of correlation for the best ANN was found to be R=0.9921 (Figure 4:5) which was similar to what Mustafa et al (2011) had found of R=0.9920 while investigating on ANN prediction of suspended sediment discharge in a River in Malaysia. Similar results were also found on data training (Table 4:8) with R=0.9999, MAE=0.1273 and Mustafa *et al*. (2011) had found 0.9999 and 0.1202 respectively. This agreement confirmed that the data was well trained and the best ANN architecture chosen. A further analysis with Nash-Sutcliffe model efficiency coefficient gave a NSE of 0.9999, which was the best amidst the four ANN.

Patil *et al.* (2016) while researching on prediction of sediment deposition in reservoirs using ANN had found almost similar results on regression with an overall value of R=0.98. He also found that the best validation performance was at epoch 6 but in this research it was epoch 5. In addition, he found the best ANN architecture as 3-10-5-1. This differs with the output of this research of 1-9-1, the reason for the difference was that Patil had used three input variables contrary to this research of two input variables. Khairi *et al*. (2015) while using ANN approach for predicting

the water turbidity level using Optical Tomography found closely found similar results where R =0.9991 and MSE= 0.1432 on training.

4.2.4 Calculation of optimum hydraulic parameters

Using Table 4.3 and Figure 4.10 the time for each turbidity drop was noted and Equation 4.2 was applied to calculate the optimum area required to settle the particle at that flow rate. The depth of the tank was considered as 0.4 m as per the physical model but this can be varied as per the designs.

To calculate for 5.7 L/min

From Figure 4:1 Optimum time to settle the particles is at 110 and 170 minutes.

Q = A x V (from Equation 4.2)

But V = AH

Where;

A = Surface area of the tank (m^2)

V = Settling velocity (m/s)

H = depth of the tank

Hence, Q = 5.7L/min so if 1 min =5.7 ($0.0057m^3$) what will be the volume in 110 minutes.

Taking H = 0.4m (tank depth)

A = 0.0057 x110/0.4 = 1.5675 m^2

For 170 minutes

A = 0.0057 x 170/0.4 = 2.4225 m^2

This means that with a settling tank of between 1.5675m^2 and 2.4225m^2 surface area the particles can be settled to the desired turbidity drop of 152.8500 NTU. This process was down for three-flow rate that is 5.7l/min, 8.7l/min and 11.1 l/min. A graph of flow rate against optimum areas was plotted as shown in Figure 4.12.

From Figure 4.12 a quadratic equation was developed for calculating the optimum surface area required to settle the particles and different flow rates.

Using Equation 4.4, the optimum surface areas for the five flow rates were calculated and the results given in Table 4.9.

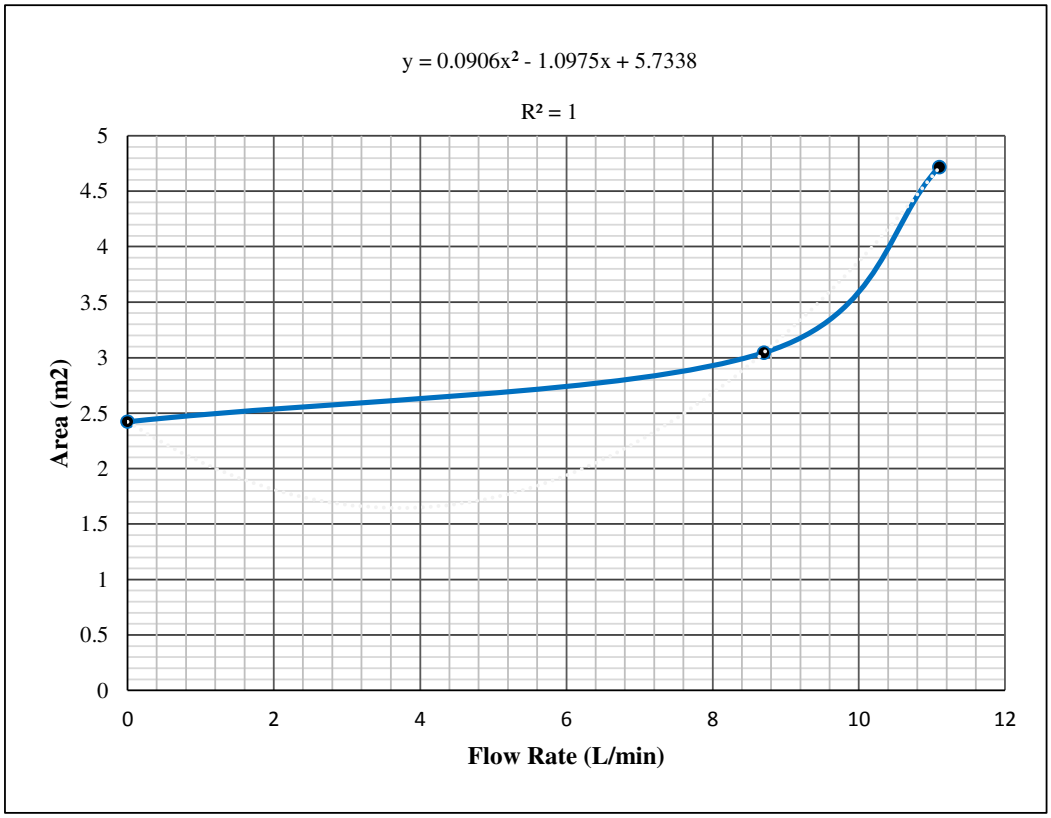

Figure 4.11: Flow rate against the optimum surface area

Equation 4.4 is given as;

$$Y = 0.0906X^2 - 1.0975X + 5.7338 \quad (0.4)$$

Where;

Y = Optimum Surface area of the tank (m^2)

X = Flow rate (L/min)

It is evident that the sediment concentration at the sludge zone increased with increase in flow rate as shown in Table 4.1. This corresponds to what (Martin, 2006) had found while researching on sediment load and sediment concentration prediction whereby the author observed that the highest sediment concentration was with high flows. (Haiyan *et al.,* 2013) drew the same conclusion where flow rate significantly affected the concentration of heavy metals in water and (Weixing *et al*., 2015) found that there was increase in turbidity and sediment density at the bottom of reservoirs during high inflow of storm runoff.

Table 4.9: Optimum tank surface area for different flow rates

Flow Rate (L/min)	Turbidity drop (NTU)	Calculated Area (m^2)	Optimum Area (m^2)
5.7	152.85	2.50	2.42
8.7	185.00	2.08	3.04
9.9	259.33	1.92	3.75
10.5	243.33	2.08	4.20
11.1	155.00	1.72	4.71

4.3 The Evaluation of Effects of Continuous Sediment Flushing

Table 4.10 shows the results on the sediment flushing in the basin

Table 4.10: **Weight of settled sediments with and without continuous flushing**

	Sediment Weight (g)				
	1st Experiment	2nd Experiment	3rd Experiment	4th Experiment	5th Experiment
Without Flushing	376.7000	382.1000	379.8000	369.9000	380.4000
With Flushing	171.8000	166.8000	174.2000	173.7000	175.2000

By applying Equation 3.4 on sediment flushing efficiency, it was found that the sediment removal from the tank without continuous flushing had an efficiency of 24.44%. While, the flushing efficiency for the tank with continuous flushing was calculated to be 65.53%. Matthew (2012) had found a flushing efficiency of sediment of about 53% on research carried at ABC's generating station in Kansas and therefore 65.5%found in this research was within the range of sediment removal efficiency of 50-70% (Lee, 2009).

CHAPTER FIVE

CONCLUSION AND RECOMMENDATIONS

5.1 Conclusion

This research was aimed at determination of optimum hydraulic design parameters of a settling basin for discrete particles in surface irrigation systems hence improving in design of irrigation water settling basin design and management. The following are the conclusions.

i. For flow rates of 5.7, 8.7, 9.9, 10.5 and 11.1 m^3/s, the critical settling velocity was 0.0034, 0.0044, 0.0024, 0.0026 and 0.0034 m/s respectively. Using stoke's law the critical settling velocities for discrete particles at different flow rates were calculated whereby it was found that the turbidity drop in a settling basin increased with the increase in flow rate. This is represented by a biquadratic equation 4.3. This developed equation can be used to calculate turbidity drop in a small-scale settling basin when the flow rate is given if it is within limits.

ii. The ANN model developed in this study performed well in predicting the sediment settlement potential with an acceptable level of confidence. ANN model with a architecture of 1-9-1 can be adapted to predict the turbidity of water in a settling basin. A quadratic equation 4.4 was developed for calculating optimum surface area required for settling discrete particles for different flow rates. The optimum areas for the five flow rates was calculated as; 5.7 L/min (2.42m^2); 8.7 L/min (3.04 m^2); 9.9 L/min (3.75 m^2); 10.5 L/min (4.20 m^2) and 11.1 L/min (4.71 m^2). And their corresponding turbidity drop as 152.85,185.00, 259.33, 243.33 and 155.00 NTU respectively.

iii. Settling tanks with continuous sediment removal have a higher sediment removal efficiency at 65.5% against 24.4% for those without a flushing

component. This shows that water flowing from the settling basin to the conveyance pipe from a settling tank without continuous flushing carry more sediment which eventually reduce the irrigation efficiency of the project and also cause regular maintenance of appurtenances within the system. .

5.2 Recommendations

i) While the limitation on the number of input variables was deliberate, it may be useful to explore other combinations of the most influential variables that may affect the sediment settling, such as water temperature, drag force and rainfall patterns of an area.

ii) For design engineers and hydrologists to predict the storage capacity of settling basins and not resulting to over designing leading to high cost of irrigation project, ANN is recommended for turbidity prediction. There is need for more research in order to improve the ANN turbidity predictive model results by investigating different topologies and training algorithm. This study used only Levenberg-Marquardt algorithm.

iii) Simulation of sediment flushing with more observed data on settling basin for small-scale irrigation projects with the use of baffles in consideration is recommended.

.

REFERENCES

Abdul, R.G., Mohammud, A.K.T., Ashfaq, A. T. (2004). Investigation of Optimal use of Canal water in Pakistan. International Conference on water resources and Arid Environment. Taxila, Pakistan.

Akif, R., & Amina, A. (2015). Optimal Artificial Neural Network modeling of sedimentation yield and runoff in high flow season of Indus River at Besham Qila for Terbela dam. *International journal of science and Research*, 4 (1), 479-483.

Al-Abed, N.A., & Whiteley, H.R. ((2002). Calibration of the hydrological simulation program FORTRAN (HSPF) model using automatic calibration and geographical information systems. *Journal of Hydrological processes*, 96, 3169-3188.

Ammar, H. K. (2008). Application of a hydrodynamic Mike 11 model for the Euphrate River in Iraq. *Slovak Journal of Civil Engineering*, 2, 1-7.

Ansari, M.A.,& Athar, M. (2013). Artificial neural networks approach for estimation of seiment removal efficiency of vortex settling basins. *Journal of Hydraulic Engineering*, 19(1),38-48.

Antle, S., Jones, J.W., & Rosenzweig, C. (2017). Towards a new generation of Agricultural system models, data and knowledge production. *Journal of Agricultural systems,* 155, 186-194.

Anzy, L., Zony, W.G.,& Kyung-Duck, S. (2016). Determination of optimal initial weights of a artificial neural networks by using the Harmony search Algorithm. *Journal of Applied Sciences*, *6*(6), 163-178.

APHA. (1975). Method 208D, Total non-filterable residue dried at 103-105^{0}C in Standard methods for examination of water and wastewater, Washington D.C: American public health Association,.

Archana, S. (2008). Artificial neural network models for estimation of sediment load in an alluvial river in India. *Journal of Aquartic Procedia*, *4,* 1070-1077.

Archana, S. & Pranshant, P. (2015). River water quality modeling using artificial neural network. *Journal of Environmental Hydrology*, *16*, 30-39.

Arnold, J.G., Williams, J. R.,& Sammons, N.B. (1990). SWRRBWQ, *A basin scale simulation model for soil and water resources management*: Texas A & M press, College station, TX.

Arnold, J.G., Engel, B.A., & Srinivasan, R. (1993). A continuous Time, Grid cell watershed model: in proceedings of Application of Advanced Technology for the management of Natural resources, *American society of Agricultural Engineers,* 17-19

ASCE Task committee on application of Artificial Neural Networks in Hydrology. (2000).Atificial neural networks in Hydrology. II Hydrological applications. *Journal of Hydrologic Engineering, ASCE*. 5(2), 124-137.

Bar-Zeev, E., Belkin, N., Liberman, B., Berman, T., & Berman-Frank, I. (2012). Rapid sand filtration pretreatment for SWRO: *Microbial maturation dynamics and filtration efficiency of organic matter*, 120-130.

Benham, B., & Ross, B. (2009).Filtration, treatment and maintenance considerations for micro-irrigations systems. Virginia state university, Petersburg, VA.

Bicknell, B.R., Imhoff, J.C., Kittle, J.L., & Donigian, A.S. (1996). *Hydrological simulation program-FORTRAN: User's manual for release 11* Davis, California: Hydrologic Engineering Center, Corps of Engineers.

Bjorneberg, D.L., & Sojka, R.E. (2002). *Irrigation Erosion processes. United States department of Agriculture*. Kimberly: Idaho.

Bouzeria, H., Ghenim, A.N., & Khanchoul, K. (2017). Using artificial neural networks for prediction of sediment loads, application to the Mellah catchment, Northeast Algeria. *Journal of Water and Land development*, *33*, 47-55. Doi: 10.1515/jwld-2017-0018.

Brownell, L.E., & Young, E.H. (2004). *Process Equipment Design*, Wiley India private limited, New Delhi.

Chan, L.W., & Fallside, F. (1987). An adaptive training algorithm for back-propagation networks. *Journal of computer speech and Language*, *2,* 205-218.

Chan, K.H., Patterson, D.W.,& Tan, C.M. (1993). Time series forecasting with neural nets; a comparative study. In *proceedings of the international conference on neural network applications to signal processing*, (P 269-274).

Chandra, R.,& Zhang, M. (2012). Cooperative coevolution of Elman recurrent neural networks for chaotic time series prediction. *Journal of Neurocomputing*, *86*,116-123.

Chang, C.L., Lo, S.L., & Hu, C.Y. (2007). An analysis of required parameters in WinVAST model for runoff simulation. *Journal of Advances in Asian Environmental Engineering, 6*(1), 7-12.

Chen, S.& Malone, R.F. (1991). Suspended solid control in recirculating Aquacultural system. In *the proceedings from Aquaculture symposium*. 170-186. Comell University. New York.

Chia-Ling, C., & Chung-Sheng, L. (2012). Parameter sensitivity analysis of ANN for predicting water turbidity. *International journal of Environmental, Chemical, Ecological, Geological and Geophysical Engineering*, *6*(10), 657-660.

Chiang, C.F., Tsai, C.T., Lo, H.M., Chao, K.P., & Pai, T.Y. (2010). Analyzing the design criteria of primary settlersof small sewerage treatment systems: A national survey in Taiwan. *Journal of Hazardous material*, *175*, 945-919.

Chintokoma, G.C., Machunda, R.L.,& Njau, K.N. (2015). Design and Optimization of sedimentation tank coupled with inclined plate settlers as a pre-treatment for ultra-filtration. *Journal of Environment and Earth Sciences, 5*(17), 140-146.

Chudley, R., & Greeno. R. (2008). Building construction hardbook 7th edition, Butterworth-Heinemann, Oxford. UK.

Chung, E.S.,& Lee, K.S. (2009). Prioritization of water management for sustainability using hydrologic simulation model and multi-criteria decision-making techniques. *Journal of Environmental management, 90*, 1502-1511.

Chutachindakate, C., & Sumi, T. (2007). Sediment yield and transportation analysis: case study on Managwa River basin, Japan. *Journal of Hydraulic Engineering*, *52*,212-219.

Cigizoglu, H.K., & Ozgur,K. (2006). Methods to improve the neural network performance in suspended sediment estimation. *Journal of Hydrology*, *317*, 221-238.

Cigizoglu, H.K. (2004). Estimation and forecasting of daily-suspended sediment data by Multi-layer perceptron. *Journal of Advances in Water Resources*, *27*, 185-195.

Clark, E.H., Havercamp, J.A., & Chapman, W. (1985). Eroding soils; the off-farm impacts. *American Journal of Alternative Agriculture*, *1*(2), 95-96.

Clemmens, A.J., Holly, F.M. (1992). Description and Evaluation of program, Duflow. *Journal of Irrigation and Drainage Engineering*, *119*(4), 724-734.

Collobert, D.A., Bergio, S., Fessat, F. (1995). Time series forecasting with neural nets; a comparative study. *In the proceedings of international workshop on application of neural networks to telecommunication,* 308-315.

Compton, J.S., Maake, L. (2007). Source of the suspended load of the upper Orange River, South Africa. *South African Journal of Geology*, *110*, 339-348.

Concha, F., Burger, R. (2002). A century of research in sedimentation and thickening. *KONA powder and particle Journal*, *20*, 38-70.

Crites, R., Tchobanoglous, G. (1998). *Small and decentralized wastewater management systems*. The McGraw Hill companies. Boston, Massachusetts.

Csabragi, A., Molnar, S., Tanos, P., Kovacs, J. (2015). Forecasting of dissolved oxygen in the River Danube using neural networks. *Journal of Hungarian Agricultural Engineering*, *27*, 38-41.

Daliakopoulos, I.N., Coulibaly, P., Tsanis, I.K. (2005). Ground water level forecasting using artificial neural networks. *Journal of Hydrology*, *309*, 229-240.

Davey, N., Edwards, T., Frank, R.J., Tansley, D.S.W. (1997). Traffic trends analysis using neural networks. *In proceedings of the international workshop on application of neural networks to telecommunication*, 157-164.

Delft Hydraulics (1994). Delft software Australia. Milton Qld 4064. Netherlands.

Demuth, H., Baele, M. (2002). Neural networks toolbox for use with MATLAB version 4-Users' guide. The Mathworks Inc.

Dinshaw, N.C., Wytze, S. (1993). Informed use and potential pitfalls of canal models. *Journal of Irrigation and Drainage Engineering*, *119*(4), 312-323.

District water office (2005). Flow rates for River Kirurumwe. Design report for Kiriku-Kiende irrigation project.

Dorffner, G. (1996). Neural networks for time series processing. *Journal of Neural network world*, *4*(96), 447-468.

Doroodchi, E., Zhou, J., Fletcher, D., Galvin, K.P. (2006). Particle size classification in a fluidized bed containing parallel inclined plates. *Journal of Mineral Engineering*, *19*, 162-171.

Ehasan, R., Mohamed, M., Saeed, R. (2010). Sensitivity Analysis of river flood routing model to input data. *Journal of Environmental sciences and Development*, *1*(3), 256-259.

Engel, B. A., Srinivasan, R., Arnold, J.G., Rewerts, C., Brown, S.J. (1993). Non-point Source pollution modeling using models integrated with GIS. *Journal of Water science Technology*, *28*(3), 685-690.

EPA (2012). *Turbidity in water. Monitoring and Assessment,* Pennsylvannia, Washington: EPA

EPA (2003). *Wastewater technology fact sheet screening and grit removal. United States environmental protection Agency*. Pennsylvannia, Washington.EPA

Emamgholizadeh, S., Kashi, H., Marofpoor, I., Zalaghi, E. (2014). Prediction of water quality parameters of Karoon River, Iran by artificial intelligence based models. *International Journal of Environmental Science and Technology*, *11*(3), 645-656.

Engelbrecht, A. (2007). *Computational intelligence: An introduction*, (2nd Ed.) New York: John Wiley and Sons

Fuhrman, S.E., Levier, C. (1990). The cascade-correlation learning architecture. *In advanced in neural information processing systems 2*, 524-532.

FAO. (2009). Coping with a changing climate; consideration for adaption and mitigation in Africa, Rome, Italy.

FAO. (2006). *Manual for Participatory Rapid Diagnosis and Action planning for Irrigated Agriculture*, Rome, Italy.

FAO. (2003). *Unlocking the Productivity of Agricultural Water Management to raise productivity*, Rome, Italy.

FAO. (2000). *Socio-Economic Impact of Irrigation development in Zimbabwe. Case study of ten irrigation schemes*. Harare, Zimbabwe.

Faraway, J., Chatfield, C. (1998). Time series forecasting with neural networks: A comparative study using airline data. *Journal of Applied Statistics*, *47*, 231-250.

Faro, D.O. (2010). A hybrid neural network and arima model for water quality time series prediction. *Journal of Engineering Applications of Artificial Intelligence*, *23*(4), 586-594.

Fausset, L.V. (1994). *Fundamentals neural networks: Architecture, algorithms and applications,* Prentice-Hall Englewood cliffs. New Jersey.

Fereres, E., & Maria, A.S. (2007). Deficit irrigation for reducing agricultural water use. *Journal of Experimental botany*, *58*(2), 147-159.

Fondriest, E. (2014). *Turbidity, Total suspended solids and water clarity. Fundamentals of Environmental measurements*.

Fornshell, G. (2000). *Settling basin design, Western Regional Aquculture Center. Publication no.106*. University of Washington, USA.

Frean, M. (1991). The upstart algorithm; SA method for constructing and training feed forward neural networks. *Journal of neural computation, 2*(2), 198-209.

Gagliardi, F., Alvisi, S., Franchini, M., & Guidorzi, M. (2017). A comparison between pattern based and neural network short term water demand forecasting models. *Journal of Water science and Technology*, *17*(3), 223-336.

Garcia, L.A., & Shigidi, A. (2006). Using Neural networks for parameter estimation in ground water. *Journal of Hydrology*, *318*, 215-231.

Gaya, M.S., Zango, M.U., Yusuf, L.A., Mustapha, M., Muhammad, B., Sani, A., Tijjani, A., Wahab, N.A., & Khairi, M.T.M. (2017). Estimation of Turbidity in water treatment plant using Hammerstein-Weiner and Neural network technique. *Indonesian Journal of Electrical Engineering and Computer science*, *5*(3), 666-672.

German, S., Bienenstock, E., & Doursat, R. (1992). Neural networks and the Bias-Variance Dilemma. *Journal of Neural computation. 4,* 1-58.

Ghamari, S., Borghei, A.M., Rabbani, H., Khazaei, J., & Basati, F. (2010). Modeling the terminal velocity of Agricultural seeds with ANN. *Journal of Agricultural Research*, *5*(5), 389-398.

Ghawi, A.H., & Kris, J. (2012). *A computational fluid dynamics model of flow and settling in sedimentation tanks*. Applied computational fluid dynamics, Prof. Hyoung Woo (Ed).

Ghorbani, M.A., Khatibi, R., Goel, A., Fazelifard, M.H., & Azani, A. (2016). Modeling River discharge time series using support vector machine and artificial neural networks. *Journal of Environmental earth sciences*, *75*(8), 685-998.

Ghumman, A. R., Youstry, M.G., Sohail, A.R., & Watanabe, K. (2011). Runoff forecasting by artificial neural networks and conventional model. *Journal of Alexandria Engineering*, *50*(4), 345-350.

G.O.K. (2005). Practice manual for water supply services in Kenya. Ministry of water and Irrigation, Kenya.

Gregory, R. & Edzwald, J. (2010). Sedimentation and flotation; chapter 9 in water quality and sediment, (6th Ed.). AWWA & McGraw Hill.

Guiana, Z., Yuzhu, Z., Jiliang, R., Tuanhui, Q., & Tao, W. (2012). Flow Simulation and Analysis in a vertical-flow sedimentation tank. 2012 International conference on future energy, Environment and Materials. *Energy Procedia 16*, 197-202.

Habtamu, T.K. (2009). Payment for Environmental service to enhance use efficiency and labour force participation in managing and maintaining irrigation infrastructures. *Master thesis presented in the faculty of the Graduate school of Cornel University*.

Haiyan, L., Liang, L., Mingyi, L & Xiaoran, Z. (2013). Effects of PH, Temperature, dissolved oxygen and Flow rate on Phosphorous release processes at the sediment and water interface in storm water. *Journal of Analytical methods in Chemistry*. Doi. Org/10.1155/2013/104316.

Hammerstrom, D. (1993). Working with Neural networks. *Institute of Electrical and Electronics Engineers*. *30*(7), 46-53.

Hecht-Nielsen, R. (1988). Neuro-computing, picking the human brain. *Institute of Electrical and Electronics Engineers*. *25*(3), 36-41.

Hegazy, T., Fazio, P., & Moselhi, O. (1994). Developing practical neural network applications using back-propagation. *Journal of microcomputers in Civil Engineering, 9,* 145-159.

Herbert, B., Clifford, M.M., & Hammond, M. (2002). The changing face of irrigation in Kenya: *Opportunities of anticipating change in Eastern and Southern Africa.* International Water Management Institute.

Hertz, J.A., Krogh, A., & Palmer, R.G. (1991). Introduction to the theory of neural computation, Addison-wesely publishing company, Red wood city, California.

Heydari, M.M., Mahmood, S.B., Heydari, A.K., & Hossein, S. (2013).The effect Angle of baffle on the performance of settling basin. *Journal of World Applied sciences*, *21*, 829-837.

Hoffman, A.C., & Stein, L.E. (2008). Gas cyclones and Swirl Tubes, second edition, Springer Berlin Heidelberg, New York.

Holger, R. M., & Graeme, C. D. (1996). The use of ANN for prediction of water quality parameters. *Journal of Water Resources Research*, *32* (4), 1013-1022.

Home, P.G., & Ngugi, H. N. (2012). A comparative evaluation of Irrigation efficiencies for smallholder irrigation schemes in Murang'a South District page 193. Paper presented on proceedings of the 2012 *JKUAT scientific, Technological and Industrialization conference.* Nairobi: Kenya

Hutchins, R.G. (1995). Neural network topologies and training algorithms in non-linear system identification. *Journal of intelligent systems for 21st century*, *3*, 2512-2515.

Imbenzi, J.S., Mutua, B.N., & Raude, J.M. (2014). A review for hydraulic analysis of Irrigation canals using HEC-RAS model: A case study of Mea irrigation scheme, Kenya. *Journal of Hydrology*, *2*(1), 1-5. Doi: 10.11648/j.hyd.20140201.11.

Isam, A.H., Najla, M., Fatima, S., Sahar, R., Mohammed, Z.A., Attwas, S. H., Yasmine, A., & Mohammed, A. (2013). Effectiveness Design parameters for Sedimentation of Calcium carbonate slurry. *International Journal of Chemical, Environmental and Biological Sciencies*, *1*(2), 224-228.

Islam, M.A., Amin, M.S.A., Hoinkis, J. (2013). Optimal design of an activated sludge plant, theoretical analysis. *Journal of Applied Water Science*, *3*, 375-386.

Jack, P.C. (2007). Sensitivity analysis and related analysis: A review of some statistical techniques. *Journal of Statistical Computation and Simulation*, *57*(4), 111-142.

Jacobs, R.A. (1988). Incemental rates of convergence through learning rate adaptation. *Journal of neural networks, 1,* 295-307.

Jacomino. V.M.F., Fields, D.E. (1997). A critical approach to the calibration of a water shed model. *Journal of American water Resources Association, 33*(1), 143-154.

Bicknell, Brian R., John C. Imhoff, John L. Kittle Jr, Anthony S. Donigian Jr, and Robert C. Johanson. "Hydrological simulation program-FORTRAN. user's manual for release 11." *US EPA* (1996).

Josephine, K.W. N. (2009). Challenges of water resource management and food production in a changing climate in Kenya. *Journal of Geography & Regional Planning, 2(*4), 97-103.

Jahseen, R.H.A. (2009). Efficiency of sediment settling basins. *Journal of water Resources and Hydraulic Engineering*, *14*(2), 2025-2030.

Jain, S.K. (2001). Development of integrated sediment rating curves using ANN. *Journal of Hydraulic engineering*, *127*(1), 30-37.

Jin, P.K., Wang, X.C., Hu, G. (2006). A dispersed ozone flotation (DOF) separators for tertiary wastewater treatment. *Journal of water science, 53*(9), 151-157.

Jin, X., Jin, P., Wang, X. (2015). A study on the effects of ozone dosage on dissolved-ozone flotation (DOF) process performance. *Journal of water science technology*, *71*(9), 1423-1428. Doi 10.2166/wst.2015.115.

Jones, J. W., Antle, J.M., Basso, B. (2016). Brief history of Agricultural system modeling. *Journal of Agricultural systems*, *155*, 240-254.

Juan, C., Wang, G., Mao, T., Sun, X. (2017). Artificial neural networks model based simulation of the runoff variation in response to climate change on the Qinghai-Tibet plateau in China. *Journal of Advances in Meteorology*, 1-13.

Jury, W.A., Vaux, H. (2005). The role of science in solving the World's emerging water problems. *Proceedings of the National Academy of Sciences of the USA*, *102*(44), 15715-15720. Doi: 10.1073/pnas.0506467102.

Kanda, E. K., Kipkorir, E.C., Kosgei, J.R. (2016). Dissolved oxygen modeling using artificial neural networks: A case of River Nzoia, lake Victoria basin, Kenya. *Journal of Water security*, *2*, 1-7.

Kangau, S.N., Home, P.G., Gathenya, J.M. (2012). Performance and economic evaluation of pumped irrigation system. *Journal of Agriculture, Science and Technology*, *14*(2), 601-606.

Karina, F.Z., Mwaniki, A.W. (2011). *Irrigation Agriculture in Kenya. Think Interactive limited*. Nairobi-Kenya.

Khairi, M.T.M, Ibrahim, S., Yunus, M.A., Faramarzi, M., & Yusuf, Z. (2015). Artificial neural networks approach for predicting the Water Turbidity level. *Arabian Journal for Science and Engineering*, *41*(9), 3369-3379.

Khalil, B.M., Awadallah, A.G., Karaman, H., & El-Sayed, A. (2012). Application of artificial neural networks for prediction of water quality variables in the Nile Delta. *Journal of Water Resources and Protection*, *4*(6), 388-394.

Khan, M.Y.A., Hasan, F., Panwar, S., & Chakrapani, G.J. (2016). Neural network model for discharge and water level prediction for Ramganga River catchment of Ganga basin, India. *Hydrological science Journal*, *61*(11), 2084-2095.

Kim, T.W., & Valdes, J.B. (2003). Nin-linear model for drougt forecasting based on a conjunction of wavelet transforms and neural networks. *Journal of Hydrologic Engineering*, 8(6), 319-328.

Kisi, O., Murat, A. (2011). Modeling dissolved oxygen (DO) concentration using different neural networks techniques. In: *International Balkans conference on challenges of Civil Engineering*, Tirana, Albania.

Kolen, J.F., & Pollack, J.B. (1990). Back propagation is sensitive to initial conditions. *Journal of Complex systems 4*, 269-280.

Koluvek, P.C., Tanji, K.K., & Trout, T.J. (1993). Overview of soil erosion from Irrigation. *Journal of Irrigation and Drainage Engineering*, *119*(6), 929-946.

Kumar, M., Raghuwanshi, N.S., & Sigh, R. (2011). Artificial Neural Networks approach in evapotranspiration modeling. *Journal of Irrigation Science*, *29*, 601-606. DOI 10.1007/s00271-0010-0230-8.

Kwok, T.Y., & Young, D.Y. (1995). *Constructive feed forward neural networks for regression problems. A survey technical report presented to Hong Kong University of science and Technology. Clear water Bay*. Kowloon.

Lallahem, S., & Hani, A. (2017). Artificial neural networks for defining the water quality determinants of groundwater abstraction in coastal aquifer. *AIP conference preceeedings*, *1814* (1). Doi: http//dx.doi.org/10.1063/1.4976232.

Langland, M., & Cronin, T. (2003). *A summary report of sediment processes in Chesapeake Bay and watershed. In water resources investigation report* 03-4123, New Cumberland.

Lazarovitch, N., Poulton, M., Furman, A., & Warrick, A.W. (2009). Water distribution under trickle Irrigation predicted using Artificial Neural Networks. *Journal of Irrigation Engineering Maths*, 64, 929-946. DOI 10.1007/sl0665-009-9282-2.

Lee, C.C., & Shur, D.L. (2007). Handbook of Environmental Engineering Calculations, 2nd Edition; McGraw-Hill, New York.

Lee, S., Yoon, H., Byeong, H., & Lee, K. (2017). Application of artificial neural network model for ground water level forecasting in a river Island with artificial influencing factors. *Geophysical research, 19.* EGU2017-11782-1.

Lee, T.L., & Jeng, D.S. (2002). Application of artificial neural networks in tide forecasting. *Journal of Ocean Engineering software*, *40*, 1200-1206.

Lee, T.L. (2009). Prediction of typhoon storm surge in Taiwan using ANN. *Journal of Advances in Engineering*, *29*, 1003-1022.

Leonard, H.O., & Timothy, N. (2016). *A review paper on large-scale irrigation in Kenya. A case study of maize.* Tegemeo Institute of Agricultural policy and Development, Egerton-Kenya.

Lin, B., & Namin, M.M. (2005). Modeling suspended sediment transport using integrated Numerical and ANNs models. *Journal of Hydraulic Research*, *43*, 302-310.

Liyanage, D.D., Thamali, R.J., Kumbalatara, A.A., Weliwita, J.A., & Witharana, S. (2016). An analysis of Nanoparticles settling times in liquids. *Journal of Nanomaterials*, 1, 1-7.

Logan, C.P. (2012). *Assessing performance characteristics of sediment basins constructed in Franklin County.* A MSC. Thesis submitted to the graduate Faculty of Auburn University. Alabama.

Lohani, A.K., & Krishan, G. (2015). Ground water level simulation using artificial neural networks in Southeast Punjab, India. *Journal of Geology and Geophysics*, *4*, 206-214.

Maanen, B.V., Coco, G., Bryan, K.R., & Ruessink, B.G. (2010). The use of artificial neural networks to analyze and predict alongshore sediment transport. *Journal of Non-linear processes in Geophysics*, *17*, 395-404.

Brownell, L. E., & Young, E. H. (1959). *Process equipment design: vessel design*. New York: John Wiley & Sons.

Maier, R.H., Jain, A., Dandy, C.G., & Sudheer, K.P. (2010). Methods used for development of Neural Networks for prediction Water resources variables in River systems: Current status and future directions. *Journal of Environmental modeling and Software. 25*(8), 891-909.

Maier, R.H., & Dandy, C.G. (2000). Neural Networks for prediction and forecasting of water resources variables. *Journal of Environmental modeling and Software. 15,* 101-124.

Al Shamisi, M. H., Assi, A. H., & Hejase, H. A. (2011). Using MATLAB to develop artificial neural network models for predicting global solar radiation in Al Ain City–UAE. In *Engineering education and research using MATLAB*. InTech.

Malaterre, P. O., & Baume, J. P. (1997, April). SIC 3.0, a simulation model for canal automation design. In *International Workshop on the Regulation of Irrigation*

Canals: State of the Art of Research and Applications, RIC97, Marrakech (Morocco) (Vol. 1, pp. 68-75).

Maren, A.C.H., & Pap, R. (1990). *Handbook of Neural computing applications,* San Diego, California: Academic Press

Margarita, J., Jaime, M., & Arturo, T. (2017). Model of suspended solids removal in the primary sedimentation tanks for the treatment of urban wastewater. *Journal of Water, 9*,448-460. Doi: 10.3390/w9060448.

Martin, B. (2006). Sediment load and suspended Sediment concentration prediction. *Journal of soil and water Resources*, *1*(1), 23-31.

Masters, T. (1993). *Practical neural network recipes in C++*, San Diego. California: .Academic press,

Mati, B. M. (2011). Optimizing Agricultural water Management for green revolution in Africa. Innovations as key to the green revolution in Africa. Springer, 83-94.

Matthew, D.B. (2012). Operational performance of sedimentation basins. A master thesis submitted in University of Kansas.

Mengistie, D., & Kidane, D. (2016). Assessment of the impact of small-scale Irrigation on Household Livelihood improvement at Gubalafto District, Ethiopia. *Journal of Agriculture*, *27* (6), doi: 10.3390.

Merkley, G. P. (1995). A hydraulic simulation model for unsteady flow in branching canal networks. Utah State University, Logan, USA.

Metcalf, E., Tchobanoglous, G., Burton, F.L. &, Stensel, H.D. (2003). *Wastewater Engineering : Treatment and resource recovery*. McGraw-Hill: London, UK.

McCelland, J.L., & Rumelhart, D.E. (1988). *Explorations in parallel distributed processing*, MIT press, Cambridge.

McCulloch, W.S.,&b Pitts, W. (1943). A logical calculus of ideas imminent in nervous activity. *Journal of Bulletin and mathematical Biophysics, 5*, 115-133.

Michelbach, S., Wohrle, C. (1994). Settleable solids from combined sewers: Settling, storm-water treatment and Sedimentation rates in rivers. *Journal of water Science and Technology, 29*(2), 95-102.

Mohamed, A.S. (2003). *Use of ANN for predicting settlement of shallow foundations on cohensionless soils*. Thesis presented in the university of Adelaide, school of Civil and Environmental Engineering.

Mohd, F.M., Hafizan, J., Nuraainaa, R., Isahak, M., & Norlafifah, R. (2011). Artificial Neural Networks comined with sensitivity analysis as a prediction model for water quality index in Juru River, Malaysia. *International journal of Environmental protection*, *1*(3), 1-8.

Montano, J.J., & Palmer, A. (2003). Numeric sensitivity analysis applied to feedforward neural networks. *Journal of neural computing and applications*, *12*, 119-125.

Moriasi, D.N., Arnold, J.G., Van Liew, M.W., Bingner, R.L., Harmel, R.D., & Veith, T.L. (2007). Model evaluation guidelines for systematic quantification of accurancy in watershed simulations. *ASABE, 50*(3), 885-900.

Moselhi, O., Hegazy, T., & Fazio, P. (1992). Potential applications of neural networks in construction. *Journal of Civil Engineering*, *19*, 521-529.

Mubiru, J. (2008). Predicting total solar irradiation values using artificial neural networks. *Journal of Renewable Energy*, *33*(10), 2329-2332.

Muhanned, A., & Mohammed, R. (2013). Studying the factors affecting the settling velocity of solid particles in Non-Newtonian fluids. *Nahrain University, College of Engineering Journal, 16*(1), 41-50.

Murphy, S. (2007). General information on solids. USGS water quality monitoring, City of Boulder. http://bcn.boulder.co.us/basin/data/NEW/info/TSS.html.

Mukherjee, A. & Deshpande, J.M. (1997). Modeling initial design process using ANN. *Journal of computing in Civil Engineering*, *11*(2), 145-146.

Mustafa, M.R., Isa, M.H., & Rezaur, R.B. (2011). A comparison of artificial neural networks for prediction of suspended sediment discharge in River-A case study

in Malaysia. *Journal of Civil, Environmental, Structural, Construction and Architectural Engineering*, *5*(9), 368-372.

Nagy, H. M., Watanabe, K., & Hirano, M. (2002). Prediction of sediment load concentration in Rivers using ANN model. *Journal of Hydraulic Engineering*, *128*(6), 588-595.

Najah, A., El-Shafie, A., Karim, O. A., Jaafar, O. & El-Shafie, A. H. (2011). An application of different artificial intelligences techniques for water quality prediction. *International Journal of the Physical Sciences*, *6*(22), 5298-5308.

Nash, J.E., & Sutcliffe, J.V. (1970). River flow forecasting through conceptual models: part 1. A discussion of principles. *Journal of Hydrology*, *10*(3), 282-290.

Ngenoh, E., Kirui, L.K., Mutai, B.K., Maina, M.C. (2015). Economic Determinants of the Performance of Public Irrigation Schemes in Kenya. *Journal of Development and Agricultural Economics, 7*(10), 344-352.

Nikolos, I. K., Stergiadi, M., Papadopoulou, M.P., & Karatzas, G. P. (2008). Artificial neural networks as an alternative approach to ground water numerical modeling and environmental design. *Journal of Hydrological processes*, *22,* 3337-3348.

Nourani, V., Alami, M.T., & Aminfar, M.H. (2009). A combined neural-wavelet model for prediction of Ligvanchai watershed. *Journal of Engineering in Applied Artificial Intelligence*, *22*, 466-472.

Onyando, J.O., Kisoyan, P., & Chemelil, M.C. (2005). Estimation of potential soil erosion for River Perkerra catchment in Kenya. *Journal of Water Resources management, 19*(2), 133-143.

Palani, S., Liong, S.Y., & Tkalich, P. (2008). An ANN application for water quality forecasting. *Journal of Marine pollution bulletin*, 56(9), 1586-1597.

Pande, P.K. (2015). *Sediment management in Hydropower plants. International conference on Hydropower for sustainable development*. New Delhi: Dehradun.India.

Patil, R.A., & Shetkar, R.V. (2016). Prediction of sediment deposition in reservoir using artificial neural networks. *International Journal of Civil Engineering and Technology, 7*(4), 1-12.

Pedras, C.M.G., Pereira, L.S., & Gonçalves, J.M. (2009). A decision support system for design and evaluation of micro-irrigation systems. *Journal of Agricultural water management*, Amsterdam, *96*, 691 – 701.

Qingzhen, Y., Xiaojing, W., Huimin, J., Hongtao, C., & Zhigang, Y. (2015). Characterization of particle size fraction associated with heavy metals in suspended sediments of Yellow River. *International Journal of Environmental Research and Public health*, *12*(6), 6725-6744. Doi 10.3390/ijerph120606725.

Raghuwanshi, N.S., Sigh, R., & Reddy, L.S. (2006). Runoff and sediment yield modeling using Artificial Neural networks. *Journal of Hydrologic Engineering, 11*(1), 133-138.

Rahim, A., & Amina, A. (2015). Optimal; Artificial neural networks modeling of sedimentation yield and run-off in high flow season of Indus River at Besham Qila for Terbela dam. *International journal of Science and Research*, *4*(1): 479-483.

Rai, R.K., & Mathur, B.S. (2008). Event-based sediment yield modeling using ANN. *Journal of water resources management*, *22*(4), 423-441.

Raju, K.G., Kothyari, U.C., Srivastar, S., & Saxena, M. (1999). Sediment Removal Efficiency of settling basins. *Journal of Irrigation and Drainage Engineering*, *125*(5), 308-314.

Rajurkar, M.P., Kothyari, U.C., & Chaube, U.C. (2002). Artificial neural network for daily rainfall-runoff modeling. *Journal of Hydrological sciences*, *47*(6), 865-877.

Ramapulana, N. (2011). *Artificial Neural Networks modeling of flood prediction and early warming.* Master thesis presented in University of Free State. South Africa.

Ranjithan, S., Eheart, J.W, & Garrret, J.H. (1993). Neural network based screening for groundwater reclamation under uncertainty. *Journal of water resources*, *29*(3), 563-574.

Reckendorf, F. (1995). Sedimentation in Irrigation water bodies Reservoirs, canals and ditches. A *paper presented to United States department of Agriculture*. Paper no. 5.

Rehman, H., Chaudhry, M.A., & Akhtar, N. (2009). Assessment of sediment flushing efficiency of reservoirs. *Pakistan Journal of Sciences*, *61*(3), 181-187.

Revel, N.M.T., Ranasari, L.P., Rathnayake, R.M., & Pathirana, K.P. (2013). Estimation of sediment trap efficiency in reservoirs. *European international Journal of Science and Technology, 2*(10), 134-146.

Reynolds, T., & Richards, P. (1996). Unit operations and processes in Environmental Engineering. PWS publishing company. Boston, Massachusetts.

Rietjes, T.M., & De Vos, N.J. (2008). Multi objective training of artificial neural networks for rainfall-runoff modeling, *Journal of water Resources, 44,* 365-415.

Ripley, B.D. (1996). *Pattern recognition and neural networks*, Cambridge: Cambridge university press.

Rumelhart, D. E., Hinton, G. E., & Williams, R. J. (1985). *Learning internal representations by error propagation* (No. ICS-8506). California Univ San Diego La Jolla Inst for Cognitive Science..

Saenyi, W.W. (2002). *Sediment management in Masinga reservoir, Kenya*. A PhD thesis submitted at Insitute for management, Hydrology and Hydraulic Engineering. University of Agricultural Sciences (BOKU), Vienna, Austria.

Saharia, M., Bhattacharjya, R.K. (2012). Geomorphology based time lagged recurrent neural networks for runoff forecasting. *Journal of Civil Engineering*, *16*(5), 862-869.

Sarle, W.S. (1994). In neural networks and statistical models, in *proceedings of the Nineteenth Annual SAS users' Group International conference, SAS institute*: 1538-1550.

Sasikala, S., Muthurama, G. A. (2016). Laboratory study of the treatment of turbidity and Total hardness bearing synthetic wastewater/Ground water using Moringa Oleifera. *Journal of Industrial Chemistry*, 2, doi 10.4172/2469-9764.

Schladow, S.G., Hamilton, D.P. (1997). Prediction of water quality in lakes and reservoirs: Part II-model calibration, sensitivity analysis and application. *Journal of Ecological modeling*, *96*, 111-123.

Sengorur, B., Koklu, R., Ates, A. (2015). Water quality assessment using artificial intelligence techniques: A case study of Melen River, Turkey. *Journal of Water Quality Exposure and Health*, *7*(4), 469-490.

Shaopei, L., Boru, D. (1998). *Modeling of Fuzzy machine learning and fuzzy neural networks in structural design*. *Uncertainity modeling and analysis in Civil Engineering*, New York: CRC press,

Sharma, N., Zakaullah, M., Tiwari, H., & Kumar, D. (2015). Runoff and sediment yield modeling using ANN and support vector machines: A case study from Nepal watershed. *Journal of Modeling Earth Systems and Environment*, *1,* 23-31.

Shen, H.W. (2010). Flushing sediment through reservoirs. *Journal of Hydraulic Research*, *37(*6), 743-757.

Shetab-Boushehri, M. S., Shetab-Boushehri, S. (2010). Design of settling basins in Irrigation network using simulation and mathematical programming. *Journal of Irrigation and Drainage Engineering*, *136* (2), 99-106.

Shrestha, B. V. (2012). 3D *Numerical investigation on settling basin layout.* An MSC. Thesis submitted to Norwegian University of Science and Technology.

Sietsma, J.,& Dow, R. J. F. (1991). Creating artificial neural networks that generalize. *Journal of neural networks*, *4*, 67-79.

Sigh, G.,& Arun, K. (2013). A review of de-silting basins used in small hydropower plants. *International Journal of Emerging Technology and Advanced Engineering*, *3*(5), 440-443.

Singh, G., & Kumar, A. (2016). Performance evaluation of desilting basins of small hydropower projects. *Journal of Hydraulic Engineering*, *22*(2), 135-141.

Sinnott, R.K. (2005). Coulson and Richardson's chemical engineering series, Chemical Engineering Design, volume 6, Fourth edition, Butterworth-Heinemann. Oxford.

Spellman, F.R. (2009). Hard book of water and wastewater treatment plant operations, CRC press, second edition.

Sultan, Q., & Naik, M.G. (2015). Estimation of trap efficiency of Sriramsagar reservoir. *International Journal of Research in Engineering and Technology*, *4*(11), 116-122.

Sunita, S.T., & Sonal, C. (2014). Assessment of coagulation efficiency of Moringa Oleifera and Okra for treatment of turbid water. *Archives of Applied Sciences Research*, *6*(2), 24-30.

Tabatabaei, Z., Mahvi, A. H., & Saeidi, M.R. (2007). Advanced wastewater treatment using two-stage sand filtration. *European Journal of scientific Research*, *17*(1), 48-54.

Toth, E., Brath, A., & Montanari, A. (2000). Comparison of short-term rainfall prediction models for real-time flood forecasting. *Journal of Hydrology*, *239*, 132-147.

Touretzky, D.S., & Pomerleau, D.A. (1998). What is hidden in the hidden layer? *Byte*,, 227-233.

Tymvios, F. S., Michaelides, S. C., & Skouteli, C. S. (2008). Estimation of surface solar radiation with artificial neural networks. In *modeling solar radiation at the earth's surface* (pp. 221-256). Springer Berlin Heidelberg.

Pappenberger, F., Beven, K., Horritt, M., & Blazkova, S. (2005). Uncertainty in the calibration of effective roughness parameters in HEC-RAS using inundation and downstream level observations. *Journal of Hydrology*, *302*(1), 46-69.

UNESCO. (2011). Sediment issues and sediment management in large river basins. Interim case study synthesis report.

Vahid, N. (2009). Using Artificial neural networks for sediment load forecasting of Talkherood River mouth. *Journal of Urban and Environmental Engineering*, *3*(1), 1-6. Doi: 10.4090/juee. 2009. V3n1.001006.

Valipour, M. (2015). Future of Agricultural water management in Africa. *Journal of Soil Science*, *61*(7), 907-927.

Vicente, H., Couto, C., Machado, J., Abelha, A., & Neves, J. (2012). Prediction of water quality parameters in a reservoir using artificial neural networks. *International Journal of Design & Nature and Eco-dynamics*, 7(3), 310-319.

Viska, M. (2011). 5-10. *Separator vessel selection and sizing* Sri Perkasa 2, Malaysia: Jalan

Vitela, J.E., & Reifman, J. (1997). Premature saturation in back propagation networks-mechanism and necessary conditions. *Journal of neural networks*, *10,* 721-735.

Walker, S. (1996). *Modeling nitrate in Tile-Drained watersheds of East-Central Illinois.* PhD. Thesis, University of Illinois at Urbana-Champain.

Walling, D.E., & Fang, D. (2003). Recent trends in the suspended sediment loads of the world's rivers. *Journal of Global and planetary change*, *39*, 111-126.

Wambua, R.M., Mutua, B.M., & Raude, J.M. (2016). Prediction of missing Hydro Meteorological data series using artificial neural networks for upper Tana River basin, Kenya. *American Journal of water Resources*, *4*(2), 35-43. Doi 10.12691/ajwr-4-2-2.

Wambua, R.M., Mutua, B.M., & Raude, J.M. (2014). Drought forecasting using Indices and Artificial neural networks for upper Tana River basin, Kenya. A

review concept. *Journal of Civil and Environmental Engineering*. *4*(4), 1-12. Doi: 10.4172/2165-784X.1000152.

Wambua, R.M., Mutua, B.M., & Raude, J.M. (2014). Performance of Standardized precipitation index (SPI) and effective drought index (EDI) in drought forecasting using artificial neural networks for upper Tana River basin, Kenya. *Journal of Engineering Research and Technology. 3* (11), 547-556.

Wang, Y., Guo, S., Xiong, L., & Liu, D. (2015). Daily forecasting model based on ANN and Data preprocessing techniques. *Journal of Water*, *7*(8), 4144-4160.

Wasserman, P.D. (1989). *Neural computing theory and practice,* New York.: Van Nostrand Reinhold,

Weiss, S., & Kulikowski, C.A. (1991). *Computer systems that learn: Classification and prediction methods from statistics, neural nets, machine learning and expert systems*. San Francisco. CA: Morgan Kaufman publishers,

Weixing, M., Huang, T., Li, X., Zhou, Z., Li, Y., & Zeng, K. (2015). The effects of storm runoff on water quality and the coping strategy of a deep canyon-shaped source water reservoir in China. *International Journal of Environmental Research and Public health*, *12*(7), 7839-7855.

Wilinski, P., & Naumczyk, J. (2012, May). Dissolved Ozone Flotation as a innovative and prospect method for treatment of micropollutants and wastewater treatment costs reduction. In *12th edition of the World Wide Workshop for Young Environmental Scientists (WWW-YES-2012)-Urban waters: resource or risks?* (No. 6). HAL-ENPC.

William, J.P. (1998). *Introduction to Matlab for Engineers*. McGraw-Hill, USA.

Williams, J.R., Nicks, A.D., & Arnold, J.G. (1985). Simulator for water resources in rural basins. *Journal of Hydraulic Engineering*, *111*(6), Doi: http//dx.doi.org/10.1061/ (ASCE) 0733-9429(1985)111.6(970).

Wisniewski, E. (2013). Sedimentation tank design for rural communities in the hilly regions of Nepal. *Journal of Humanitarian Engineering, 2,* 54-67.

Xueying, L., Jun,Q., Qianqian, S., & Fangfany, L. (2016). Simulation of reservoir sediment flushing of the three gorges reservoir using Artificial Neural Networks. *Journal of Applied Sciences*, *6,* 1-11. Doi: 10.3390/app6050148.

Yang, X. (2003). *Manual on sediment management and measurement, operational hydrology* Rep. No. 47, Geneva, Switzerland.

Yaseen, Z.M., El-Shafie, A., Jaafar, O., Afan, H.A., & Sayl, K.N. (2015). Artificial intelligence based models for stream flow forecasting. *Journal of Hydrology*, *530*, 829-844.

Yitian, L., & Gu, R.R. (2003). Modeling flow and sediment transport in a river system using ANN. *Journal of Environmental management, 31* (1), 122-134.

Yon, T.H., & Lee, S.O. (2000). Hydraulic behavior and Removal efficiency of settling tanks. *Journal of Civil Engineering*, *4* (1), 55-57.

Yun-Mei Zhu, X.X., & Yue, Z. (2007). Suspended sediment flux modeling with artificial neural networks. *Journal of Geomorphology*, *84,* 111-125.

Zhiyao, S., Tingting, W., Fumin, X., & Ruijie,C. (2008). A simple formula for predicting settling velocity of sediment particles. *Journal of water science and Engineering*, *1*(1), 37-43.

Zurada, J.M. (1992). *Introduction to Artificial neural systems*. (Vol.8). St. Paul: West: Jaikos books

APPENDICES

Appendix 1: Some small scale Irrigation projects in Embu East and West Districts

Project Name	Sub-County	No. of Members	Discharge (Q) L/sec	Irrigated Area (Ha)
Ena Irrigation project	Embu – East	278	69.55	107
Kiaga Irrigation Project	Embu West	378	93.75	150
Kiruki Kiende Irrigation Project	Embu West	250	32.50	52
Kanthitu Irrigation Project	Embu East	120	46.00	80
Itabua Irriagation water project	Embu West	377	103.50	138
Kithimu- Kithegi Irrigation Project	Embu West	339	101.25	135
Gachicori-Nthamari Irrigation Project	Embu East	122	51.25	82
Kaagari-South Irrigation Project	Embu East	360	98.00	140
Mwiria Irrigation Project	Embu North	375	78.75	150
Kamiu-Kavanga Irrigation Project	Embu west	70	22.50	36

Source: Ministry of Water, land and Environment-Embu County (2013)

Appendix 2: Different Turbidity values against different Flow rates

EXPERIMENTAL DATA

	Flow Rate (Litres/minute)									
Time (mins)	**5.7**	**8.7**	**9.9**	**10.5**	**11.1**	**4.8**	**8.7**	**9.9**	**10.5**	**11.1**
0	424.33	425.00	465.33	463.00	395.00	249.67	245.33	196.00	254.00	257.67
20	314.00	299.33	300.33	367.67	365.67	209.00	177.00	134.33	128.33	235.33
40	324.00	332.00	304.00	334.67	354.67	152.33	167.00	125.33	161.00	268.00
60	317.67	320.67	277.67	377.67	343.67	198.67	170.33	116.67	149.67	256.67
80	317.33	382.67	245.33	358.33	299.33	175.33	163.00	102.33	211.67	318.67
100	333.67	370.33	285.00	397.67	260.67	189.00	161.33	105.33	199.33	306.33
120	325.33	372.00	287.33	396.00	274.67	175.67	218.33	100.33	201.00	308.00
140	325.67	328.33	269.67	357.67	267.67	161.00	150.00	103.00	157.33	264.33
160	305.33	311.00	297.33	227.67	269.33	160.33	158.33	97.33	140.00	247.00
180	307.33	302.67	222.67	269.67	267.00	143.33	151.67	92.33	131.67	238.67
200	295.67	275.33	236.67	257.00	251.00	139.33	139.67	93.67	104.33	211.33
220	304.33	288.67	209.00	260.33	256.00	132.33	138.00	95.00	117.67	224.67
240	284.00	269.33	198.67	260.00	256.33	130.00	142.67	88.33	98.33	205.33
260	291.67	228.00	209.67	241.00	244.67	119.00	128.33	83.00	57.00	164.00
280	271.48	240.00	206.00	219.67	240.00	112.33	140.33	85.00	69.00	176.00

300	250.62	261.67	200.00	242.00	233.67	108.67	133.67	81.67	90.67	197.67

Appendix 3: Normalized turbidity data

	FLOW RATES (M^3/sec)									
Time (mins)	**$9.5x10^{-5}$**	**$1.45\ x10^{-4}$**	**$1.65\ x10^{-4}$**	**$1.75\ x10^{-4}$**	**$1.85\ x10^{-4}$**	**$8.0\ x10^{-5}$**	**$1.5\ x10^{-4}$**	**$1.65\ x10^{-4}$**	**$1.7\ x10^{-4}$**	**$1.8\ x10^{-4}$**
0	1.0000	1.0000	1.0000	1.0000	1.0000	1.0000	1.0000	1.0000	1.0000	1.0000
20	-0.2703	-0.2758	-0.2375	0.2164	0.6364	0.4232	-0.1681	-0.0787	-0.2758	0.5231
40	-0.1552	0.0558	-0.2100	-0.0548	0.5000	-0.3806	-0.3390	-0.2362	0.0558	1.2206
60	-0.2281	-0.0592	-0.4075	0.2986	0.3636	0.2766	-0.2821	-0.3878	-0.0592	0.9786
80	-0.2319	0.5702	-0.6500	0.1397	-0.1860	-0.0544	-0.4074	-0.6385	0.5702	2.3025
100	-0.0439	0.4450	-0.3525	0.4630	-0.6653	0.1395	-0.4359	-0.5860	0.4450	2.0391
120	-0.1398	0.4619	-0.3350	0.4493	-0.4917	-0.0496	0.5385	-0.6735	0.4619	2.0747
140	-0.1360	0.0186	-0.4675	0.1342	-0.5785	-0.2577	-0.6296	-0.6268	0.0186	1.1423
160	-0.3701	-0.1574	-0.2600	-0.9342	-0.5579	-0.2671	-0.4872	-0.7259	-0.1574	0.7722
180	-0.3470	-0.2420	-0.8200	-0.5890	-0.5868	-0.5083	-0.6011	-0.8134	-0.2420	0.5943
200	-0.4814	-0.5195	-0.7150	-0.6932	-0.7851	-0.5650	-0.8063	-0.7901	-0.5195	0.0107
220	-0.3816	-0.3841	-0.9225	-0.6658	-0.7231	-0.6643	-0.8348	-0.7668	-0.3841	0.2954
240	-0.6157	-0.5804	-1.0000	-0.6685	-0.7190	-0.6974	-0.7550	-0.8834	-0.5804	-0.1174
260	-0.5274	-1.0000	-0.9175	-0.8247	-0.8636	-0.8534	-1.0000	-0.9767	-1.0000	-1.0000
280	-0.7598	-0.8782	-0.9450	-1.0000	-0.9215	-0.9480	-0.7949	-0.9417	-0.8782	-0.7438
300	-1.0000	-0.6582	-0.9900	-0.8164	-1.0000	-1.0000	-0.9088	-1.0000	-0.6582	-0.2811

Appendix 4: The intake of Kiriku-Kiende irrigation project

The Intake of Kiriku-Kiende Irrigation project

Appendix 5: Photo of the settling basin Model

The fabricated physical model for settling basin